2mip

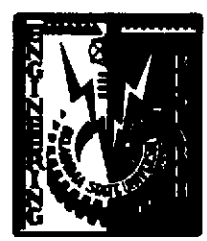

OKLAHOMA STATE UNIVERSITY

OPTIMAL CONTROLLER DESIGN FOR HIGH PERFORMANCE AIRCRAFT UNDERGOING LARGE DISTURBANCE ANGLES

FINAL REPORT

TO

NASA

LANGLEY

RESEARCH

CENTER

NASA Grant NGR 37-002-096

February 28, 1974

FINAL REPORT

OPTIMAL CONTROLLER DESIGN FOR HIGH PERFORMANCE AIRCRAFT UNDERGOING LARGE DISTURBANCE ANGLES

NASA Grant NGR 37-002-096

Principal Investigator

Ronald P. Rhoten

School of Electrical Engineering

Oklahoma State University

Stillwater, Oklahoma

February 28, 1974

CONTENTS

FINAL REPORT

OPTIMAL CONTROLLER DESIGN FOR HIGH PERFORMANCE AIRCRAFT UNDERGOING LARGE DISTURBANCE ANGLES

I. INTRODUCTION AND PROBLEM STATEMENTS

This document represents the final report for the research supported by NASA Grant NGR 37-002-096. The program was initiated on February 1, 1973 and terminated on January 31, 1974.

The research focused on an examination of two aircraft controller structures applicable to on-line implementation. The two controllers, a linear regulator model follower and an "inner-product" model follower, were applied to the lateral dynamics of the F8-C aircraft.

Any controller design must satisfy certain performance criteria. First, of course, the resulting aircraft handling characteristics must be "acceptable", in an as yet to be defined sense. Second, the performance must not deteriorate significantly when the real physical constraints of control surface rate and magnitude deflection limits are considered. Third, the design must be amenable to on-line implementation, in that as the aircraft changes flight condition, the linear perturbation model must be modified and a new control law rapidly and accurately evaluated. Finally, the standard regulator technique to be considered is designed under the assumption of zero pilot commands, and performance should not be adversely affected by significant command signals.

For the purposes of this research effort, the lateral dynamics of the F8-C aircraft were considered. The controller designs were evaluated

for four flight conditions, described in detail in the Appendix. Additionally, effects of pilot input, rapid variation of flight condition and control surface rate and magnitude deflection limits were considered, to be discussed in summary in the next section and in detail in later sections.

II. SUMMARY OF RESULTS

At the outset of this research project, it was noted that standard regulator model following designs suffered from three possible design difficulties:

(i) Since zero pilot commands were assumed during design, significant pilot inputs would degrade performance.

(ii) Rapid changes in flight condition would introduce nonlinear effects and degrade performance.

(iii) Control surface rate and magnitude limits would degrade performance.

In contrast, the proposed inner-product model follower possessed the following properties:

(i) By treating pilot commands as arbitrary variables, no performance degradation would result from their introduction.

(ii) By measuring (or evaluating) state derivatives, nonlinear effects would be noted and undesirable effects minimized.

(iii) Again through sensing state derivatives, limitations due to rate and magnitude constraints would be noted and effects minimized.

The extensive simulations of flight trajectories to be presented will illustrate the following general conclusions and observations:

(i) Non-zero pilot commands did degrade performance of the standard design, yet caused no reduction in performance

of the inner-product design.

(ii) The inner-product design unexpectedly proved to be more sensitive to control surface rate and magnitude constraints than the standard. While various gain weighting constants could be "tuned" to a particular flight condition and amplitude of pilot input, a change would then result in an unsatisfactory design. While even more extensive simulations might provide a single satisfactory result, such improvements as were noted seem too minor to justify the considerable effort required.

(iii) Nonlinear effects did degrade performance, though at least for those nonlinearities considered, not so significantly as to give rise to serious instabilities. As expected, the inner-product design offered improved performance before consideration of rate and magnitude constraints. With these constraints in effect, however, the improvements in performance were not substantial.

(iv) In summary, then, the primary result of this effort is that rapid changes in flight condition can sufficiently degrade performance that considerable attention should be devoted to this problem. If on-board computational speed limitations do not allow evaluation of new feedback gains for the standard design sufficiently fast, other alternatives, mentioned in the CONCLUSIONS AND RECOMMENDATIONS of this report, should be considered.

III. THE CONTROLLER STRUCTURES

The Linear Regulator Design

Suppose that the linearized equations of lateral motion of the aircraft are given by

$$\dot{x} = Ax + B\delta \tag{1}$$

$$\delta = \delta^a + H\delta^p \tag{2}$$

$$y = Dx, \tag{3}$$

where x is the state vector of roll rate, yaw rate, sideslip and bank angle; δ is the control vector of aileron (δ_a) and rudder (δ_r); δ^a and δ^p are automatic control and pilot commands respectively; and y is the primary output vector of roll rate, yaw rate and sideslip.

Suppose further that a mathematical model of desired characteristics has been constructed and is represented by

$$\dot{x}_m = A_m x_m + B_m \delta^p \ , \tag{4}$$

where x_m is the model state vector of roll rate, yaw rate and sideslip and δ^p is again the pilot command vector.

Since the design objective is to select δ^a such that y follows the model response x_m, and to pose the problem in optimal regulator form, consider the augmented system

$$\dot{x}^* = \begin{bmatrix} \dot{x} \\ - - \\ \dot{x}_m \end{bmatrix} = \left[\begin{array}{c|c} A & 0 \\ - & - \\ 0 & A_m \end{array}\right] x^* + \begin{bmatrix} B \\ - - \\ 0 \end{bmatrix} \delta^a + \begin{bmatrix} B\ H \\ - - \\ B_m \end{bmatrix} \delta^p$$

$$= A^* x^* + B^* \delta^a + \bar{B}\delta^p \tag{5}$$

with associated performance measure

$$J = \int_0^\infty \{x^{*T} Q^* x^* + \delta^{aT} R \delta^a\} \, dt, \tag{6}$$

where

$$Q^* = \left[\begin{array}{c|c} D^T Q D & -D^T Q \\ \hline -QD & Q \end{array}\right] \tag{7}$$

and Q and R are respectively positive semidefinite and positive definite matrices of appropriate dimension.

If the pilot commands are for the moment assumed to be identically zero, the dynamics of (5) and performance measure of (6) constitute a quadratic regulator problem, where Q* is such that the variables y will optimally approach the variables x_m.

The solution is well known to be

$$\delta^a = -R^{-1} B^{*T} K x^* \tag{8}$$

where K is the symmetric positive definite solution of the matrix algebraic Riccati equation

$$[0] = -KA^* - A^{*T} K + KB^* R^{-1} B^{*T} K - Q^*. \tag{9}$$

The question immediately encountered is how to solve (9). In an off-line mode, the answer is to merely integrate the associated matrix differential Riccati equation backwards in time until steady-state conditions are attained. In an on-line mode, when A* and B* may change

rapidly, a more rapid process is obviously required. As later simulations will indicate, an updating of gains at less that one second intervals appears to be sufficient - still a significant task for an on-board processor.

Recalling that the design to this point has assumed zero pilot commands, the feedforward gain matrix H must be found to minimize performance losses due to large inputs. This goal is best attained by selecting H by pseudo-inversion,

$$H = [DB]^{\dagger}B_m .$$

This selection minimizes excitation of the error modes, though both transient and steady state errors will exist, with their magnitudes dependent on the magnitudes of pilot commands.

The Inner-Product Design

A controller as designed above will operate satisfactorily if the aircraft's distrubance angles are small, implying that the linearized equations of motion are valid, and under conditions of limited pilot command. Unfortunately, there is no known method of altering the synthesis procedure if either of these conditions is violated. However, a completely different design process does offer a potentially useful approach to such problems. The theoretical basis for this technique may be briefly presented as follows.

Suppose the aircraft dynamics are described by

$$\dot{x} = f(x) + B\delta \tag{10}$$

$$\delta = \delta^a + \delta^p \tag{11}$$

$$y = D_1 x \ , \tag{12}$$

where x, δ, δ^a, δ^p and y represent again, respectively, state variables, control variables, automatic control signals, pilot commands and output variables. Suppose further that the desired model is described by

$$\dot{x}_m = f_m(x_m) + B_m\delta^p \tag{13}$$

$$y_m = D_2 x_m \quad , \tag{14}$$

where x_m and y_m are model state and output variables. If it is desired that the actual aircraft responses follow the model output variables, an error signal can be defined as

$$e = y - y_m. \tag{15}$$

At this point the optimization procedure proceeds in a manner entirely different from standard techniques. A performance measure is constructed which penalizes for error and the time derivative of error, rather than for error and control magnitudes, and which is completely independent of the system dynamics. Optimizing trajectories are than evaluated using the calculus of variations, and finally a control is selected to cause the system outputs to track the optimal trajectories as closely as possible.

Since the system should be penalized in a non-negative manner for both error and error derivative, a performance measure is chosen as

$$J = \int_0^\infty \{h(\rho) + \dot{\rho}^2\}dt, \tag{16}$$

where ρ is an error function defined by e^Te, the inner-product of the error signal of (15) with itself, and $h(\cdot)$ is constrained only by

$$h(\rho) > 0 \qquad \text{for all } \rho \neq 0,$$

$$h(0) = 0.$$

A solution trajectory which minimizes (16) must satisfy the Euler-Lagrange equation and associated boundary conditions

$$\begin{aligned} 2\ddot{\rho} &= dh(\rho)/d\rho \\ \rho(t_o) &= \rho_o \\ \lim_{t\to\infty} \dot{\rho}(t) &= 0. \end{aligned} \tag{17}$$

If (17) is multiplied by $\dot{\rho}$, the resulting expression can be integrated once to yield

$$\dot{\rho}^2 = h(\rho) \ , \tag{18}$$

where the initial value of (17) still applies and, by use of the final condition, the constant of integration has been found to be zero.

Since (18) is in general nonlinear in ρ, the common variational calculus problem of finding a closed-form solution of the Euler-Lagrange equation is present. However, equation (18) represents a description of the optimal trajectories, and if a controller can be found so that (18) is satisfied then it need never be solved.

To begin the solution of such a controller, the plant dynamics must be considered. Since ρ is merely $e^T e$, the time derivative of ρ is just

$$\dot{\rho} = 2e^T\dot{e} \ . \tag{19}$$

Substituting then equations (10-15) into (19) yields

$$\dot{\rho} = 2e^T [D_1 \dot{x} - D_2 \dot{x}_m]$$

$$= 2e^T [D_1 f(x) + D_1 B\delta^a + D_1 B\delta^p \qquad (20)$$

$$-D_2 f_m(x_m) - D_2 B_m \delta^p].$$

Finally, from equation (18),

$$-\frac{1}{2}\sqrt{h(\rho)} = e^T [D_1 f(x) + D_1 B\delta^a$$

$$+ D_1 B\delta^p - D_2 f_m(x_m) - D_2 B_m \delta^p]. \qquad (21)$$

Equation (21) represents an equation describing both the norm of the system solution and the norm of the trajectories minimizing the performance measure. If (21) can be solved for δ^a, the resultant system trajectories will thus be optimal. It should also be noted that the pilot commands are present as arbitrary variables, and a primary objective of controller design has thus been satisfied. Of course, the difficulty in solving (21) for δ^a will depend inherently on the system and model equations.

If the error function $h(\rho)$ is selected as $\alpha^2 \rho^2$, where α is an error vs. error derivative weighting constant, equation (21) becomes

$$-\frac{\alpha}{2} e^T e = e^T \{D_1 f(x) + D_1 B\delta^a + D_1 B\delta^p$$

$$- D_2 f_m(x_m) - D_2 B_m \delta^p\}. \qquad (22)$$

While equation (22) does not have an unique solution, it is clear that the autopilot signals may be found as

$$\delta^a = [D_1 B]^{-1} \{-\frac{\alpha}{2} e - D_1 f(x) - D_1 B\delta^p$$

$$+D_2 f_m(x_m) + D_2 B_m \delta^p\} . \qquad (23)$$

The control law is thus seen to consist of linear combinations of three primary types of functions. First, of course, the instantaneous value of error influences the control law; second, the plant and model dynamics are utilized in the control process. Finally, the actual values of pilot commands contribute to the design, thus overcoming the severe constraint of previous techniques that pilot inputs be considered as zero or known in advance.

IV. SIMULATION RESULTS

To provide continuity of text, the figures of all simulation results are provided in the Appendix.

Bare Aircraft vs. Model

The first step in the evaluation of the two controller structures was the selection of an appropriate reference model. A type of model often suggested is one which provides decoupling; that is, the rolling motions are not affected by the yaw or sideslip motions, and conversely. Similarly, the input matrix is selected so that aileron commands induce only roll, while rudder inputs excite only yaw and sideslip motions.

It is often argued that such model responses are too perfect, in that even the best handling aircraft do not possess this completely decoupled behavior, and such responses would actually be unexpected by an experienced pilot, and hence undesirable.

Nonetheless, such behavior does provide a severe test for the control law under consideration, and a decoupled model was utilized in this study to provide essentially a worst case design. All of the results to be presented would be significantly improved if a more realistic model were selected.

The model used is represented by

$$\dot{x}_m = \begin{bmatrix} -2.84 & 0 & 0 \\ 0 & -1.93 & 6.72 \\ 0 & -1.20 & -0.48 \end{bmatrix} x_m + \begin{bmatrix} 17 & 0 \\ 0 & -2.79 \\ 0 & -0.34 \end{bmatrix} \delta^p .$$

This selection gives approximately a 0.35 second time constant for the roll rate, while the yaw rate/sideslip motions are characterized by a second order system with a 3 radian/second natural frequency and a 0.4 damping factor. Input sensitivities are 6 degrees/second of roll rate per degree of aileron deflection and -0.42 degrees/second of yaw rate and 0.3 degrees of sideslip per degree of rudder deflection.

Initial simulation results utilized two standard inputs, a 5 degree aileron deflection and a 3 degree rudder deflection, acting disjointly. Figures A1 through A32 provide the responses of the bare aircraft and the model for these inputs and for each of four flight conditions described by Table A1 of the Appendix. Merely to indicate the possibilities of alternate model selections, Figures A2 and A10 indicate a model yaw rate response with an input matrix selected so that aileron deflections induced yawing motions as well as rolling motions.

Indicative of the broad range of flight conditions over which the controller must operate, the steady-state roll rate errors to a 3 degree rudder deflection ranged from a low of 2 degrees/second for flight condition C to a high of 10 degrees/second for flight condition D.

Results Without Rate or Magnitude Constraints

Even without rate or magnitude constraints, consideration must be given to the initial condition allowed the control law. Since a step input of aileron or rudder is the test signal, the inner-product controller, by sensing the input magnitude by the instantaneous values of state derivative, has a non-zero initial value. While an actual pilot input would never be a step function, due to rate constraints, such effects might be encountered due to sudden external disturbances.

If the inner-product controller is allowed to assume these instantaneous values, and with no rate or magnitude constraints, *the model variables of roll rate and sideslip are tracked with zero error independent of the magnitude of pilot commands or nonlinear effects due to rapid changes in flight condition.*

However, considering that rate and magnitude constraints will ultimately be imposed, an intermediate case has been considered wherein the initial control values have been restricted to zero. These results, presented in Figures A33 through A80, provide a realistic indication of system responses with inputs sufficiently small that rate and magnitude constraints do not seriously degrade performance.

The figures illustrate response and control trajectories for all four flight conditions both for aileron and rudder inputs. In all cases the inner-product design offers superior responses for roll rate and sideslip, with no significant degradations in yaw rate. A careful examination of the control trajectories indicates that while the inner-product controllers are in some cases excessively oscillatory, it is the standard design which results in extremely large and rapidly changing control laws. It was precisely this characteristic that seemed to indicate that the inner-product technique might prove to be superior when rate and magnitude constraints were imposed. Unfortunately, later simulations did not support this conjecture.

Rate and Magnitude Constraints Effects

Since the application of rate and magnitude constraints to a control law introduces a significant nonlinear effect, and one which successfully

resists analytical analysis, extensive simulations provide the primary evaluative procedure. In examining the two control structures under study, magnitude constraints of $\pm$ 6° rudder, $\pm$ 30° aileron and rate constraints of $\pm$ 70°/second rudder and $\pm$ 140°/second aileron were imposed. Various pilot command magnitudes were examined; changes in error weighting terms were considered; and all flight conditions examined.

As might be expected, the extensive number of simulations provided a sufficiently broad class of results that virtually any hypothesis could be supported, at least in isolated instances. However, a general feature of the results was that the inner-product design, while *capable* of providing visibly superior response characteristics, required significantly more "tuning" of error weighting terms than the standard controller. Figures A81 through A88 illustrate a typical set of response data, in that the inner-product trajectories result from some adjustment of error weights while further improvement is still possible.

Unfortunately, the simulations did not indicate a reasonable procedure or pattern for modifying these controller gains "a priori". The standard design, while not capable of approaching the *best* accuracies of the inner-product, were less sensitive to all changes and hence were almost uniformly superior to the *worst* inner-product results.

Responses with Nonlinear Effects

While the preceding discussions indicate a significant disadvantage of the inner-product design, the final feature of insensitivity to nonlinearities still merits a careful evaluation. As indicated in Section III, the inner-product error signal includes both state and

derivative information. With no limitations on the controller signal, the inner-product design will provide optimal control signals independent of any nonlinearities involved.

To evaluate this capability with initial condition and rate and magnitude constraints, the aircraft equations were simulated for an angle of attack changing from 12° to 4° and from 4° to 12° at a rate of 8°/second. The effects of this change were considered with respect to the resulting changes in c_{ℓ_p}, c_{ℓ_r}, c_{ℓ_β}, c_{n_p}, c_{n_β}, $c_{\ell_{\delta_r}}$, $c_{n_{\delta_a}}$.

Thus, the standard model following system was constrained to utilizing a fixed set of gains for this one second interval.

Again, however, effects of initial value limitations, rate and magnitude constraints and error weight adjustments were so marked that any advantages to be gained were marginal at best. A representative set of trajectories, provided in Figures A89 through A104, actually illustrates that the nonlinearities considered did not degrade performance to a completely unacceptable level. At least for the conditions considered, updates in controller gains at approximately one-half second intervals should provide acceptable response behavior.

V. CONCLUSIONS AND RECOMMENDATIONS

A careful evaluation of the results presented in the preceding section leads to the conclusion that inner-product technique disadvantages of error weighting term and rate and magnitude constraint sensitivities are at least as severe as the improvements resulting from input magnitude and nonlinearity insensitivities.

The standard linear design seems capable of providing acceptable response characteristics if it is possible to perform a new linearization and updating of controller gains sufficiently fast. At least for the nonlinearities considered, an updating of approximately every one-half second would seem to be acceptable, although many more simulations would be necessary to confirm this rate.

While the Riccati equation obviously cannot be solved exactly for the standard controller gains in less than a second with on-board computational facilities, an iterative technique can be used to provide an approximate answer. The primary difficulty with such a procedure is that it may be possible for the approximations to become less and less accurate as errors accumulate, possibly resulting in an instability.

What is needed, of course, is a procedure which is fast yet provides an exact answer. The only techniques which appear appropriate are a class of results known as "pole placing" controller designs. Until recently, all suffered from the common disadvantage of requiring the Jordon form and corresponding similarity transformation matrix for the plant matrix, an exceedingly difficult and lengthy computational process. Recently, however, new results have been presented which

do not have these restrictions, and seem to have good possibilities for on-line implementation with small air-borne processors.

It would seem appropriate that careful consideration be given these techniques, at least as a possible alternative to any procedure requiring solution of the nonlinear algebraic matrix Riccati equation.

APPENDIX

Table A1

Flight Condition Descriptions

Figures A1 - A104

Selected Response Characteristics

TABLE A 1

FLIGHT CONDITION DESCRIPTIONS

Flight Condition: A

Altitude: 50,000 ft.

Mach Number: 1.10

Angle of Attack: 8.6°

$$A = \begin{bmatrix} -1.38E+0 & 2.23E-1 & -3.31E+1 & 0. \\ -3.71E-3 & -1.96E-1 & 6.71E+0 & 0. \\ 1.15E-1 & -9.99E-1 & -1.07E-1 & 3.02E-2 \\ 9.89E-1 & 1.49E-1 & 0. & 0. \end{bmatrix}$$

$$B = \begin{bmatrix} 1.16E+1 & 4.43E+0 \\ 2.09E-1 & -1.76E+0 \\ -1.41E-3 & 1.07E-2 \\ 0. & 0. \end{bmatrix}$$

Flight Condition: B

Altitude: 50,000 ft.

Mach Number: 0.95

Angle of Attack: 5.99°

$$A = \begin{bmatrix} -1.53E+0 & 6.78E-2 & -3.00E+1 & 0. \\ -1.16E-2 & -1.50E-1 & 5.16E+0 & 0. \\ 6.98E-2 & -9.99E-1 & -9.03E-2 & 3.50E-2 \\ 9.95E-1 & 1.04E-1 & 0. & 0. \end{bmatrix}$$

TABLE A 1 - Cont'd.

$$B = \begin{bmatrix} 1.15E+1 & 5.24E+0 \\ 1.89E-1 & -1.97E+0 \\ -2.99E-3 & 1.35E-2 \\ 0. & 0. \end{bmatrix}$$

Flight Condition: C

Altitude: 12,000 ft.

Mach Number: 1.10

Angle of Attack: 1.18°

$$A = \begin{bmatrix} -8.67E+0 & -1.31E-1 & -1.55E+2 & 0. \\ 1.08E-1 & -9.96E-1 & 3.06E+1 & 0. \\ -1.45E-2 & -9.97E-1 & -5.71E-1 & 2.74E-2 \\ 9.99E-1 & 2.07E-2 & 0. & 0. \end{bmatrix}$$

$$B = \begin{bmatrix} 5.43E+1 & 4.32E+1 \\ 7.35E-1 & -9.96E+0 \\ -1.76E-2 & 5.38E-2 \\ 0. & 0. \end{bmatrix}$$

Flight Condition: D

Altitude: 4,000 ft.

Mach Number: 0.95

Angle of Attack: 1.43°

$$A = \begin{bmatrix} -1.02E+1 & -1.42E-1 & -1.48E+2 & 0. \\ 6.71E-2 & -9.61E-1 & 2.94E+1 & 0. \\ -1.01E-2 & -9.96E-1 & -5.61E-1 & 3.09E-2 \\ 1.00E+0 & 2.50E-2 & 0. & 0. \end{bmatrix}$$

TABLE A 1 - Cont'd.

$$B = \begin{bmatrix} 7.79E+1 & 4.26E+1 \\ 9.17E-1 & -1.44E+1 \\ -2.47E-2 & 8.64E-2 \\ 0. & 0. \end{bmatrix}$$

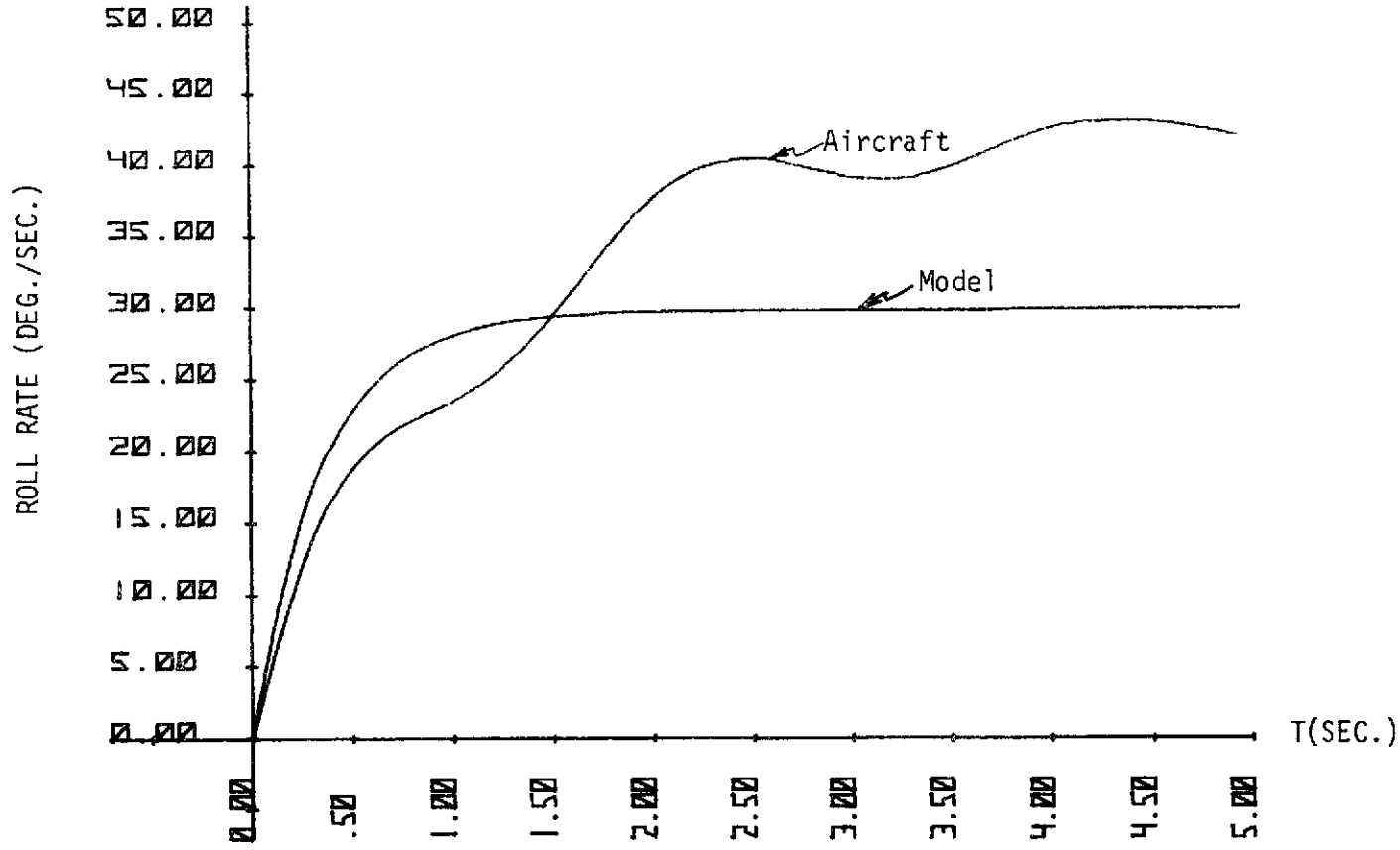

Flight Condition A; $\delta_a^p = 5^o$, $\delta_r^p = 0^o$.

Figure A1.

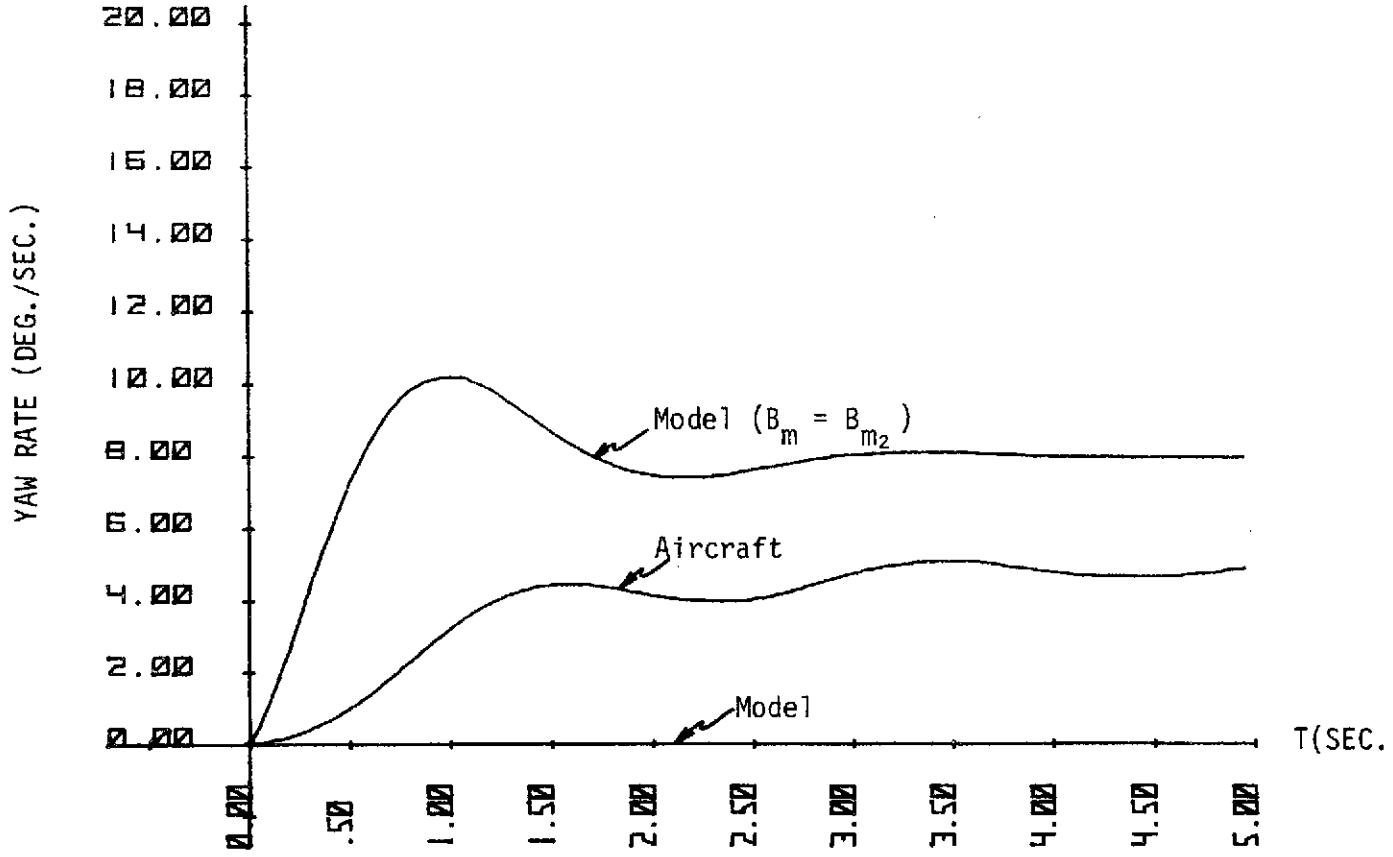

Flight Condition A; $\delta_a^p = 5^o$, $\delta_r^p = 0^o$.

Figure A2.

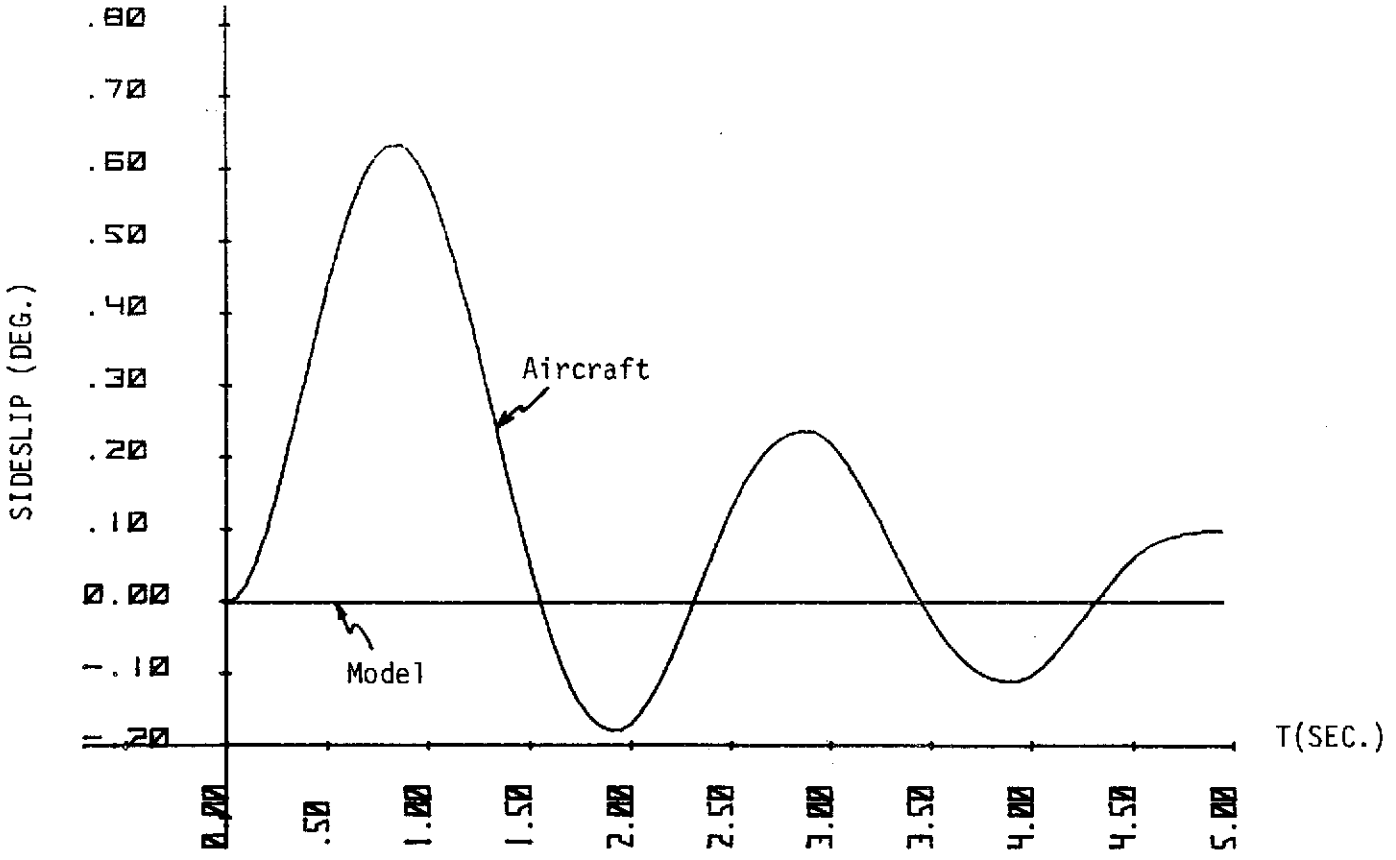

Flight Condition A; $\delta_a^p = 5^o$, $\delta_r^p = 0^o$.

Figure A3.

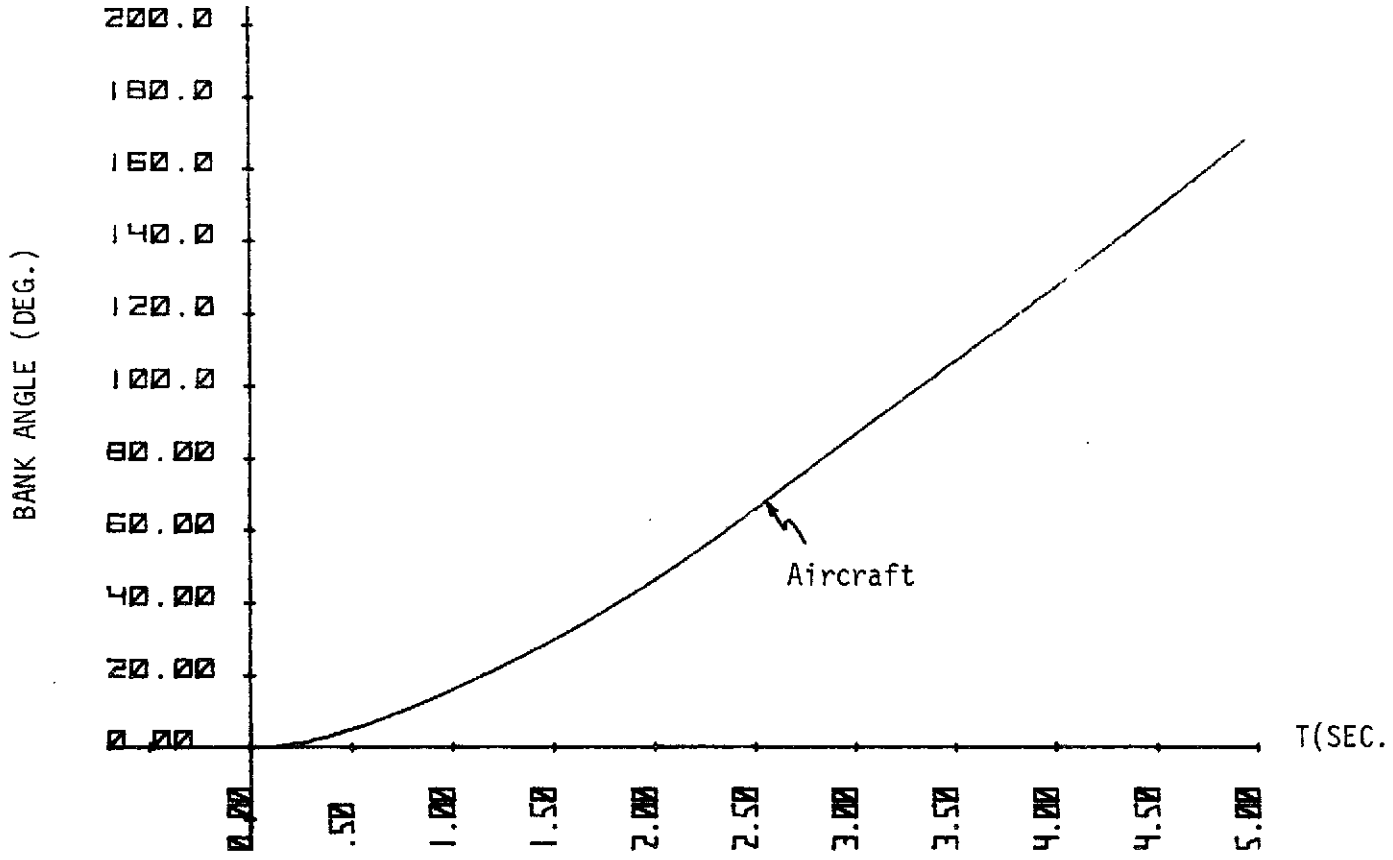

Flight Condition A; $\delta_a^p = 5, \delta_r^p = 0^o$.

Figure A4.

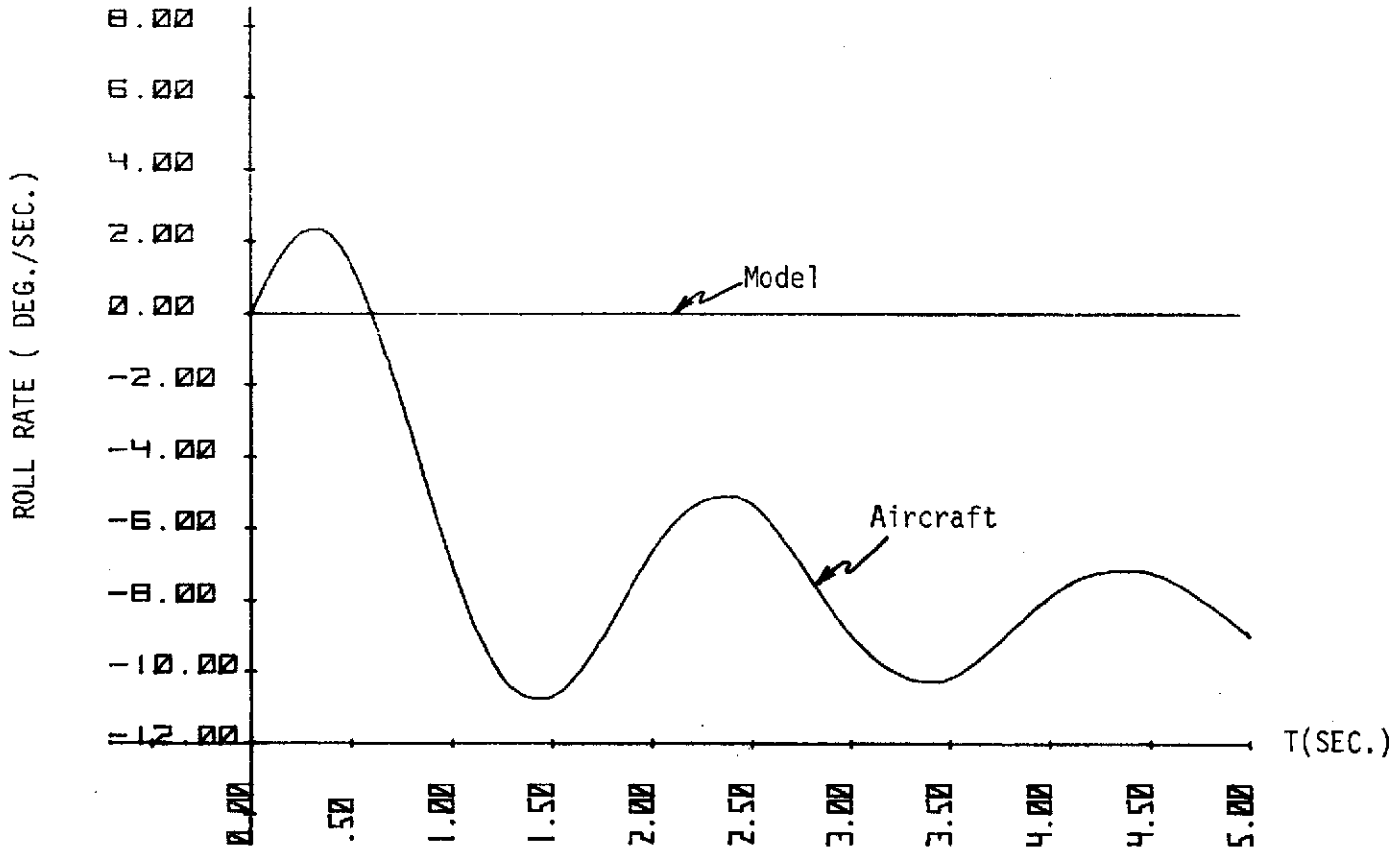

Flight Condition A; $\delta_a^p = 0^o$, $\delta_r^p = 3^o$.

Figure A5.

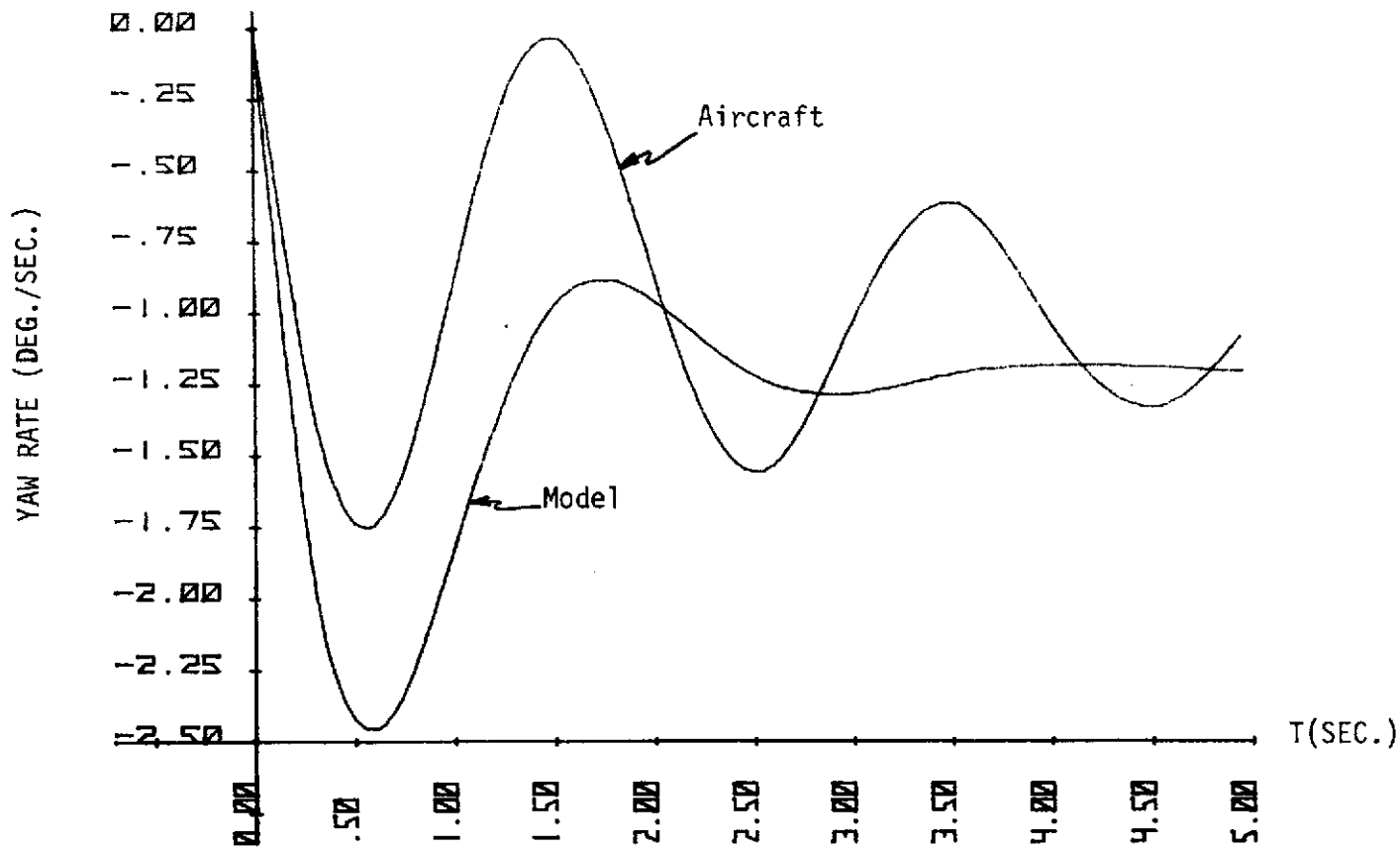

Flight Condition A; $\delta_a^p = 0^o$, $\delta_r^p = 3^o$.

Figure A6.

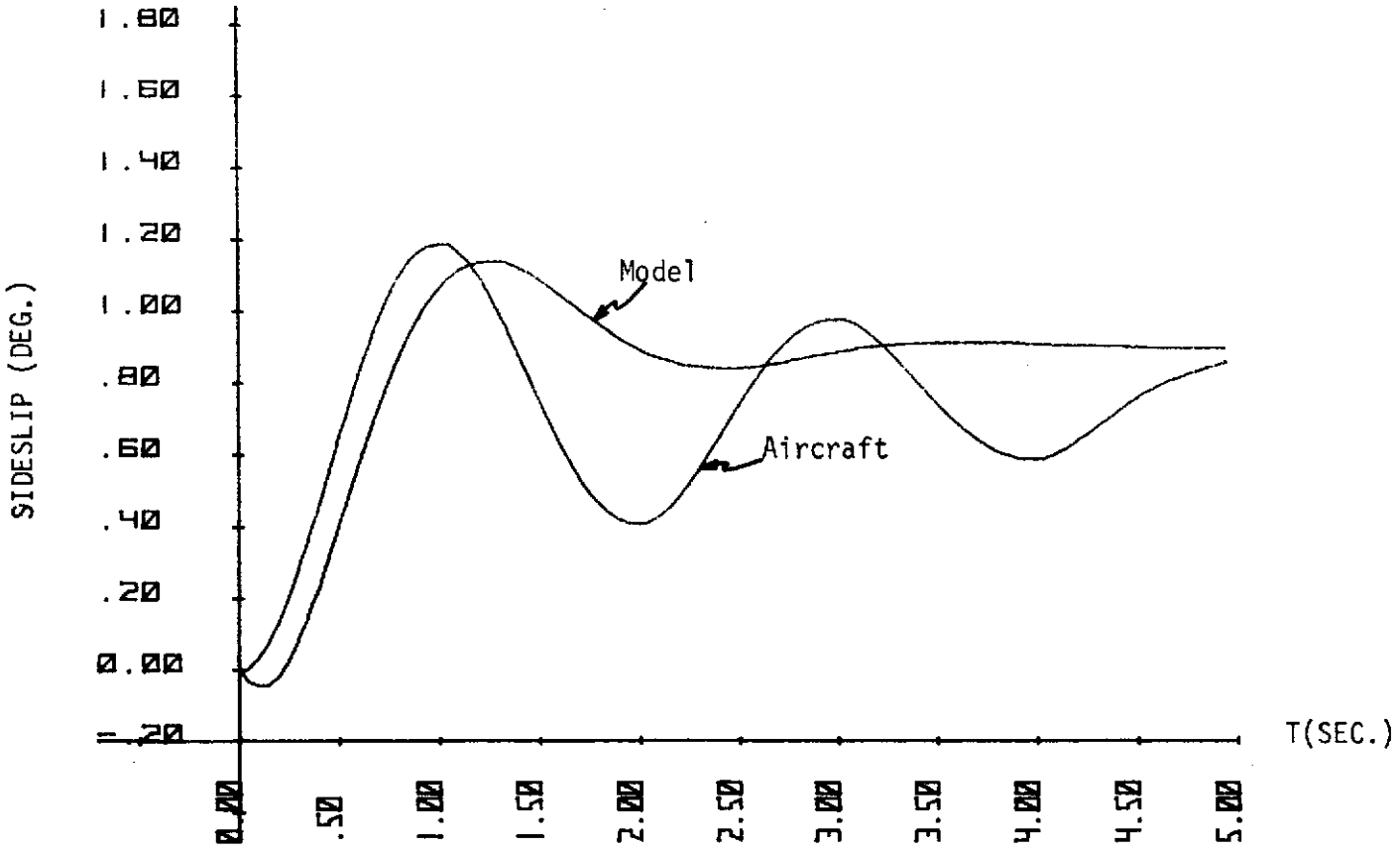

Flight Condition A; $\delta_a^p = 0^o$; $\delta_r^p = 3^o$.

Figure A7.

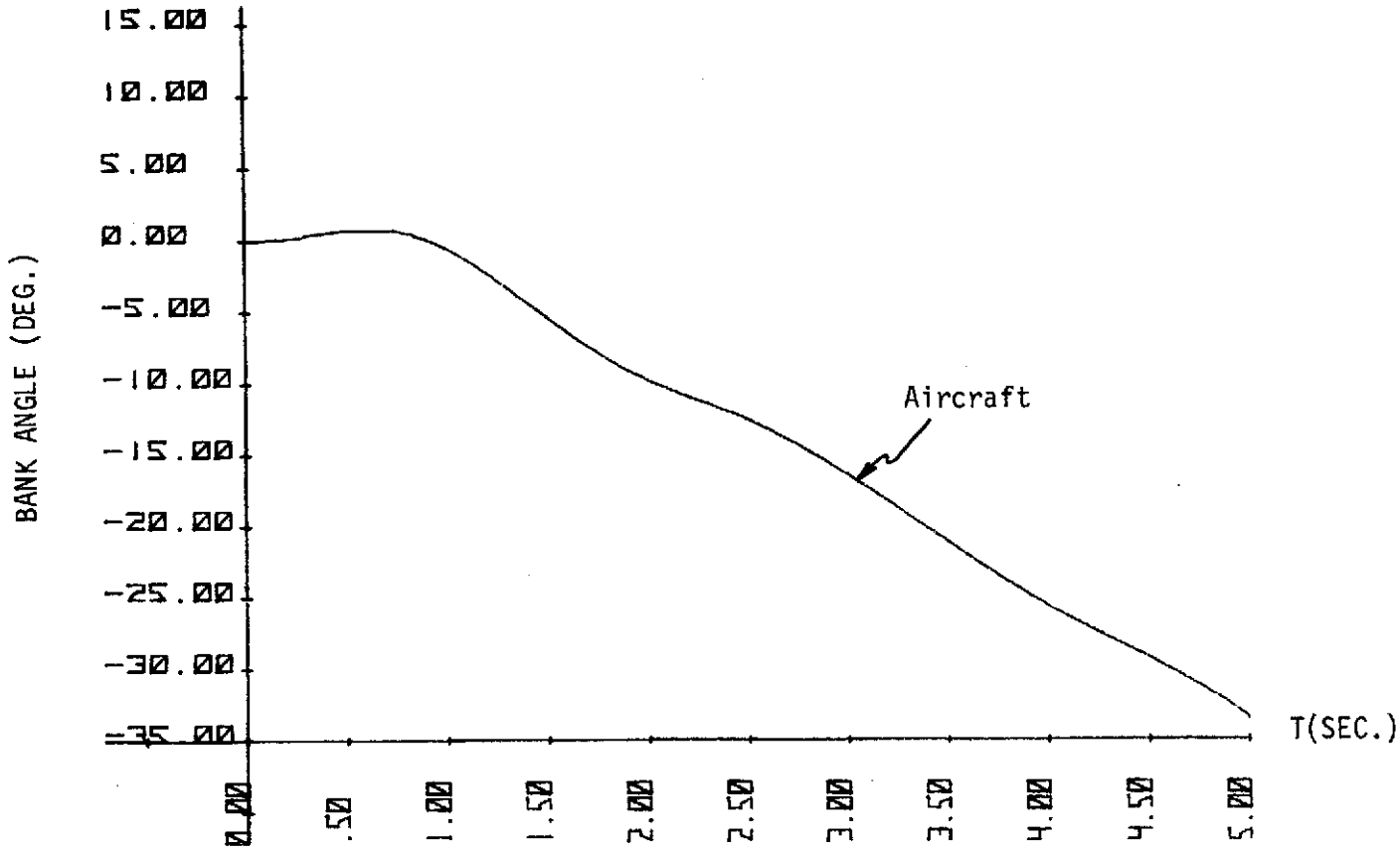

Flight Condition A; $\delta_a^p = 0^o$, $\delta_r^p = 3^o$.

Figure A8.

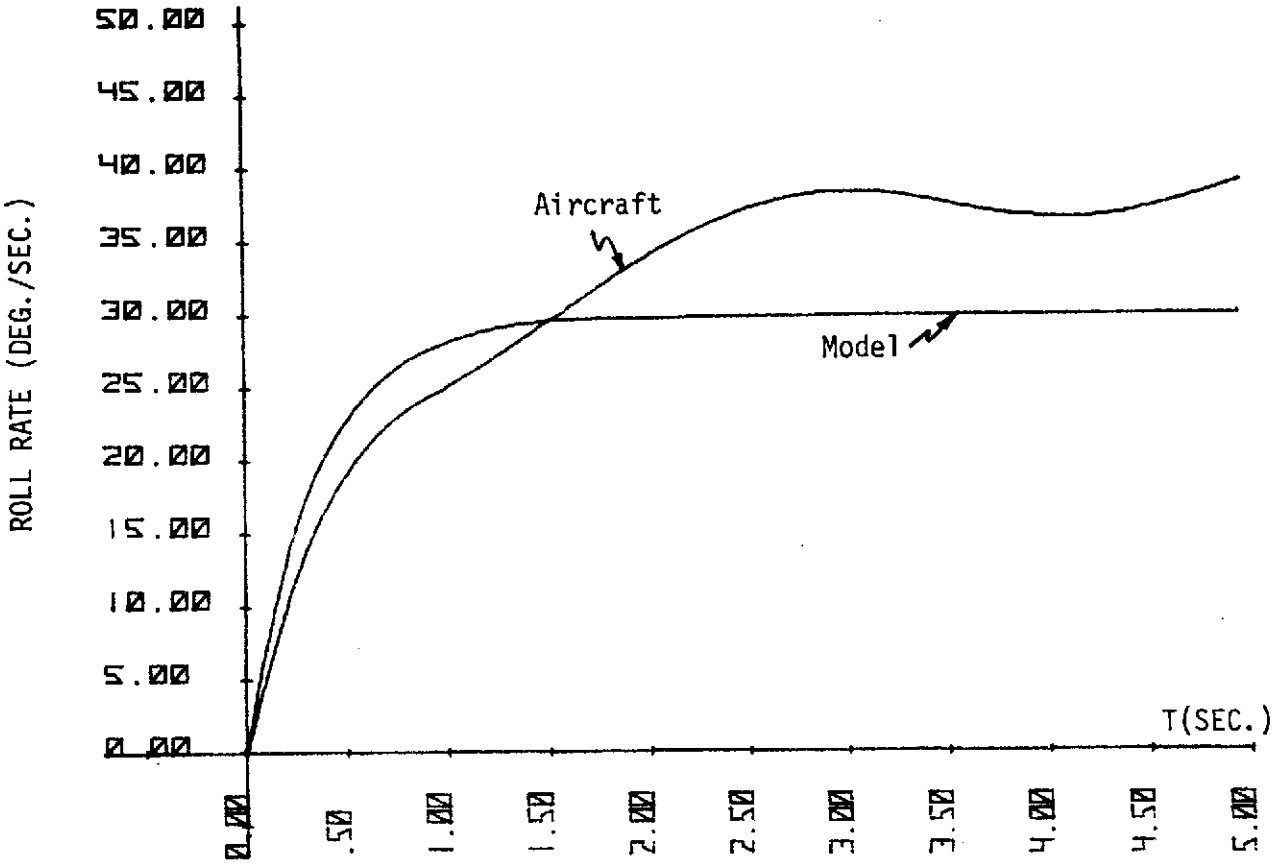

Flight Condition B ; $\delta_a^p = 5°$, $\delta_r^p = 0°$.

Figure A9.

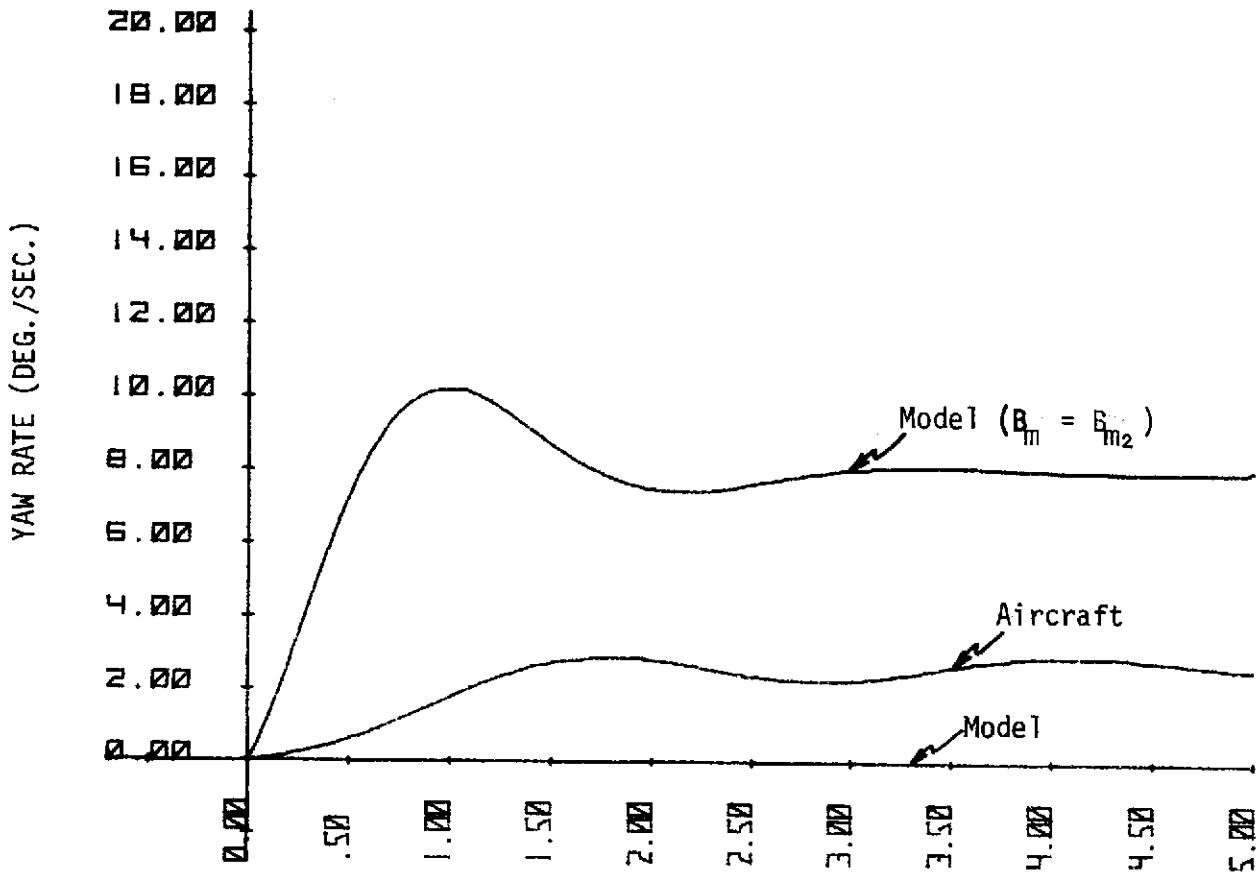

Flight Condition B ; $\delta_a^p = 5°$, $\delta_r^p = 0°$.

Figure A10.

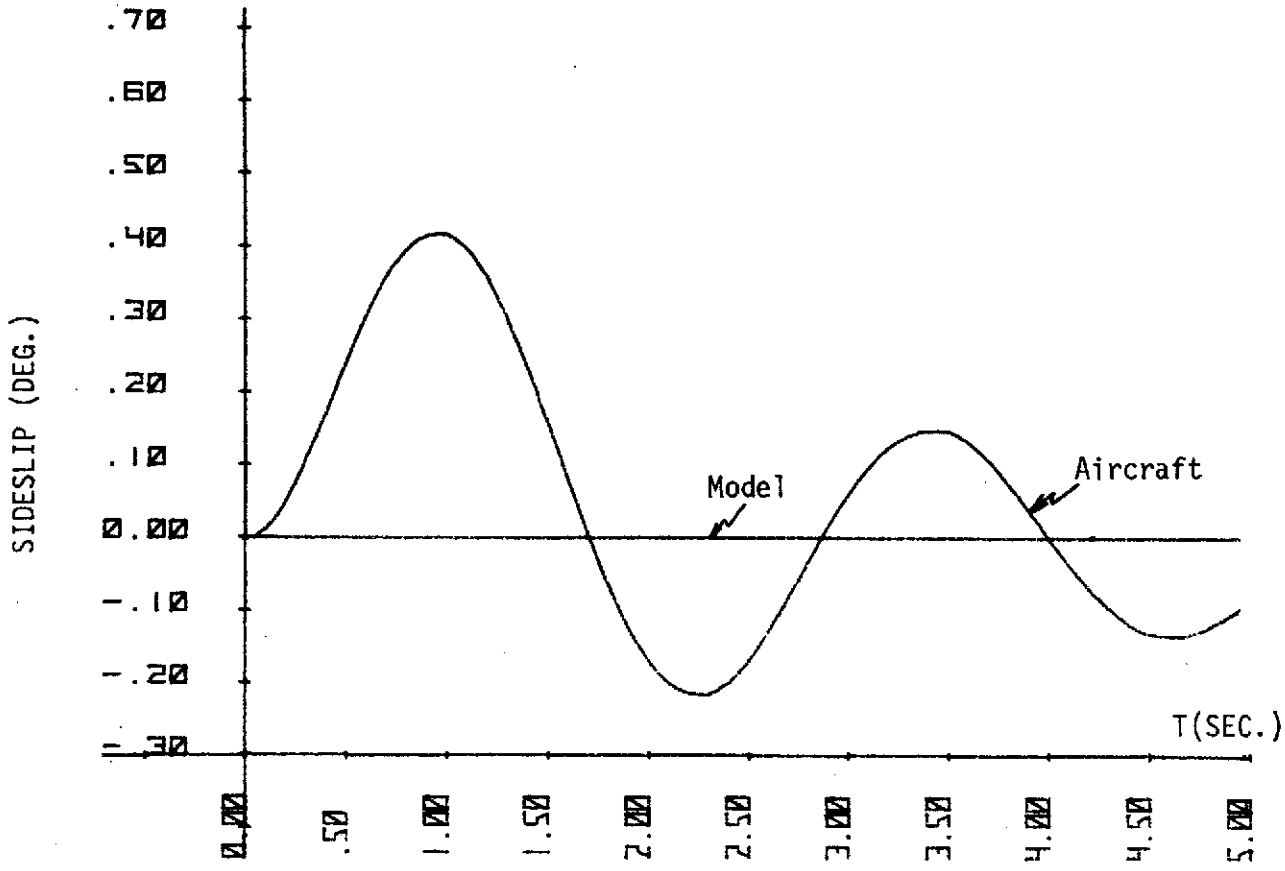

Flight Condition B ; $\delta_a^p = 5°$, $\delta_r^p = 0°$.

Figure A11.

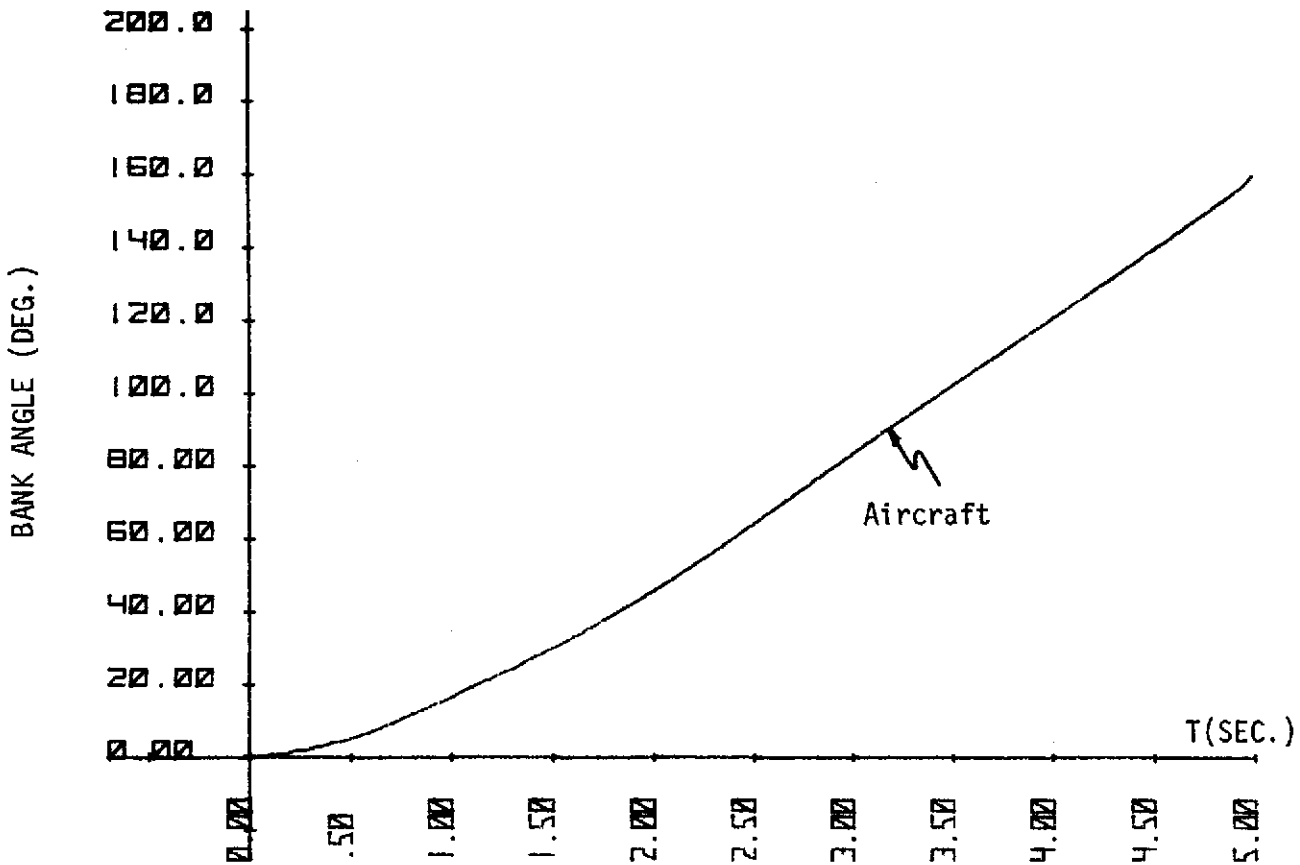

Flight Condition B ; $\delta_a^p = 5°$, $\delta_r^p = 0°$,

Figure A12.

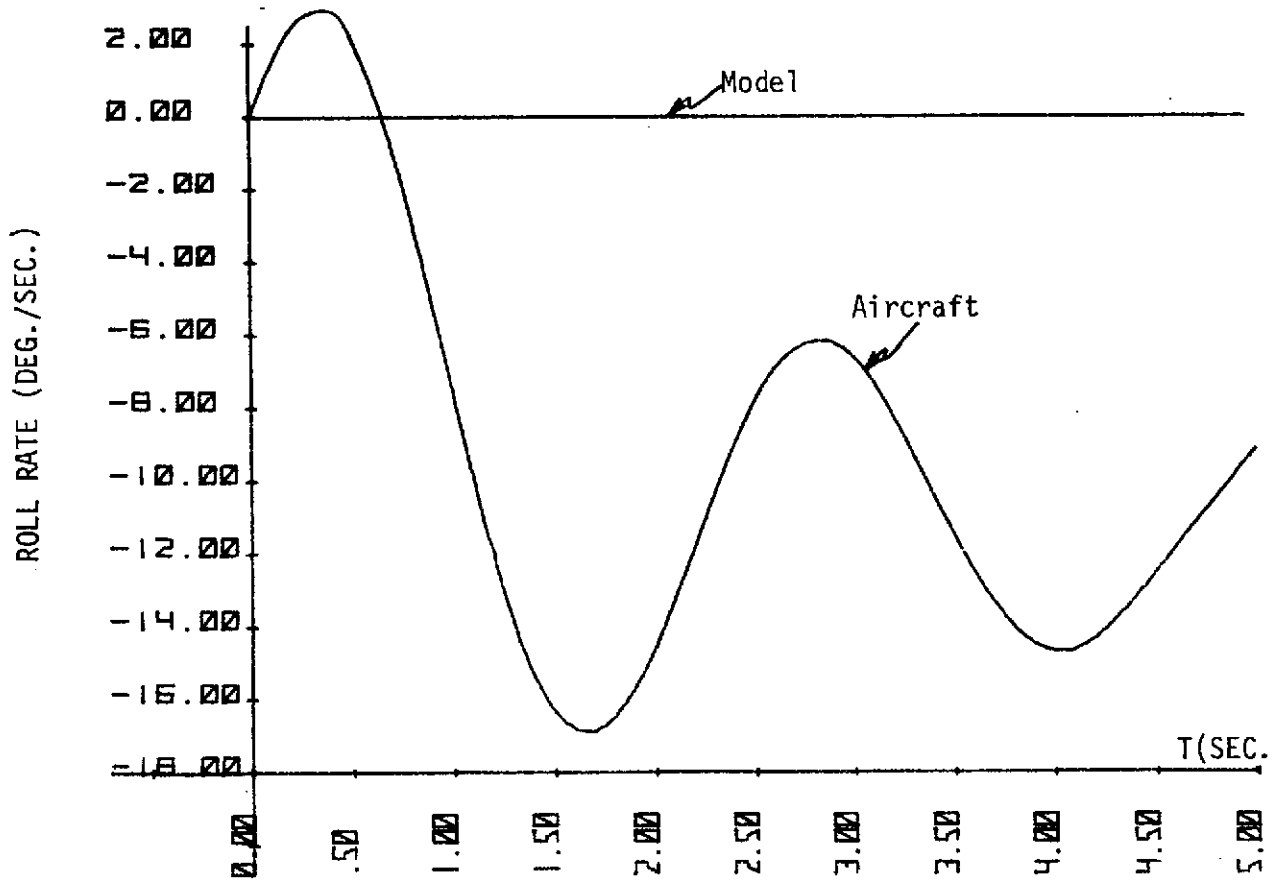

Flight Condition B ; $\delta_a^p = 0°$, $\delta_r^p = 3°$.

Figure A13.

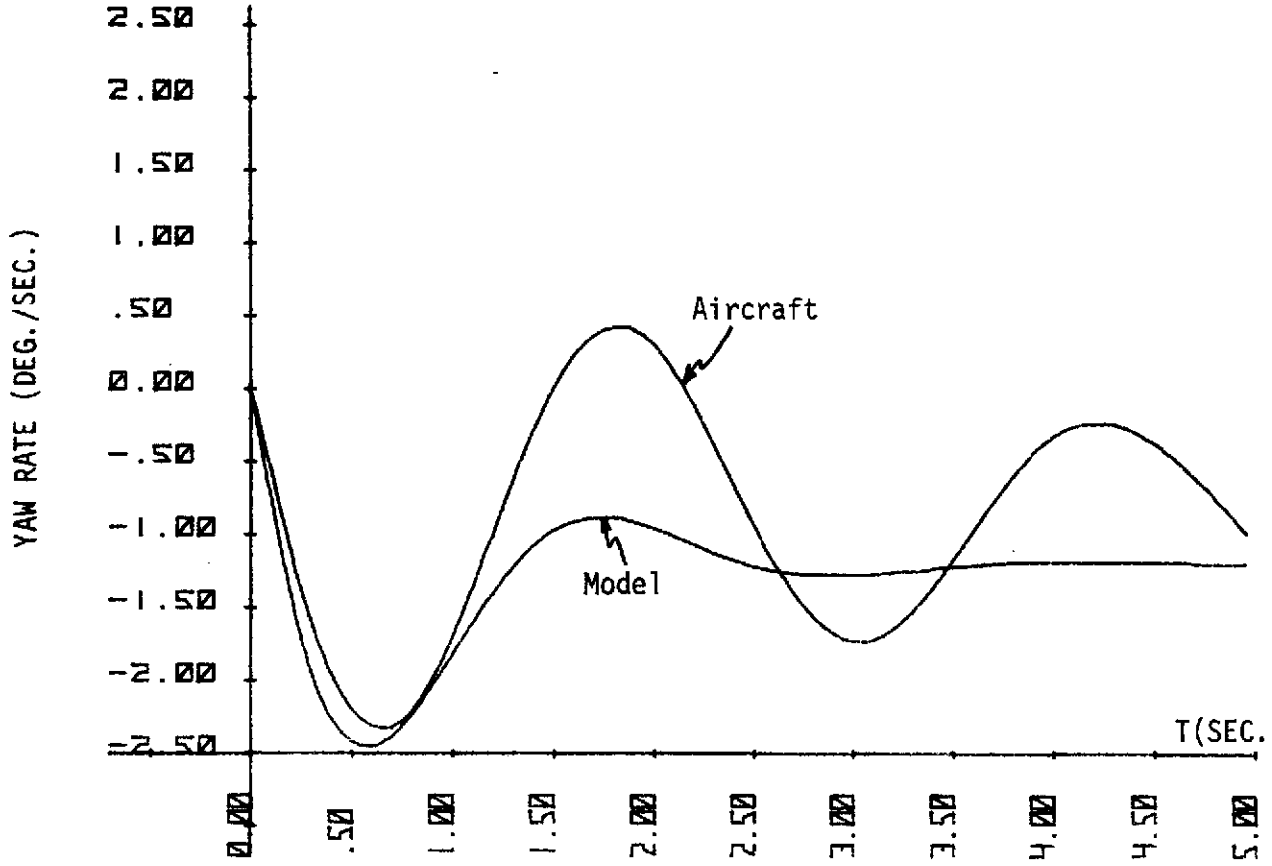

Flight Condition B ; $\delta_a^p = 0°$, $\delta_r^p = 3°$

Figure A14.

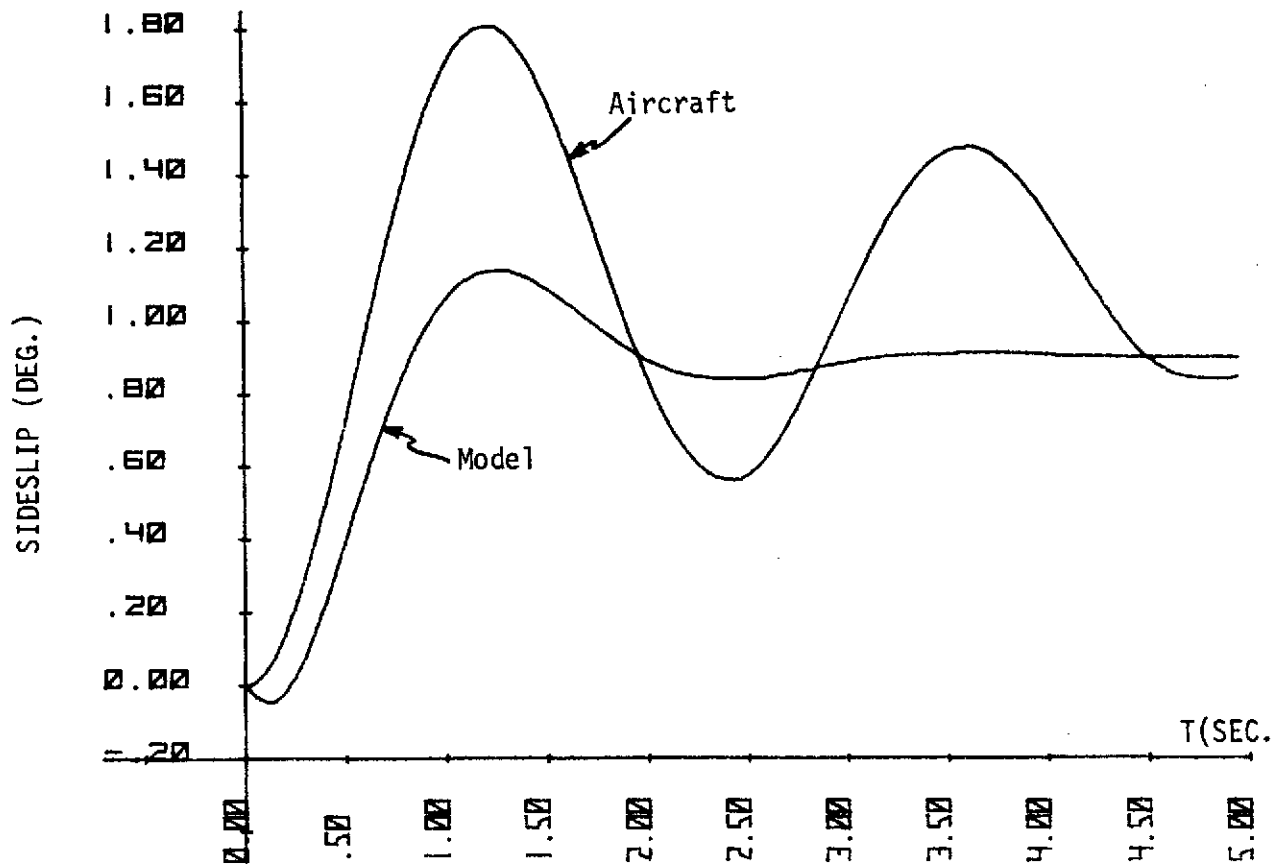

Flight Condition B ; $\delta_a^p = 0°$, $\delta_r^p = 3°$.

Figure A15.

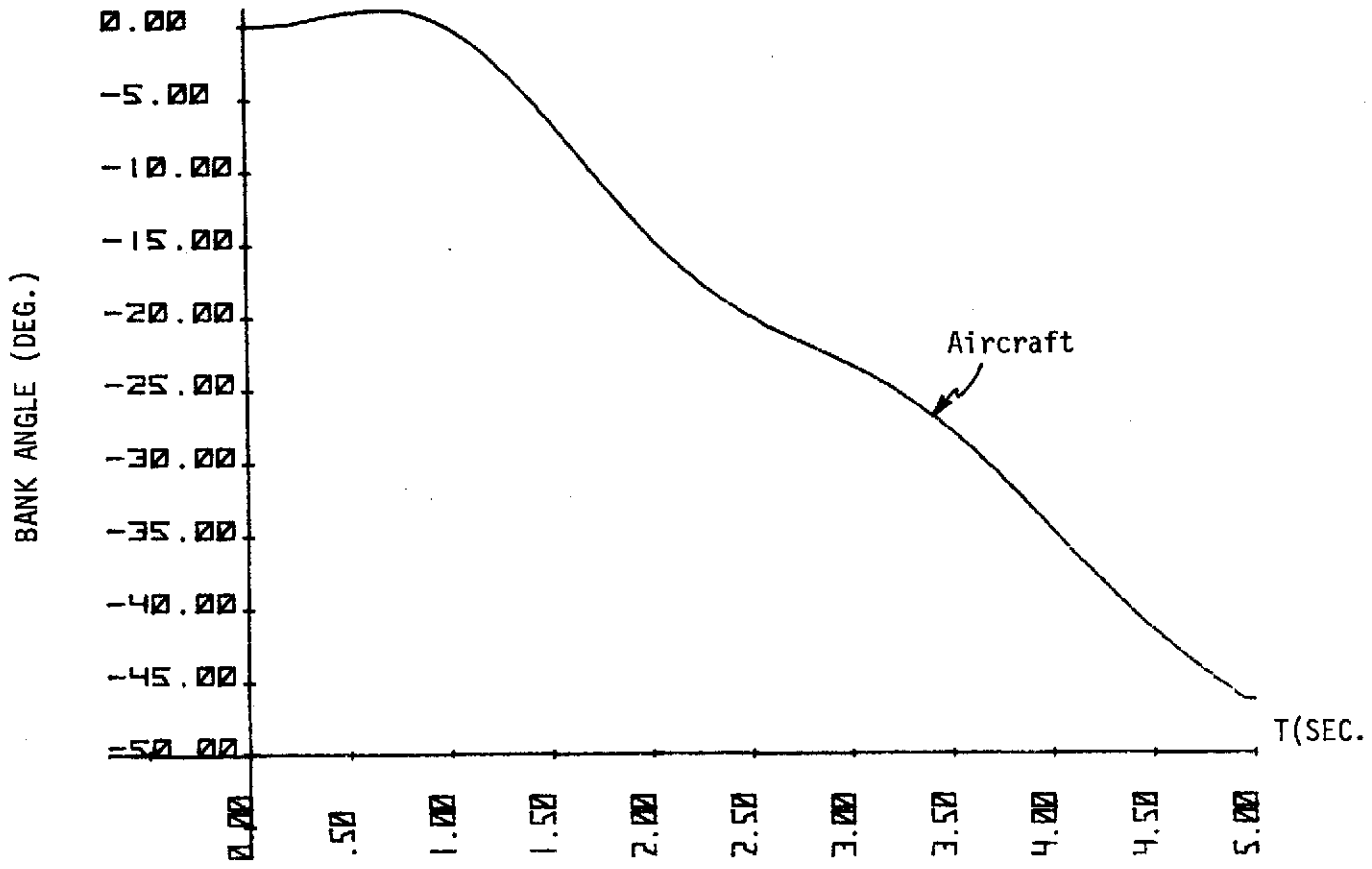

Flight Condition B ; $\delta_a^p = 0°$, $\delta_r^p = 3°$.

Figure A16.

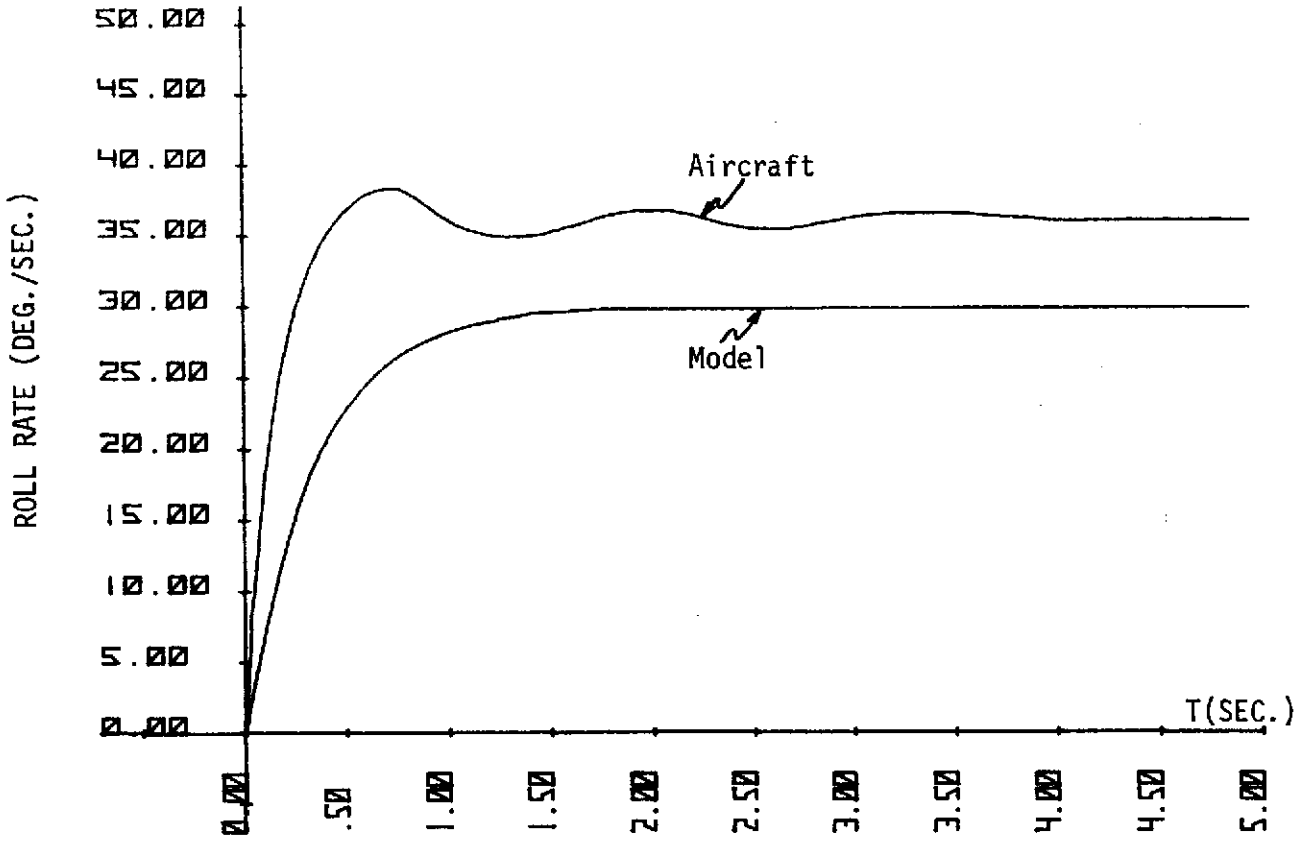

Flight Condition C ; $\delta_a^p = 5°$, $\delta_r^p = 0°$

Figure A17.

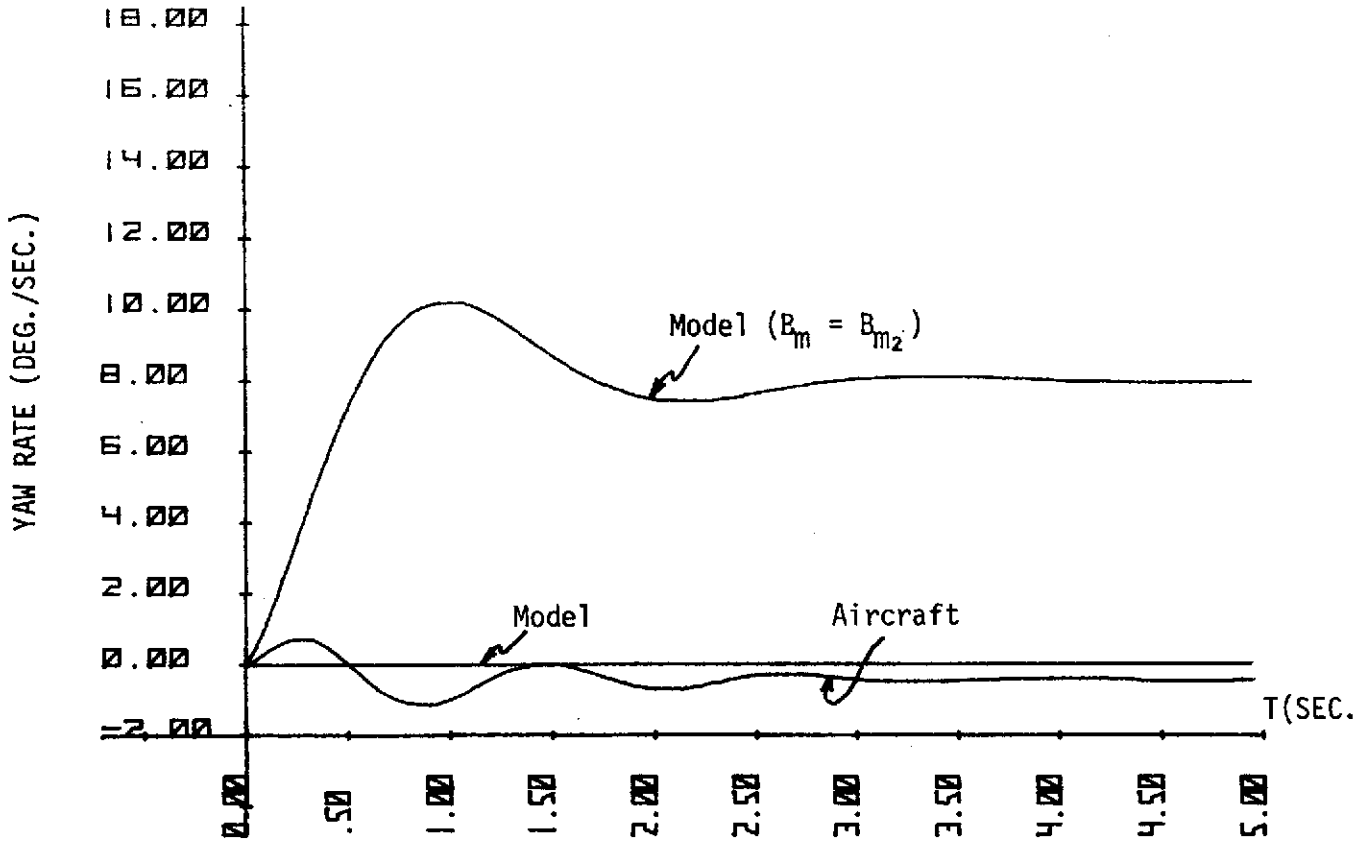

Flight Condition C ; $\delta_a^p = 5°$, $\delta_r^p = 0°$.

Figure A18.

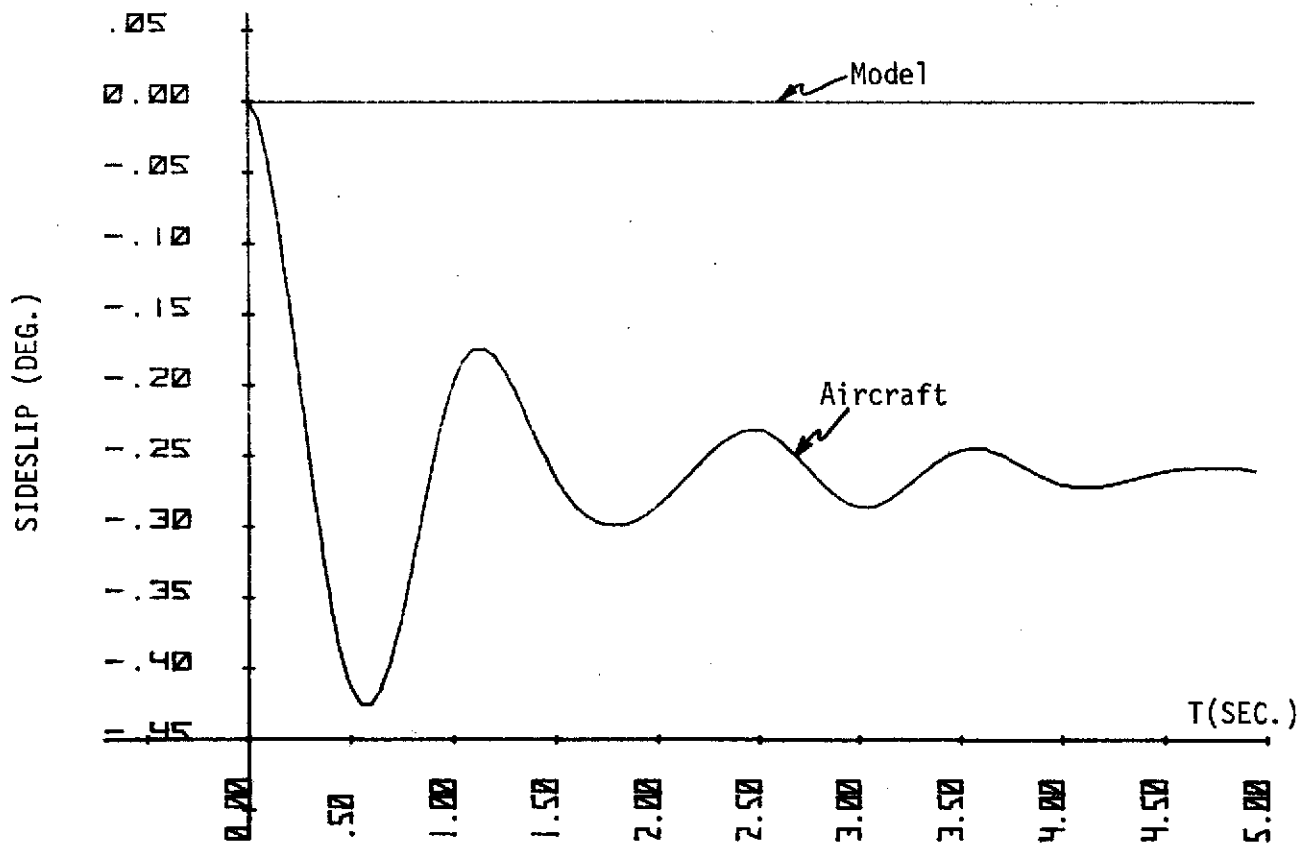

Flight Condition C ; $\delta_a^p = 5°$, $\delta_r^p = 0°$.

Figure A19.

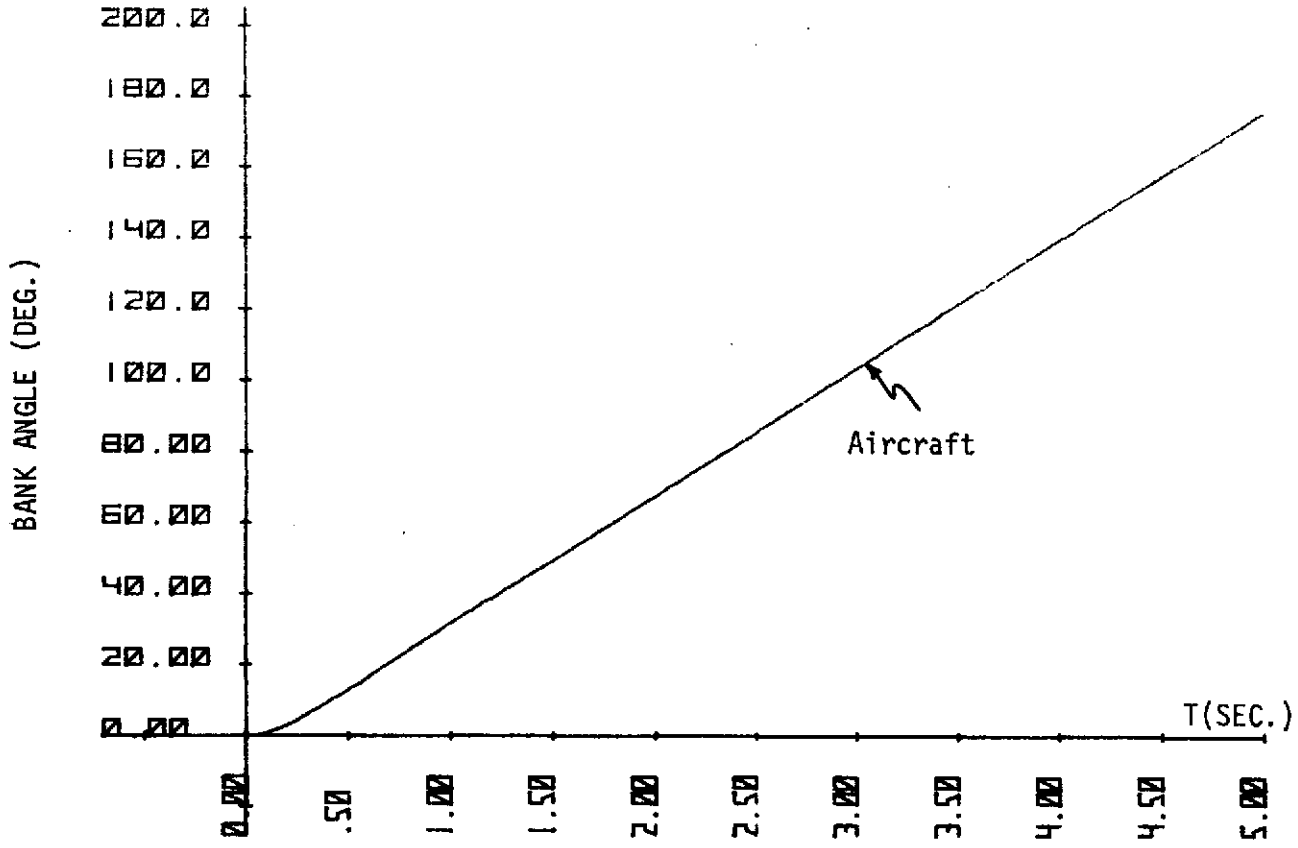

Flight Condition C ; $\delta_a^p = 5°$, $\delta_r^p = 0°$

Figure A20.

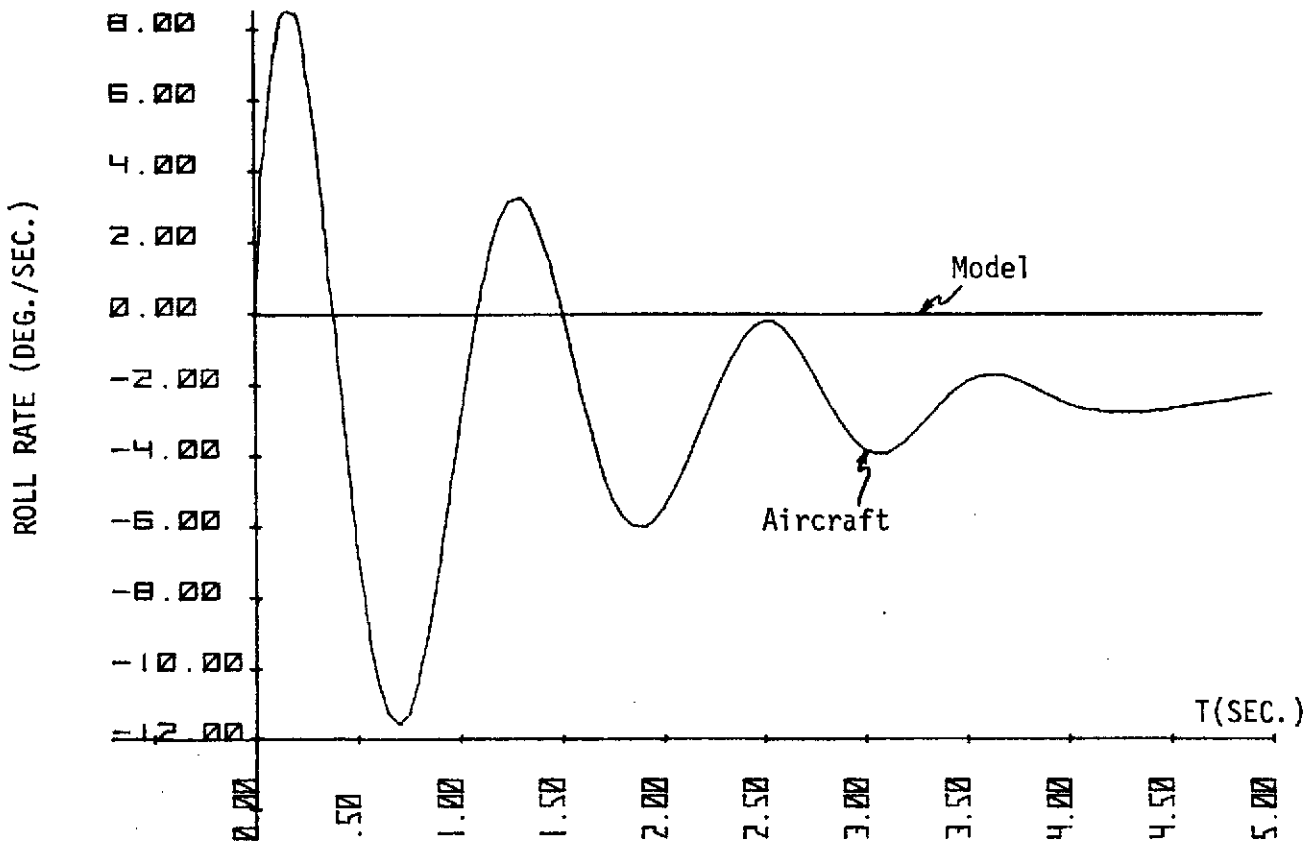

Flight Condition C ; $\delta_a^p = 0°$, $\delta_r^p = 3°$.

Figure A21.

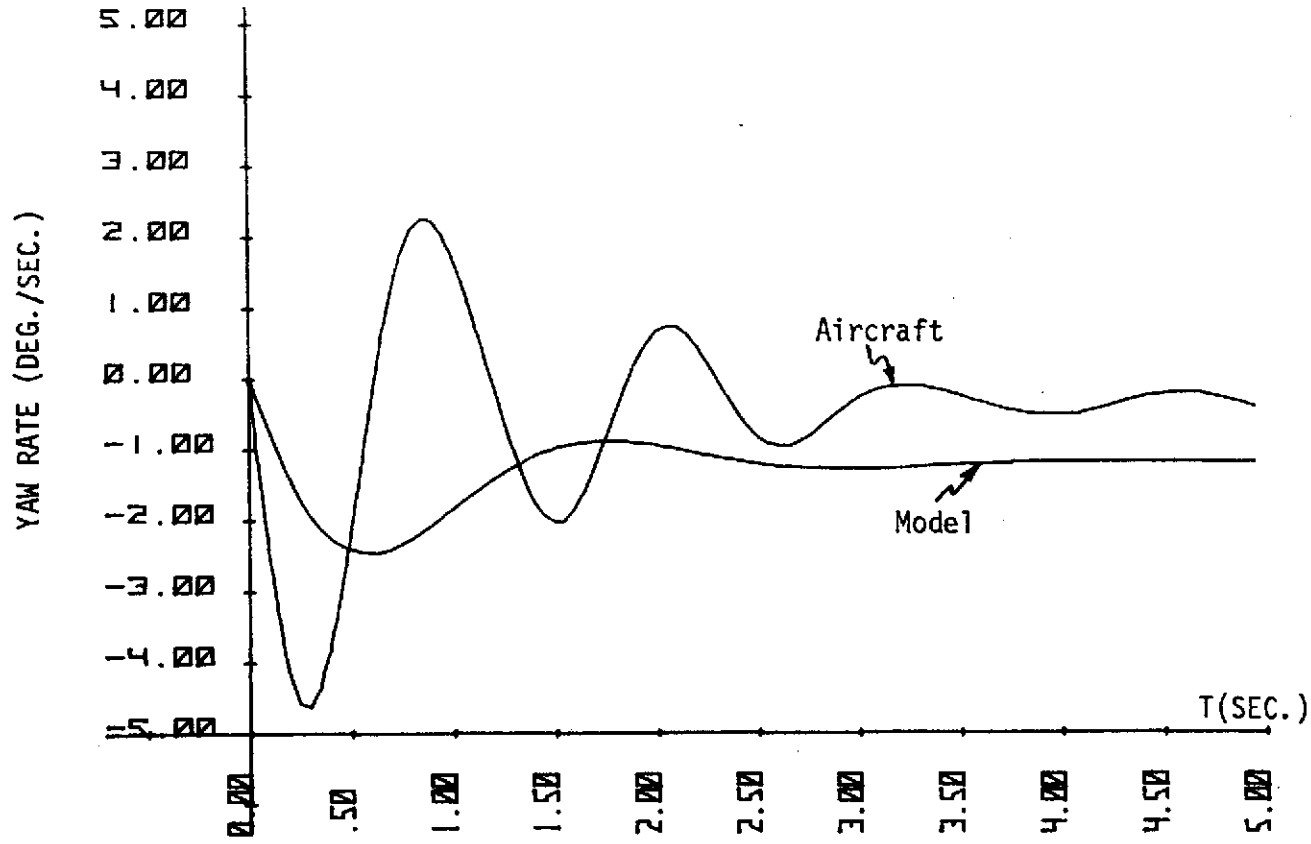

Flight Condition C ; $\delta_a^p = 0°$, $\delta_r^p = 3°$.

Figure A22.

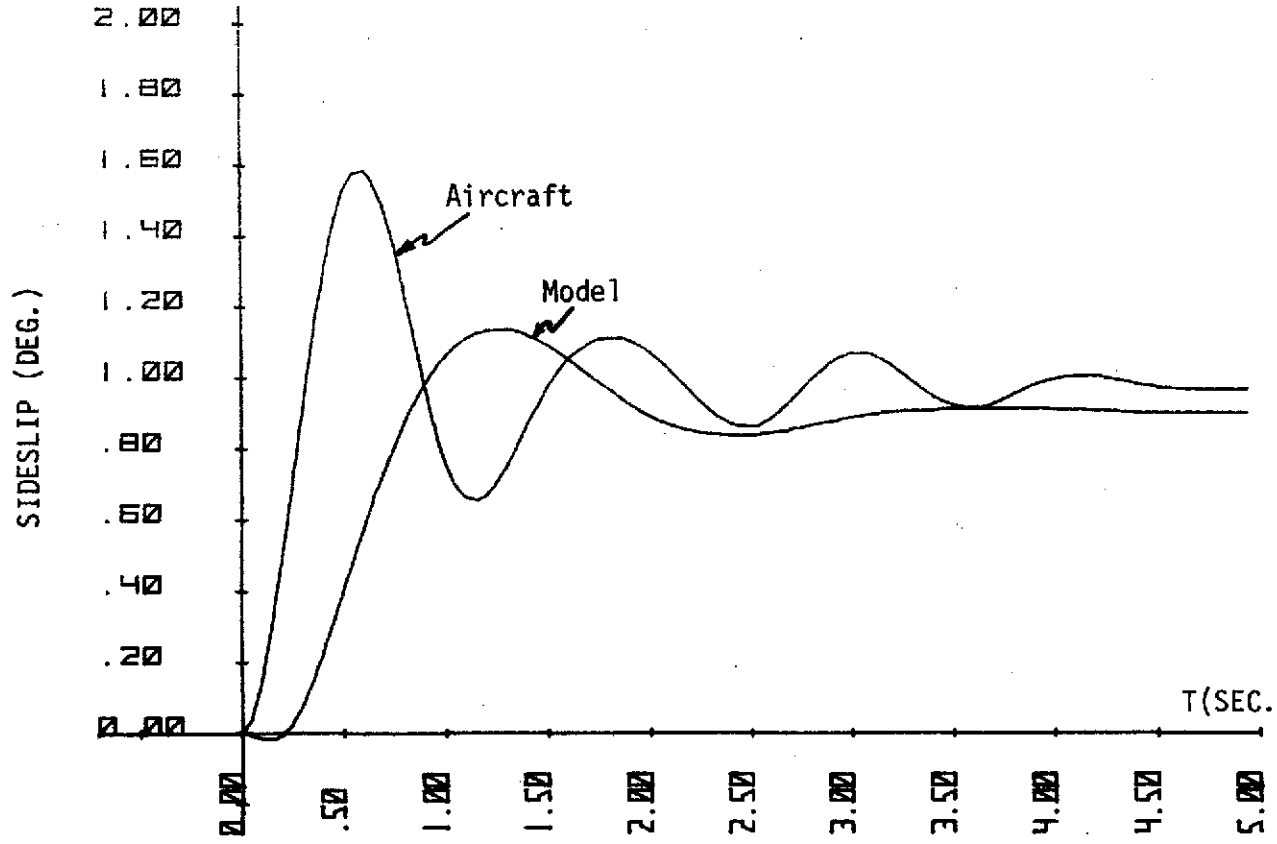

Flight Condition C ; $\delta_a^p = 0°$, $\delta_r^p = 3°$

Figure A23.

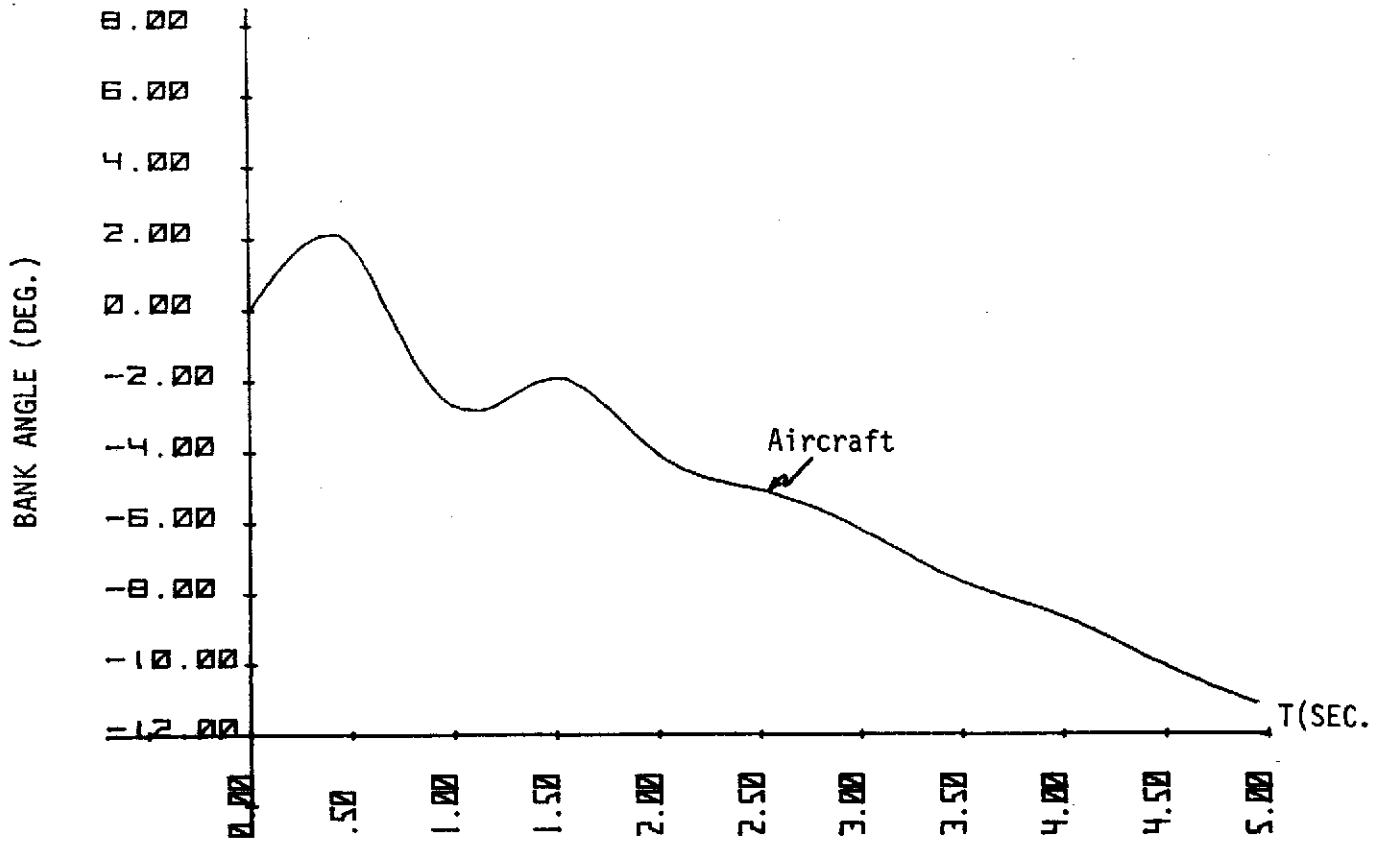

Flight Condition C ; $\delta_a^p = 0°$, $\delta_r^p = 3°$.

Figure A24.

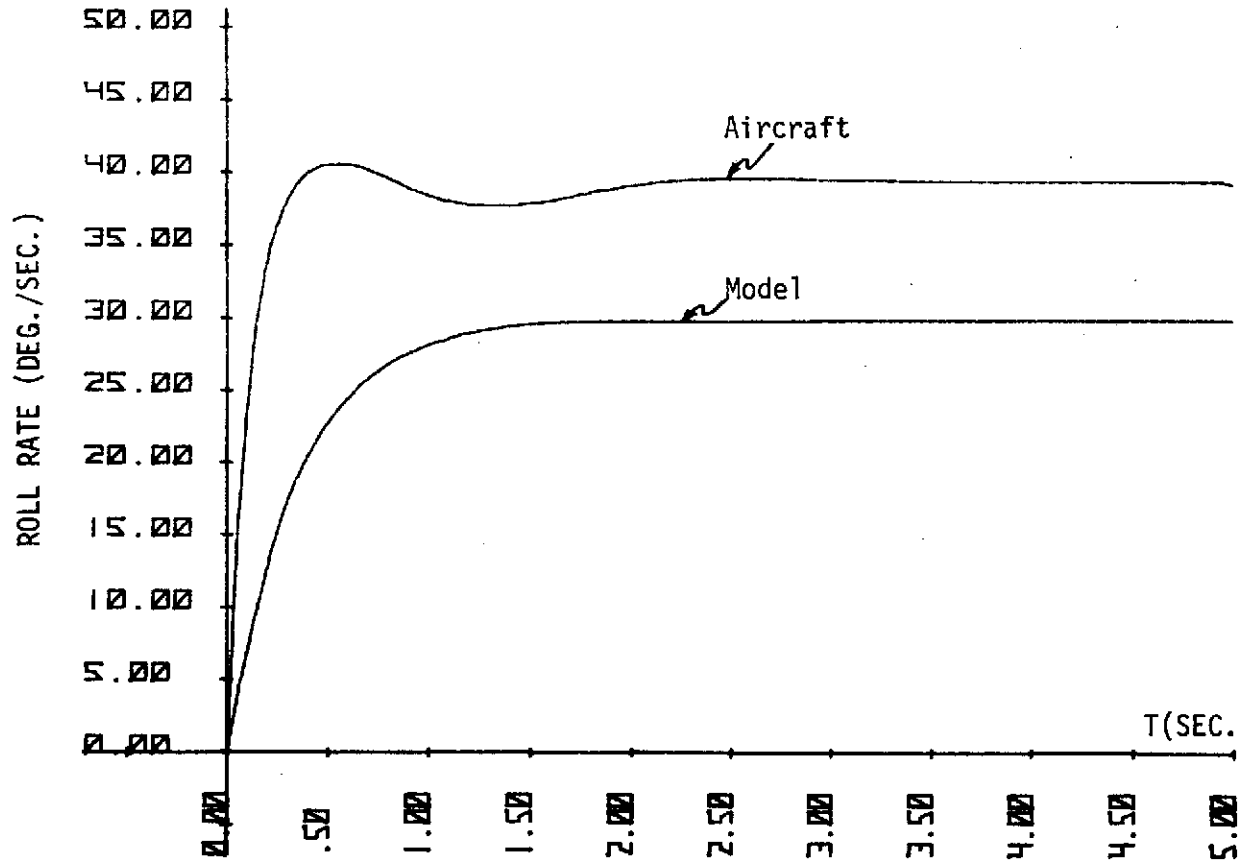

Flight Condition D ; $\delta_a^p = 5°$, $\delta_r^p = 0°$.

Figure A25.

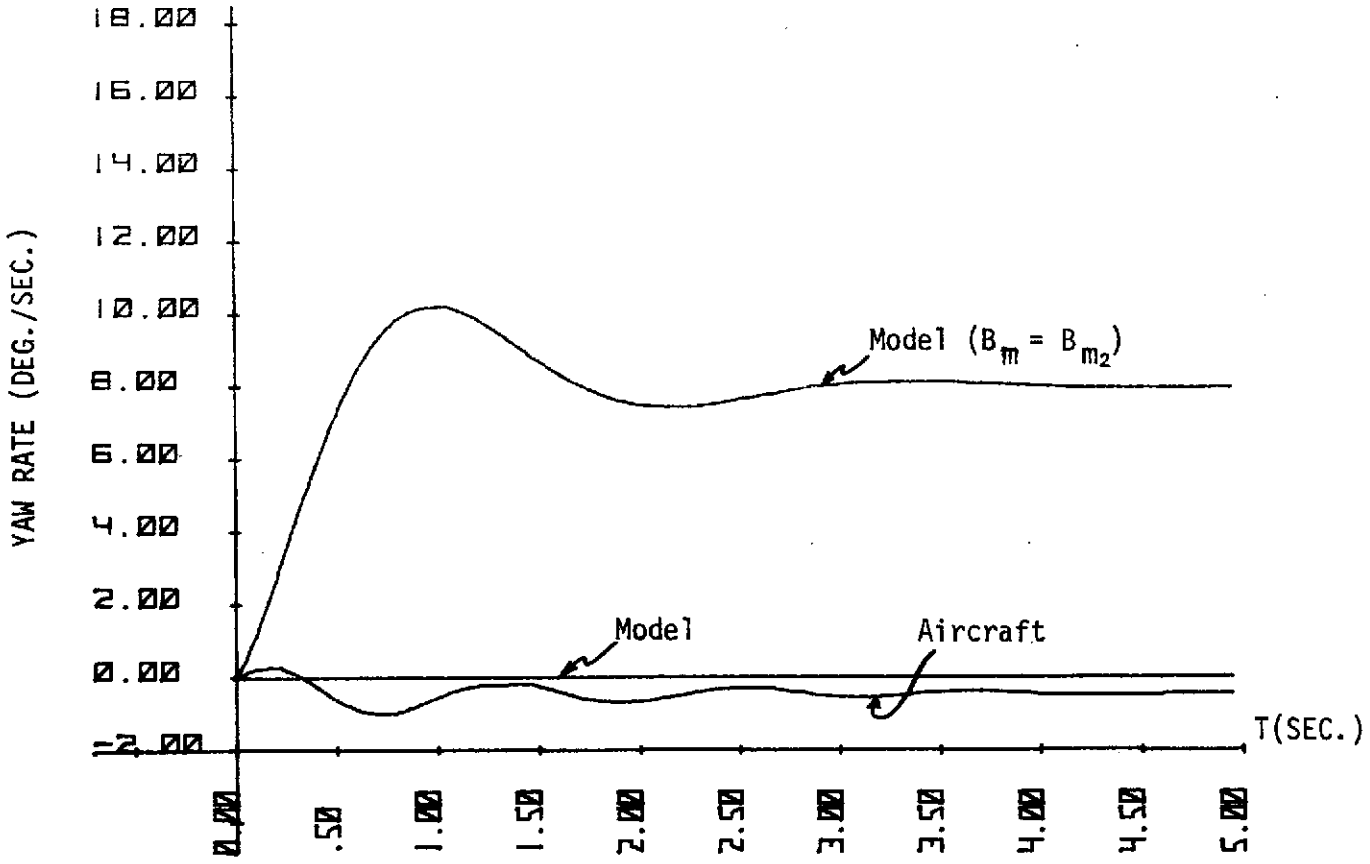

Flight Condition D ; $\delta_a^p = 5°$, $\delta_r^p = 0°$.

Figure A26.

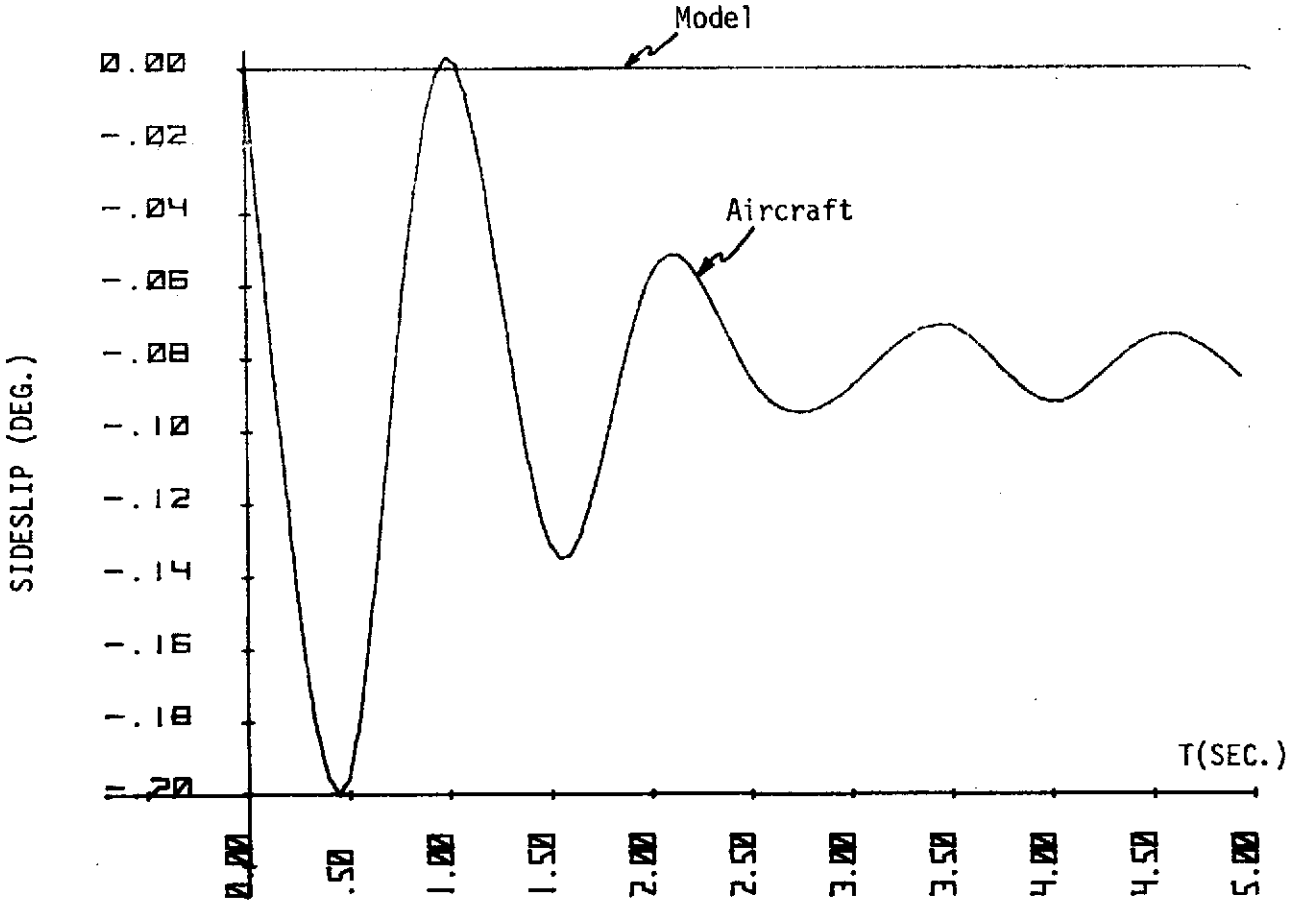

Flight Condition D ; $\delta_a^p = 5°$, $\delta_r^p = 0°$.

Figure A27.

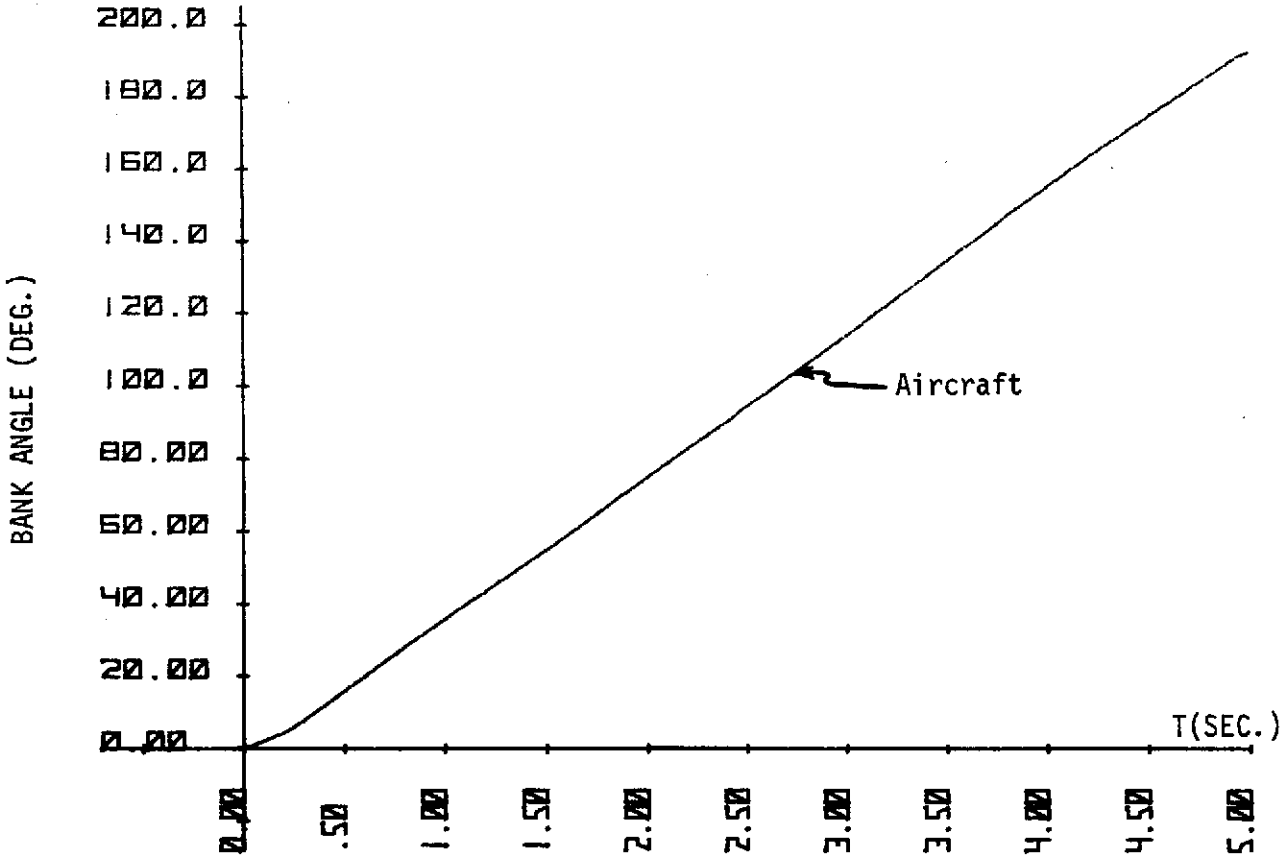

Flight Condition D ; $\delta_a^p = 5°$, $\delta_r^p = 0°$.

Figure A28.

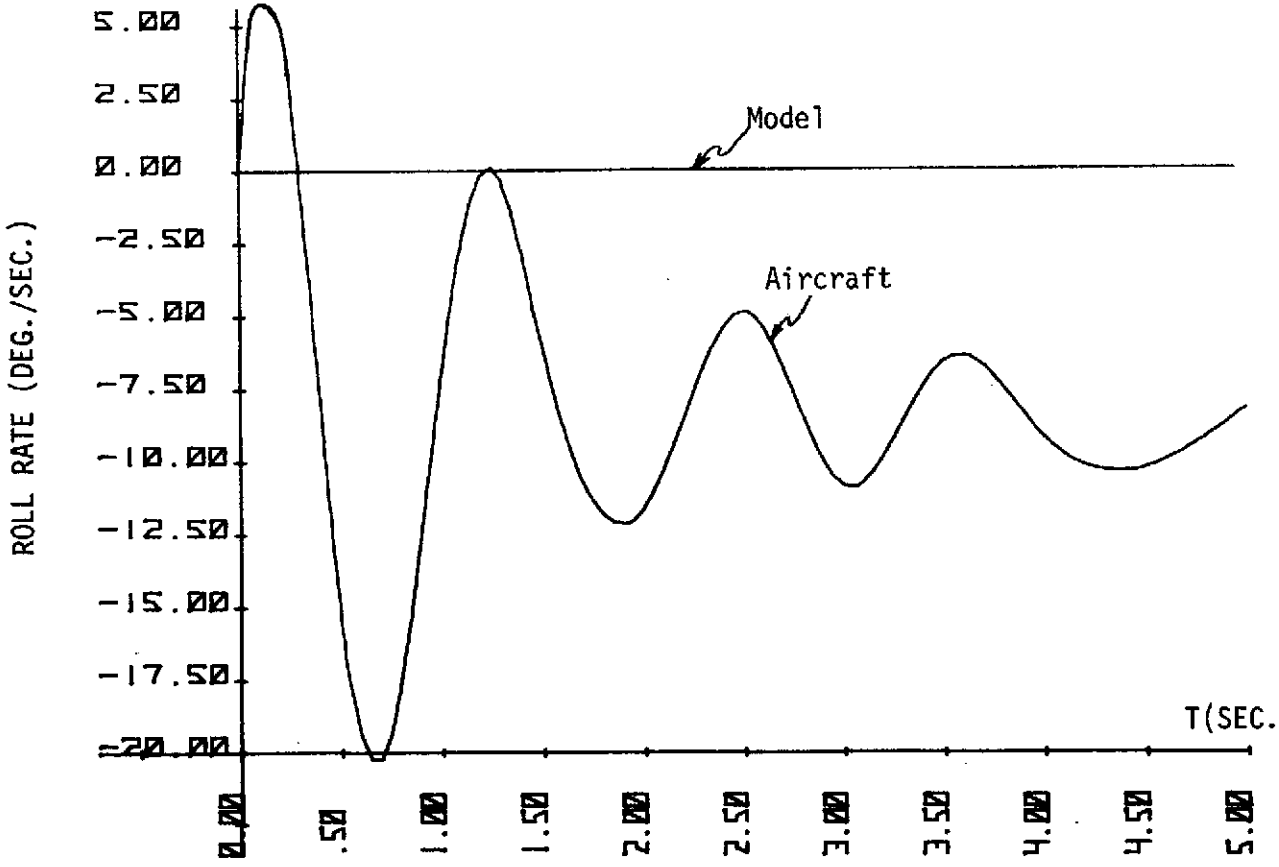

Flight Condition D ; $\delta_a^p = 0°$, $\delta_r^p = 3°$

Figure A29.

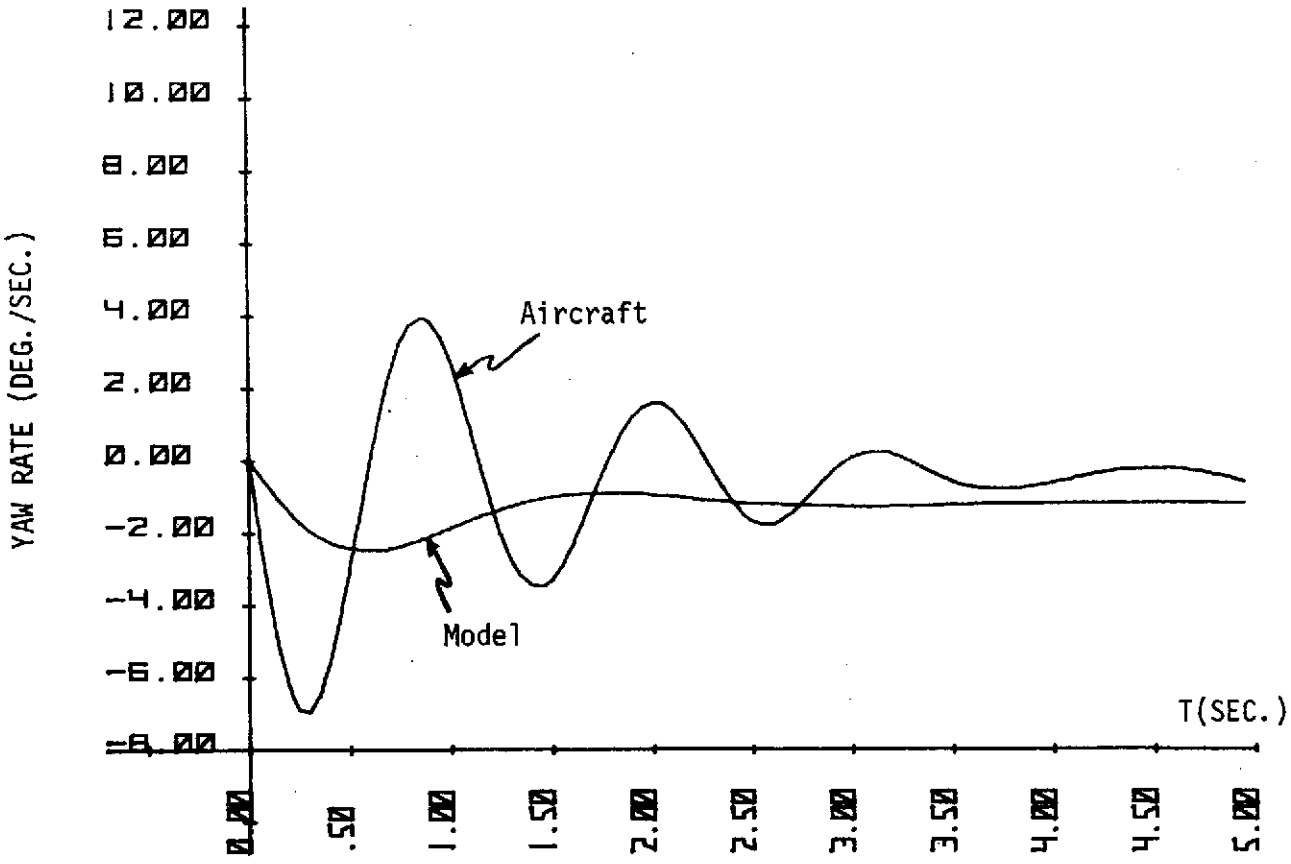

Flight Condition D ; $\delta_a^p = 0°$, $\delta_r^p = 3°$.

Figure A30.

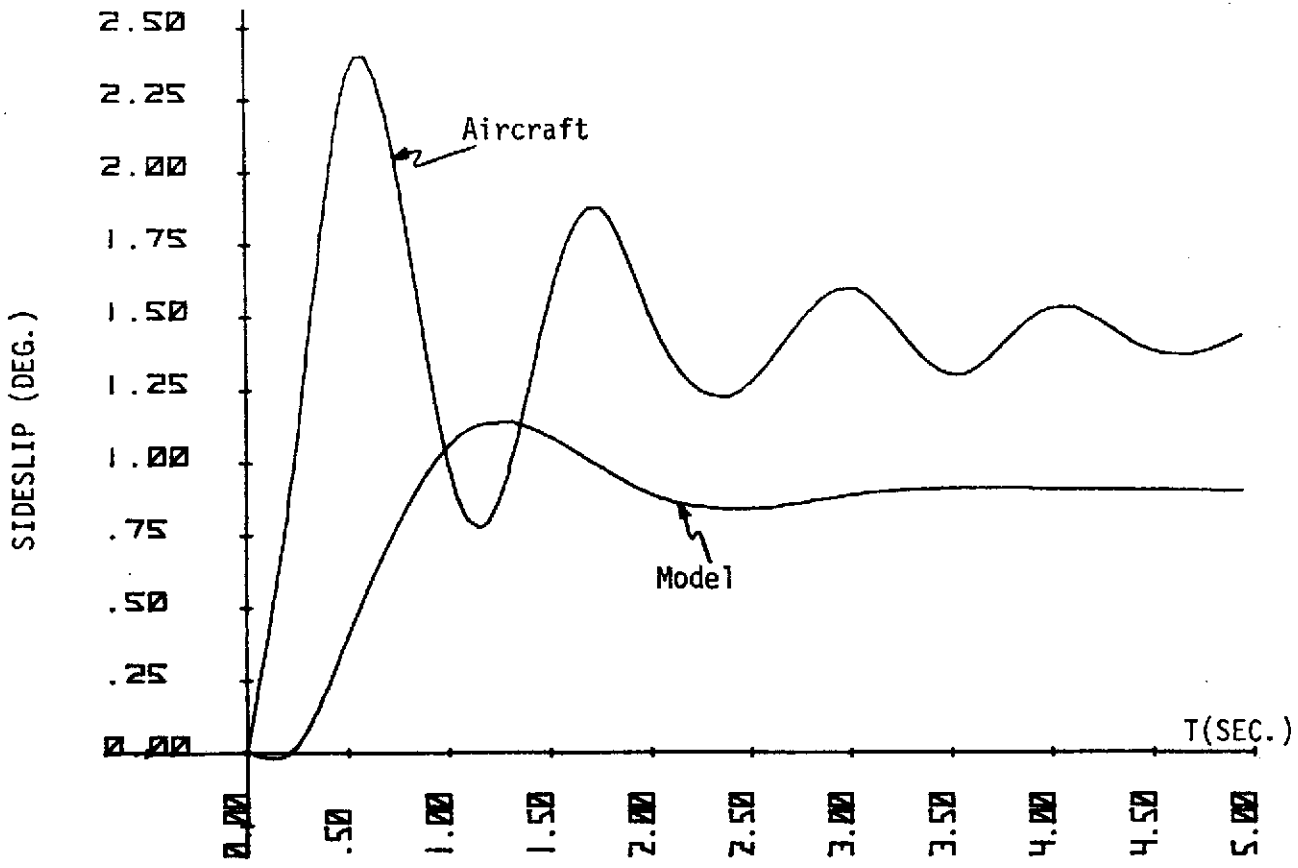

Flight Condition D ; $\delta_a^p = 0°$, $\delta_r^p = 3°$.

Figure A31.

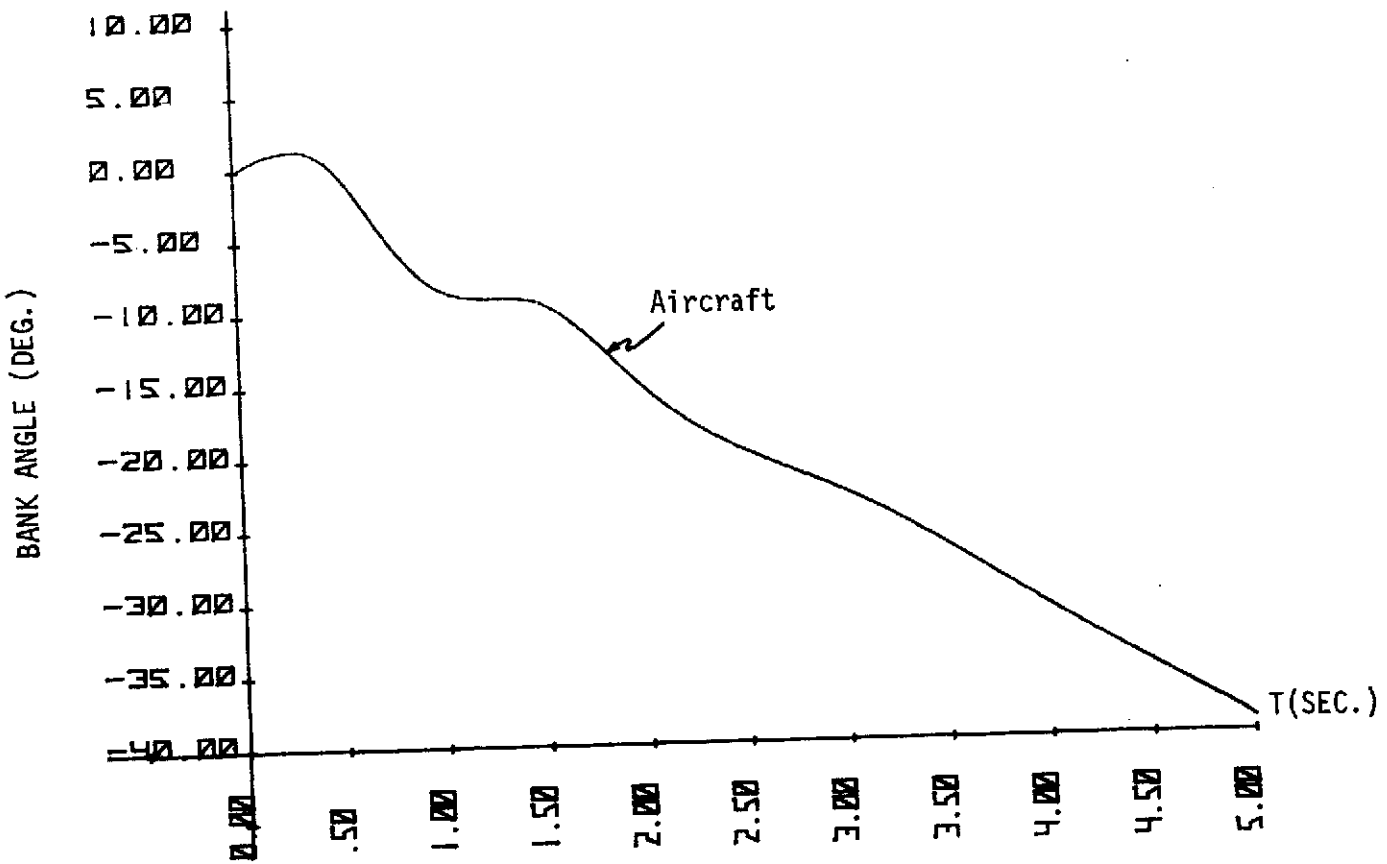

Flight Condition D ; $\delta_a^p = 0°$, $\delta_r^p = 3°$.

Figure A32.

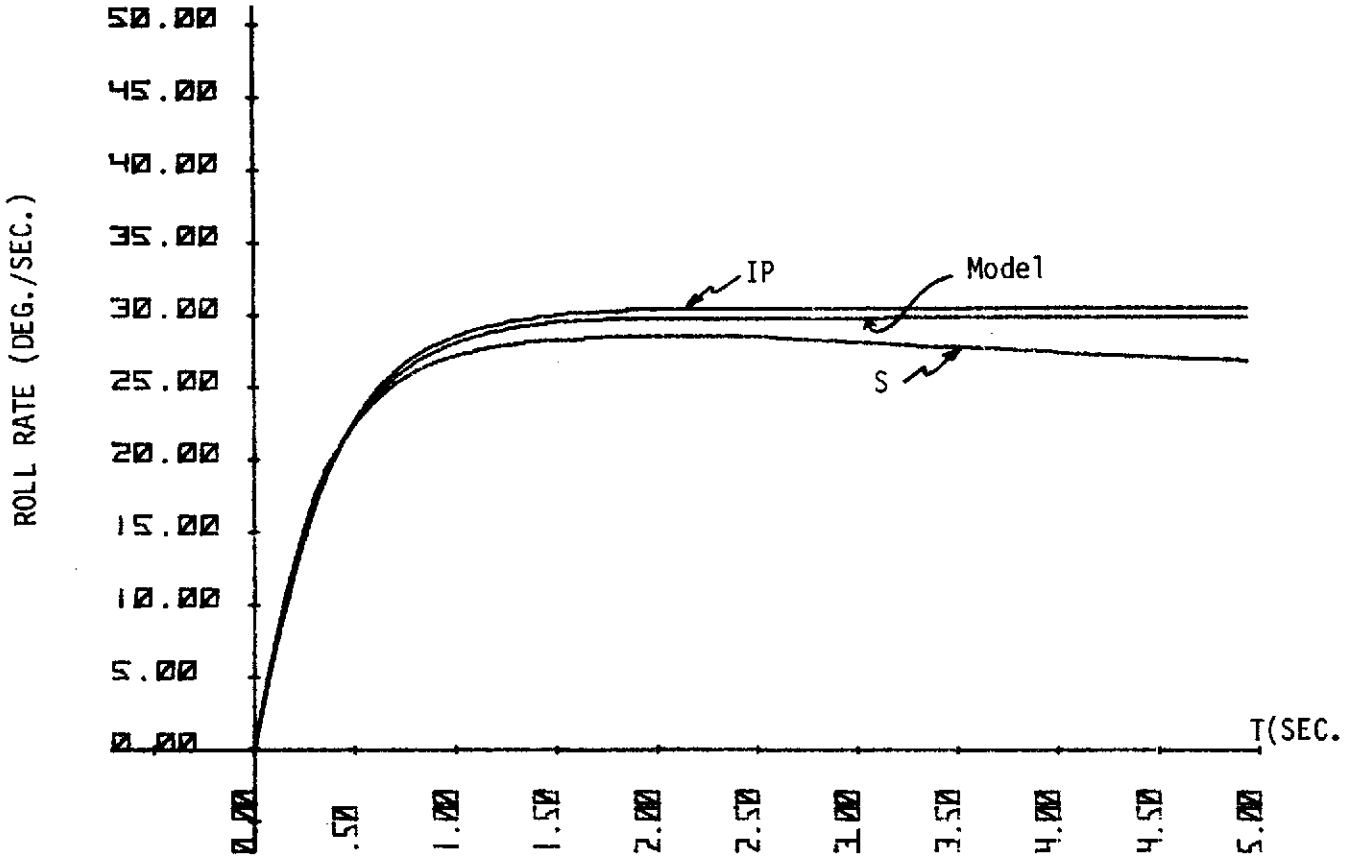

Flight Condition A ; $\delta_a^p = 5^o$, $\delta_r^p = 0^o$; $\delta^a(0) = 0^o$.

Figure A33.

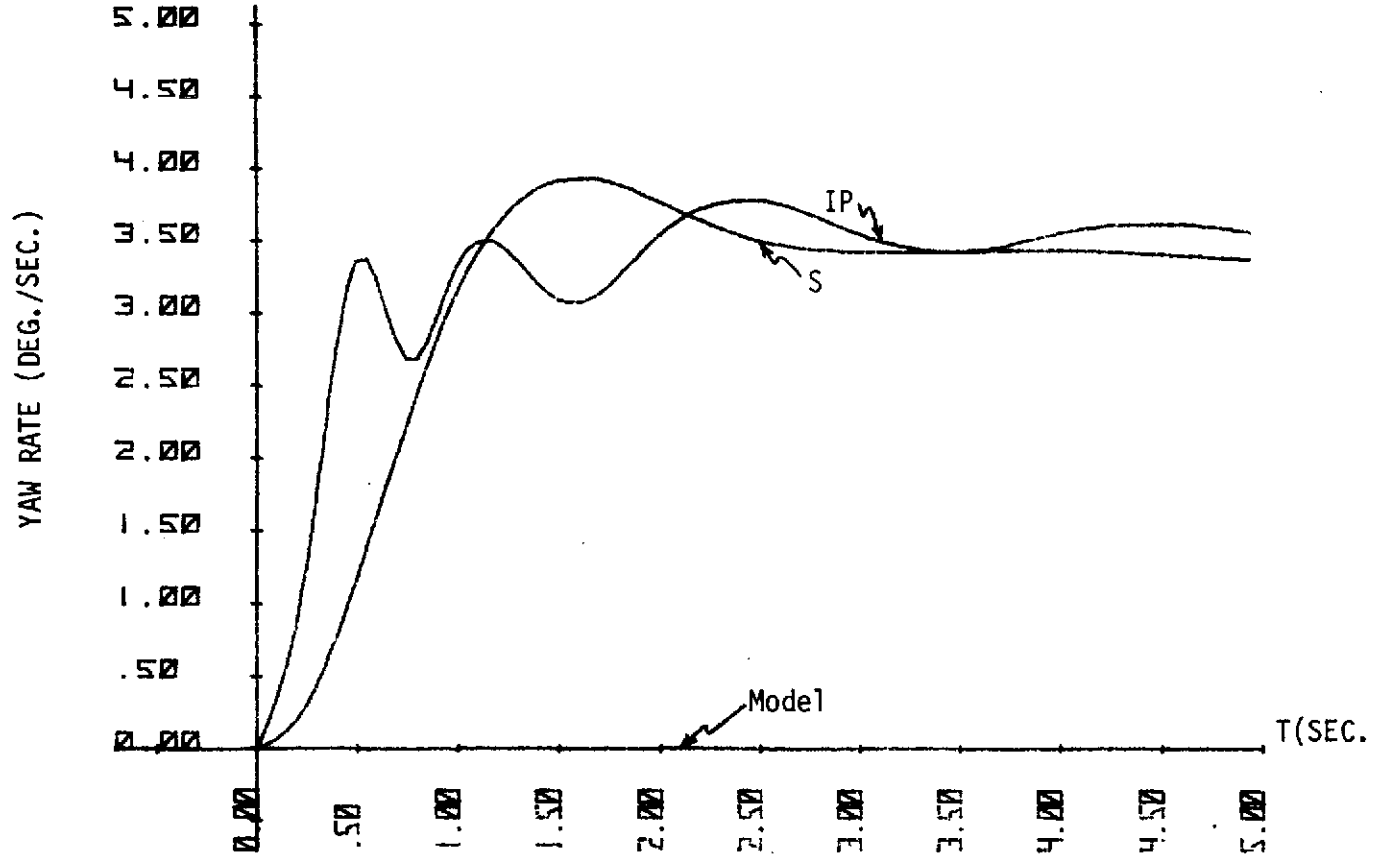

Flight Condition A; $\delta_a^p = 5^o$, $\delta_r^p = 0^o$; $\delta^a(0) = 0^o$.

Figure A34.

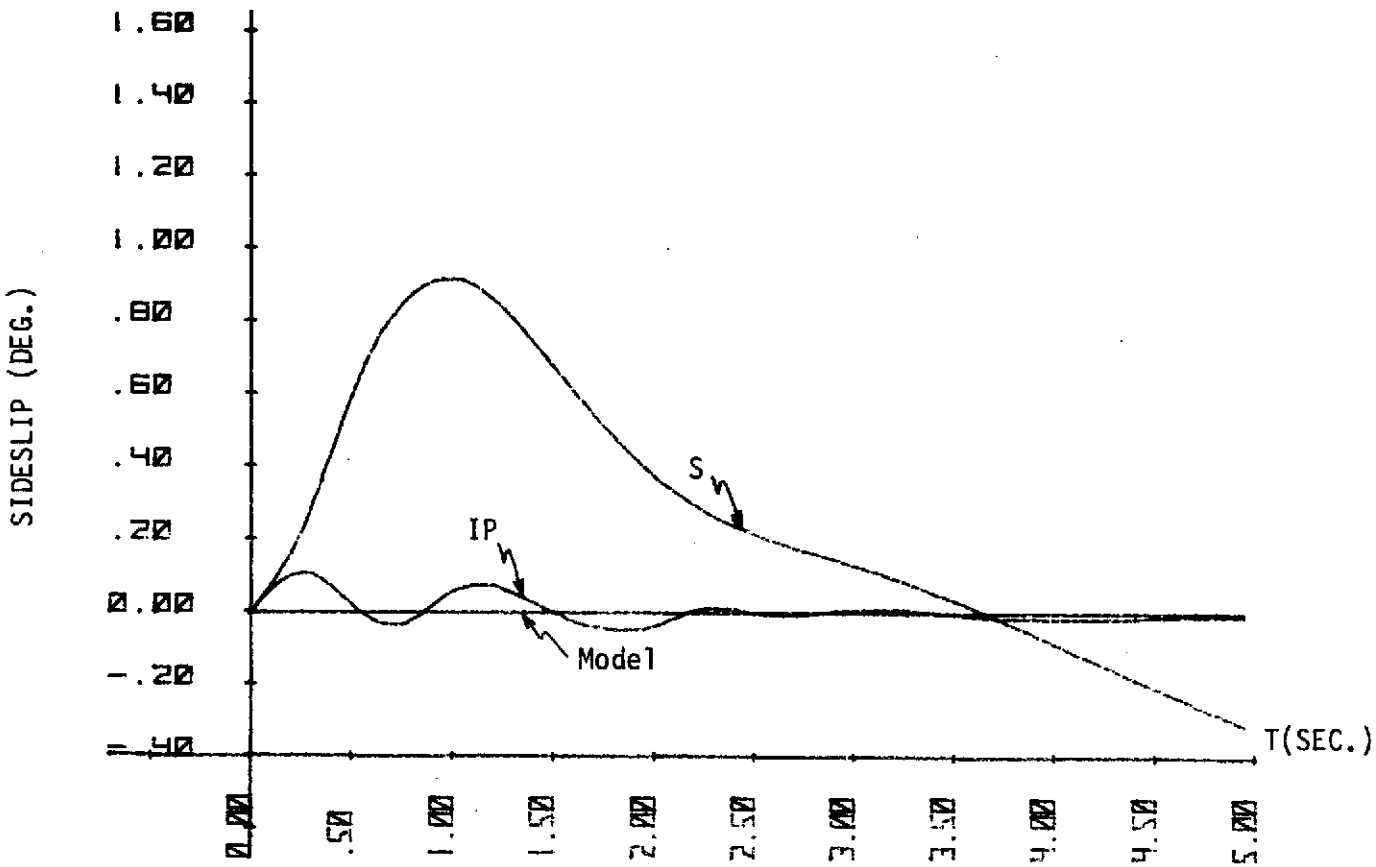

Flight Condition A ; $\delta_a^p = 5^o$, $\delta_r^p = 0^o$; $\delta^a(0) = 0^o$.

Figure A35.

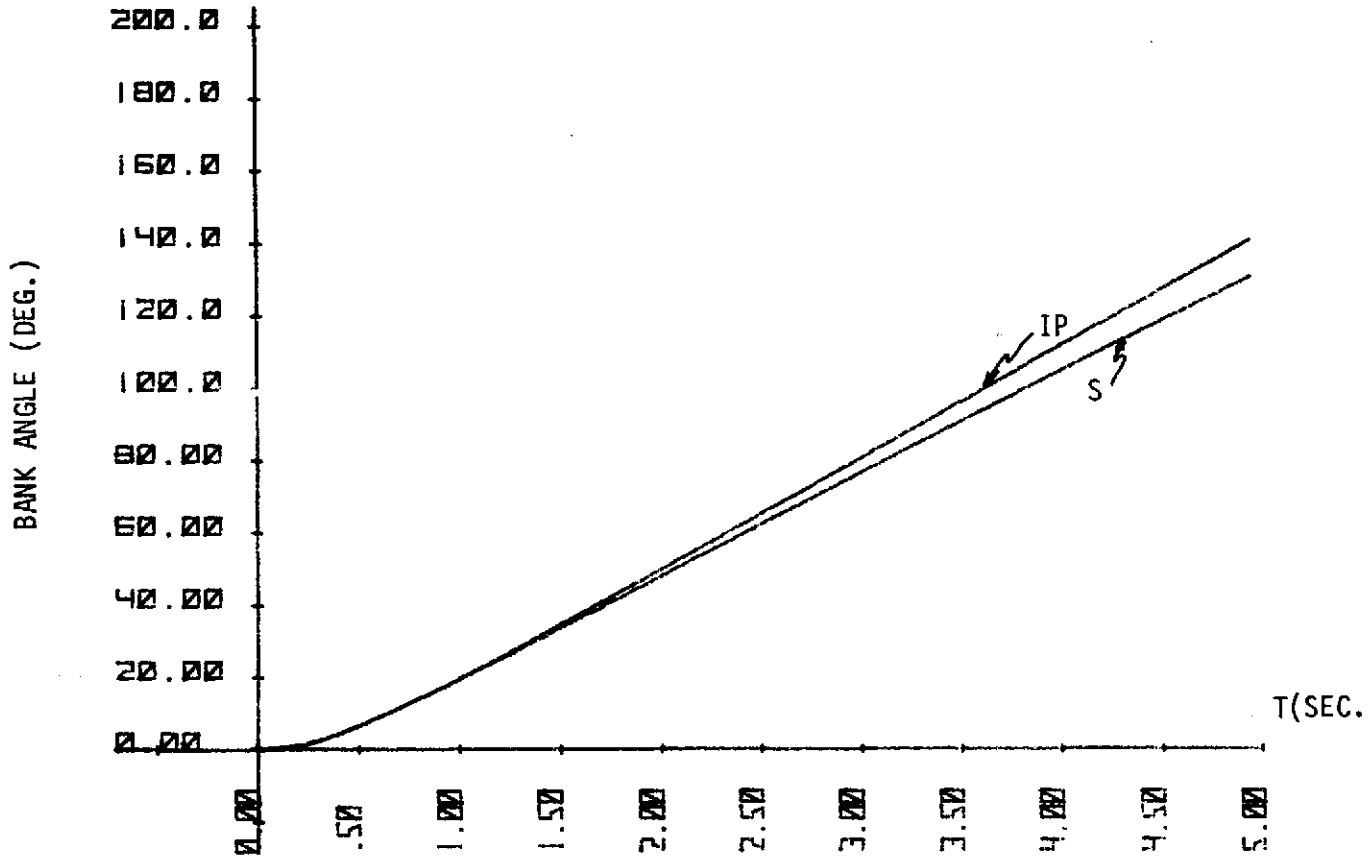

Flight Condition A; $\delta_a^p = 5^o$, $\delta_r^p = 0^o$; $\delta^a(0) = 0^o$.

Figure A36.

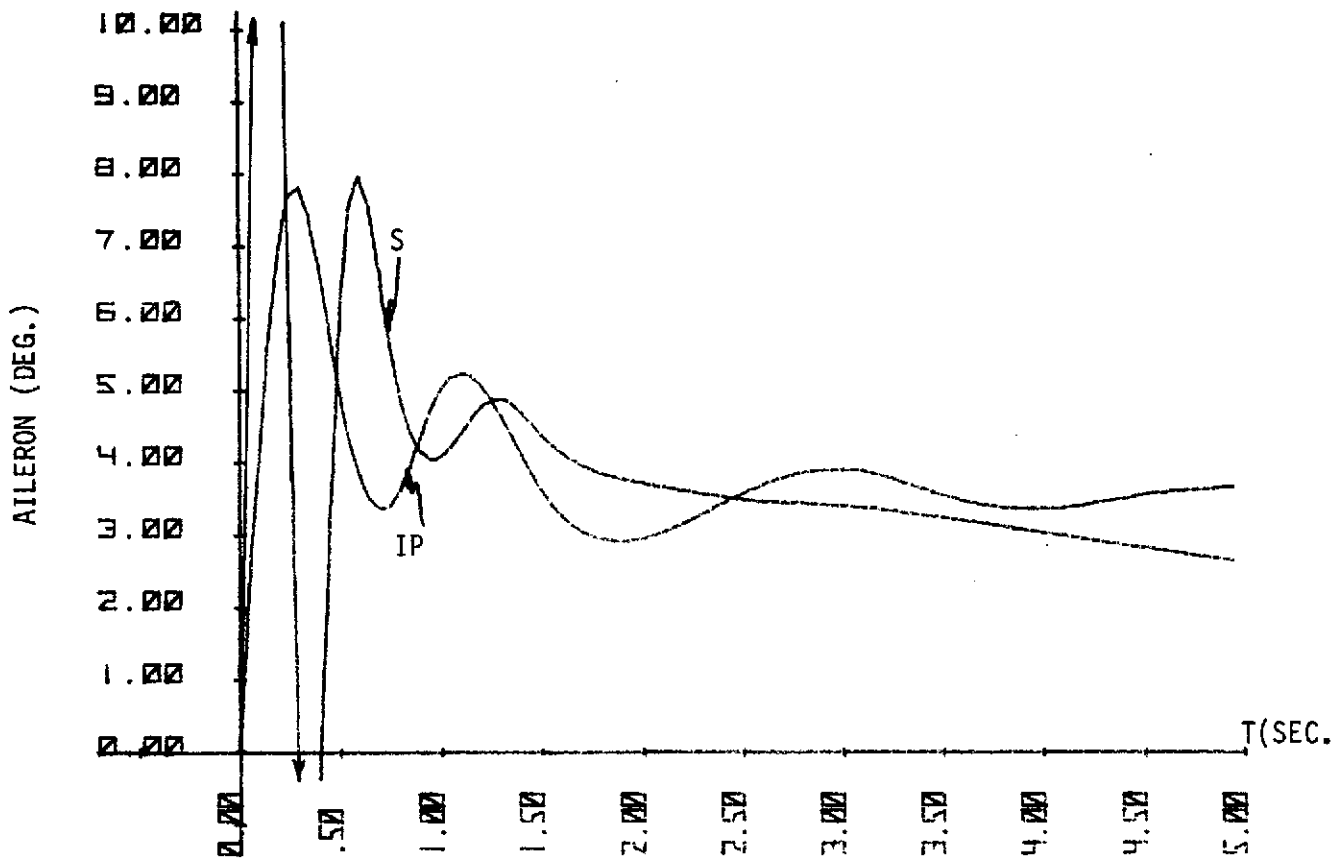

Flight Condition A; $\delta_a^p = 5^o, .\delta_r^p = 0^o$; $\delta^a(0) = 0^o$.

Figure A37.

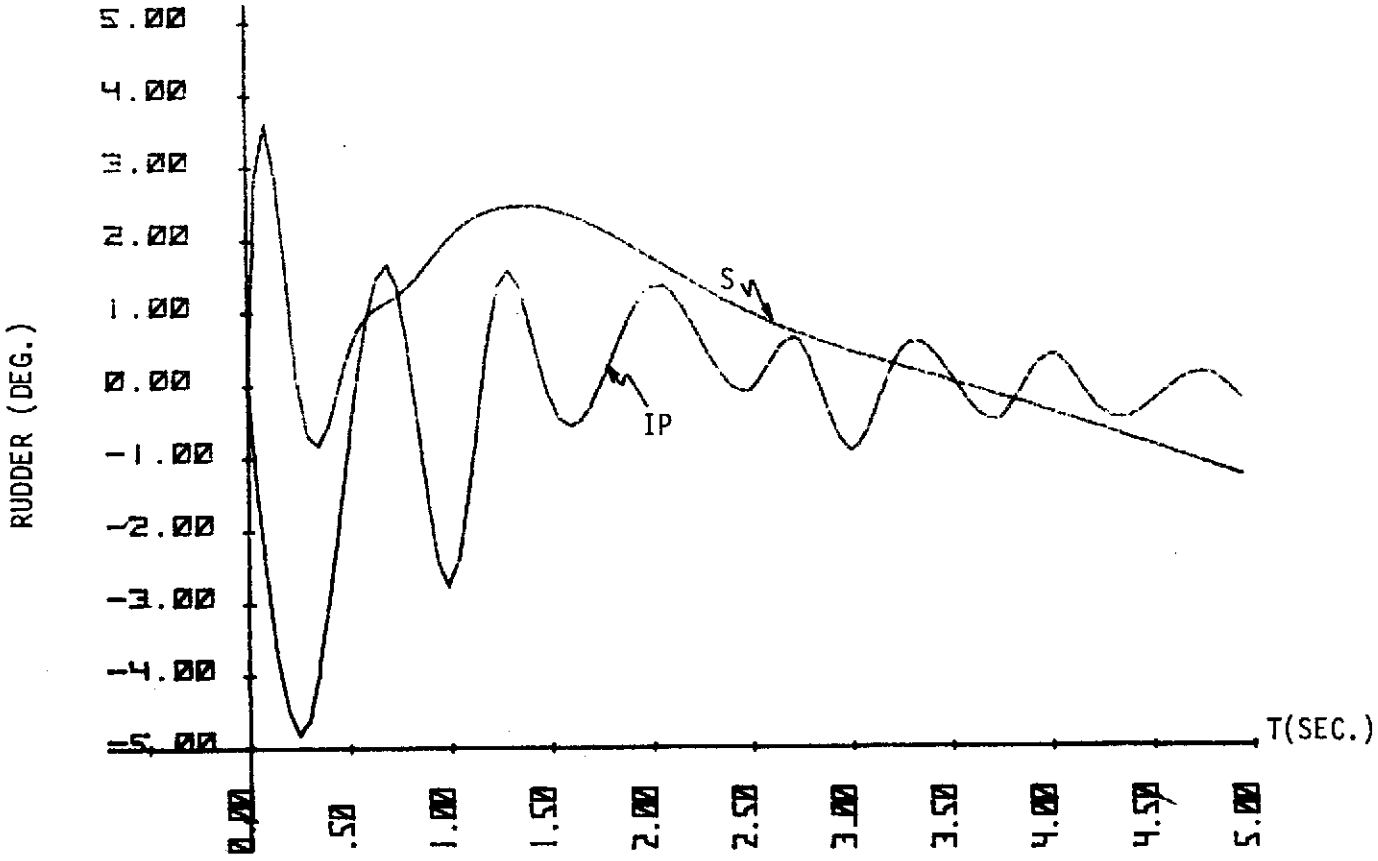

Flight Condition A ; $\delta_a^p = 5^o$, $\delta_r^p = 0^o$; $\delta^a(0) = 0^o$.

Figure A38.

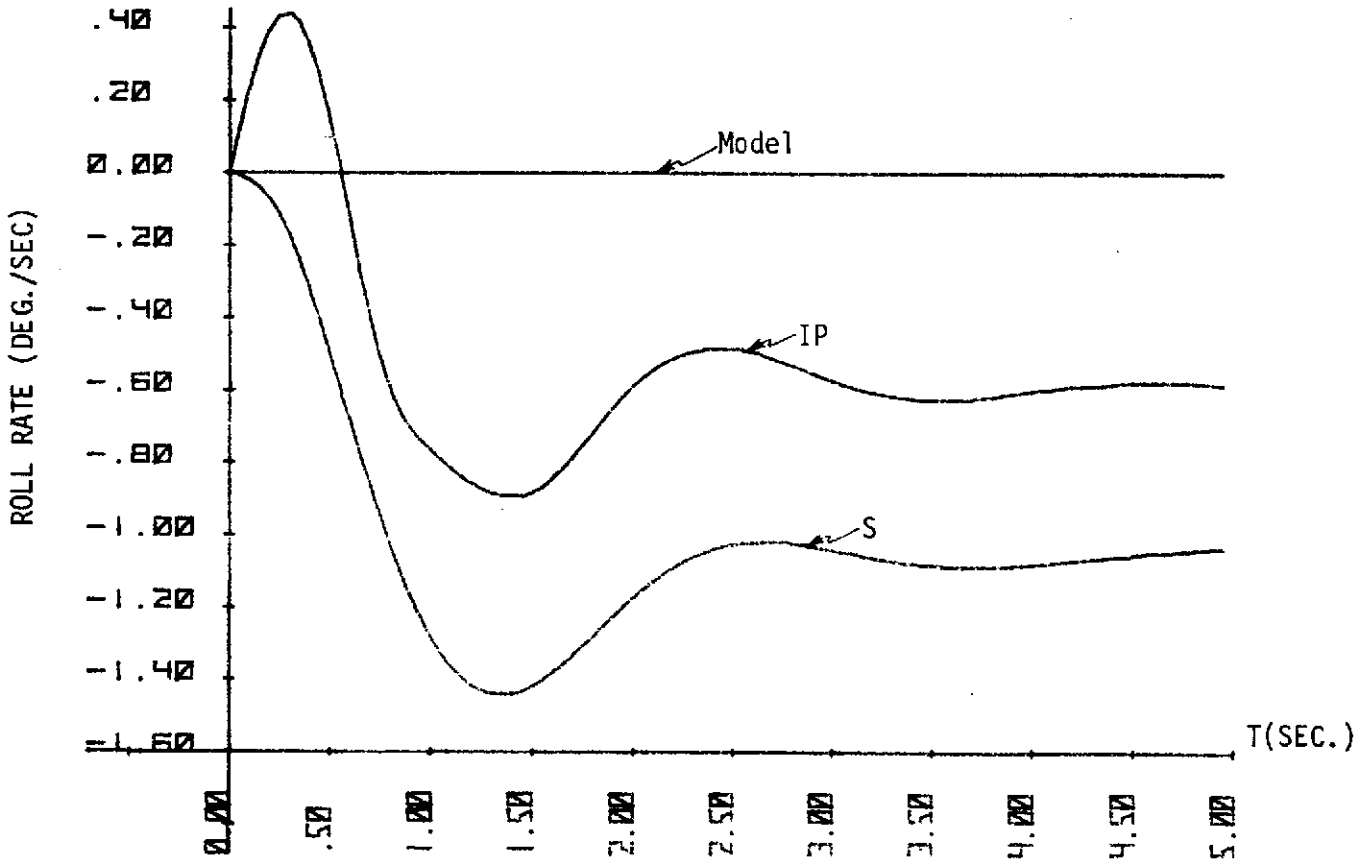

Flight Condition A; $\delta_a^p = 0^o$, $\delta_r^p = 3^o$; $\delta^a(0) = 0^o$.

Figure A39.

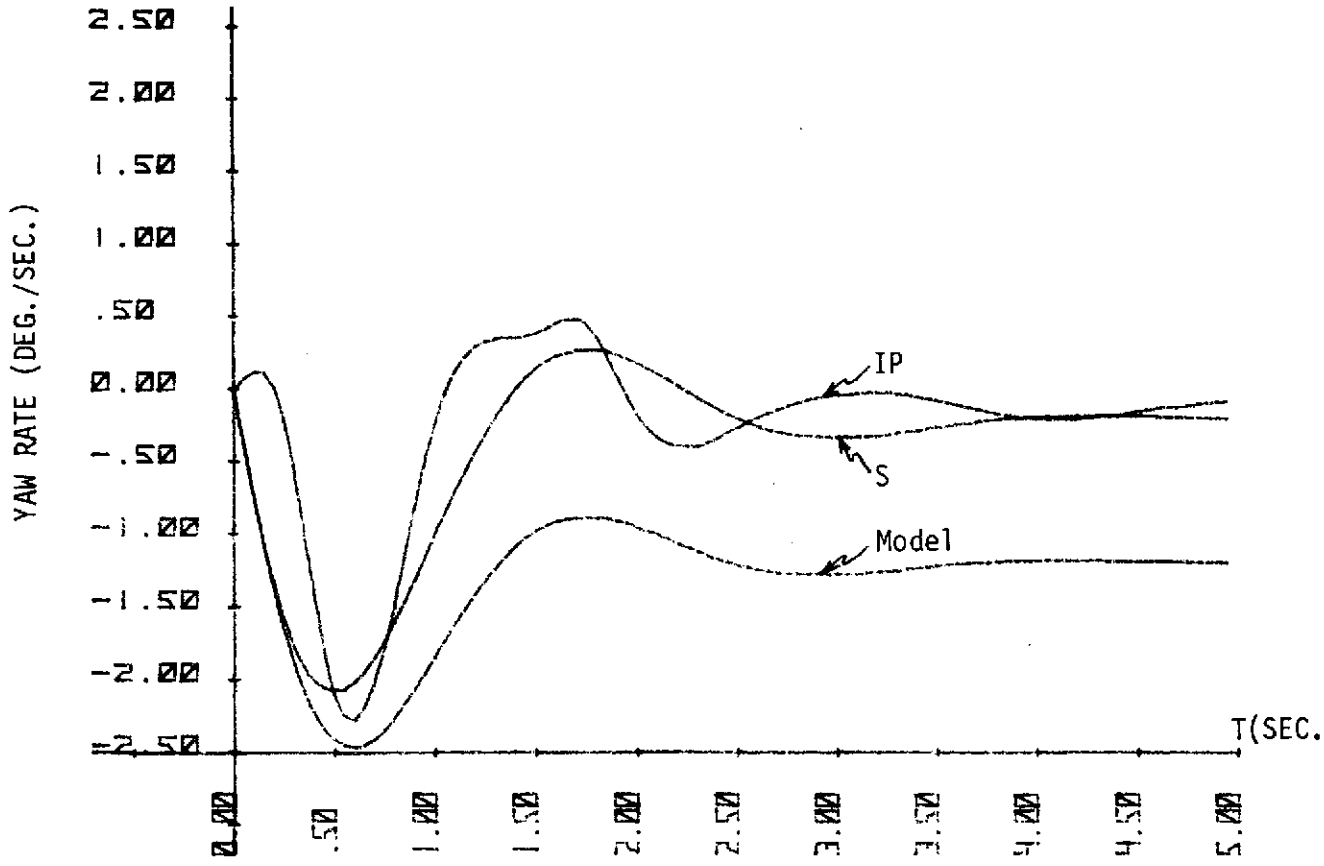

Flight Condition A ; $\delta_a^p = 0^o$, $\delta_r^p = 3^o$; $\delta^a(0) = 0^o$.

Figure A40.

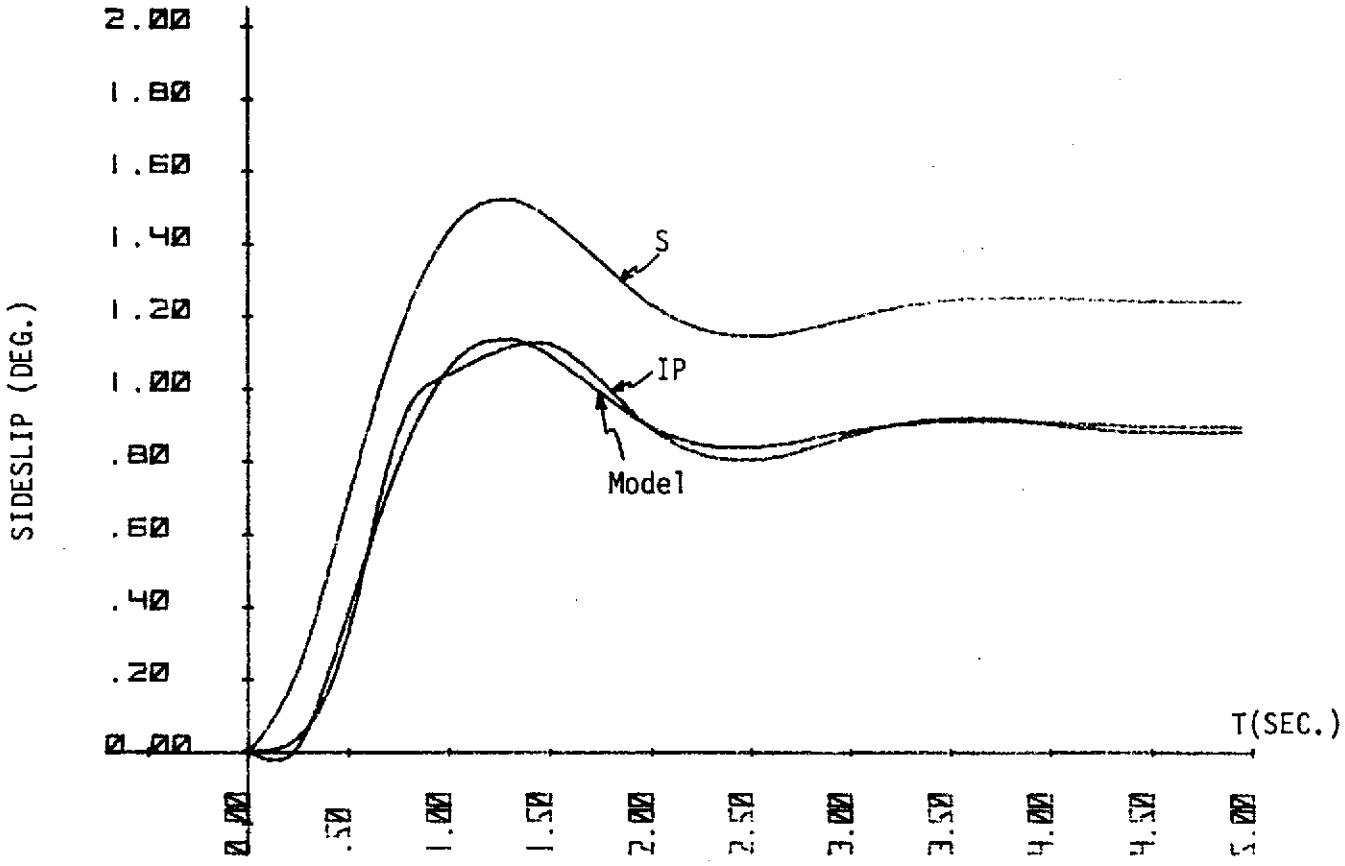

Flight Condition A ; $\delta_a^p = 0^o$, $\delta_r^p = 3^o$; $\delta^a(0) = 0^o$.

Figure A41.

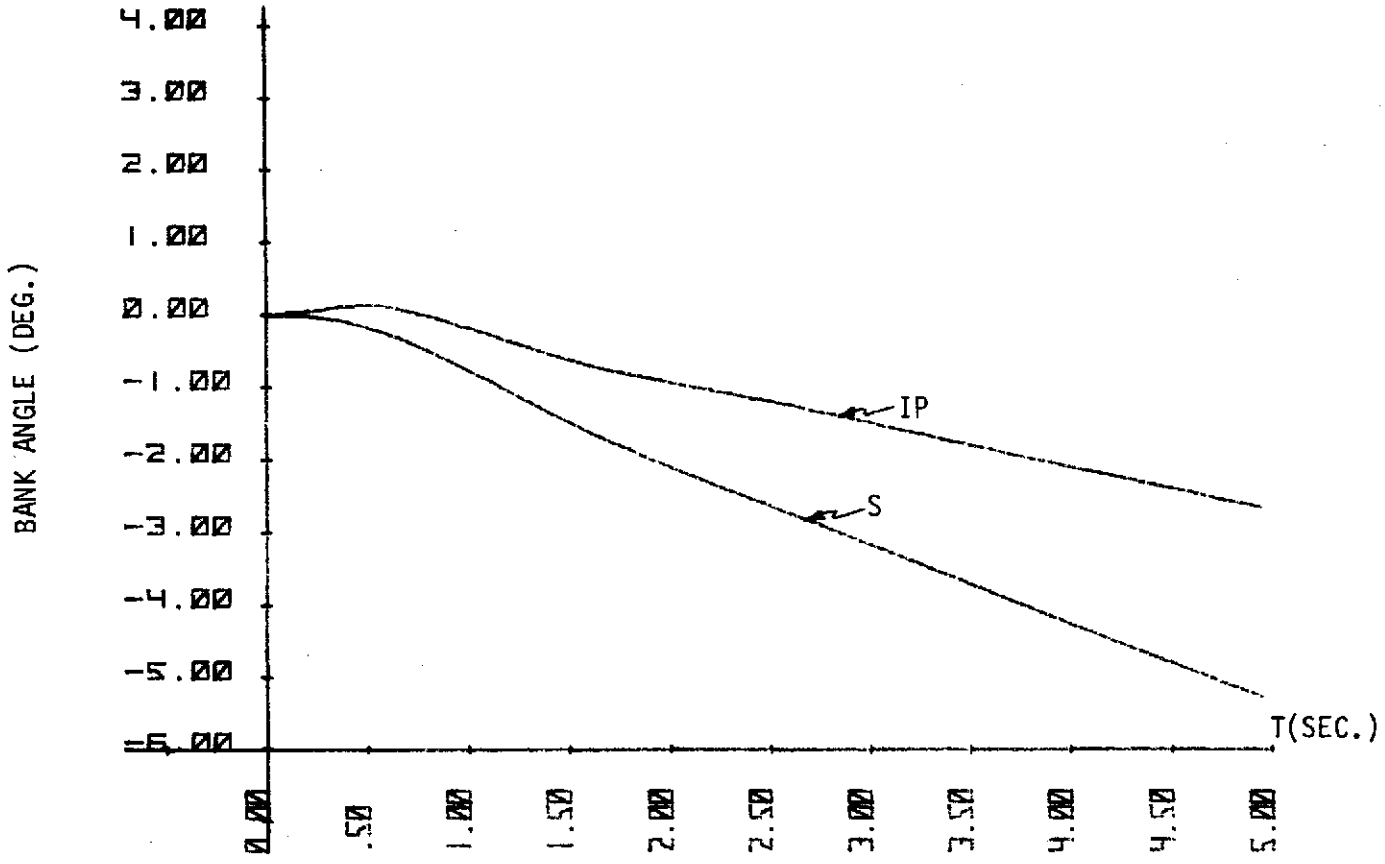

Flight Condition A; $\delta_a^p = 0^o$, $\delta_r^p = 3^o$; $\delta^a(0) = 0^o$.

Figure A42.

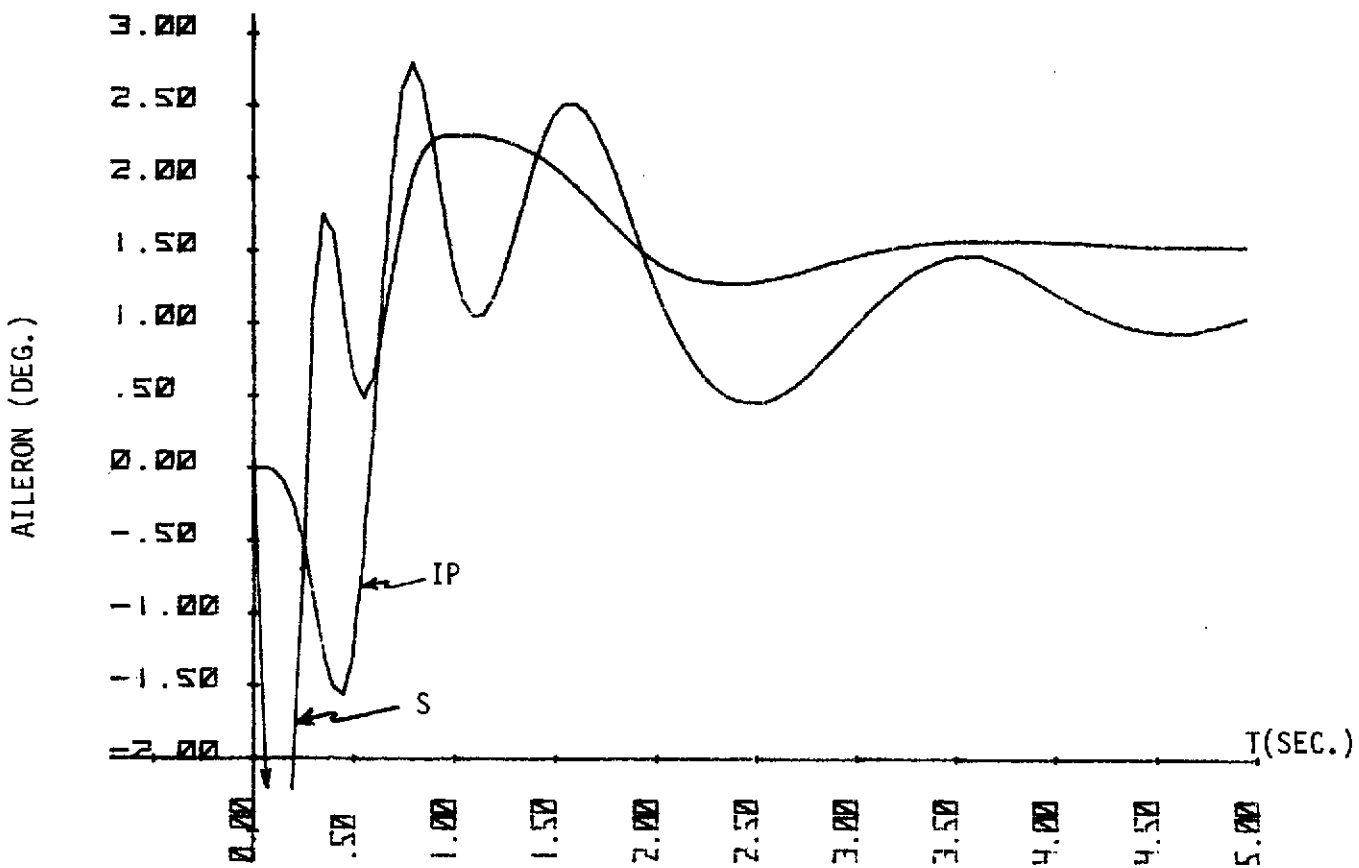

Flight Condition A ; $\delta_a^p = 0^o$, $\delta_r^p = 3^o$; $\delta^a(0) = 0^o$.

Figure A43.

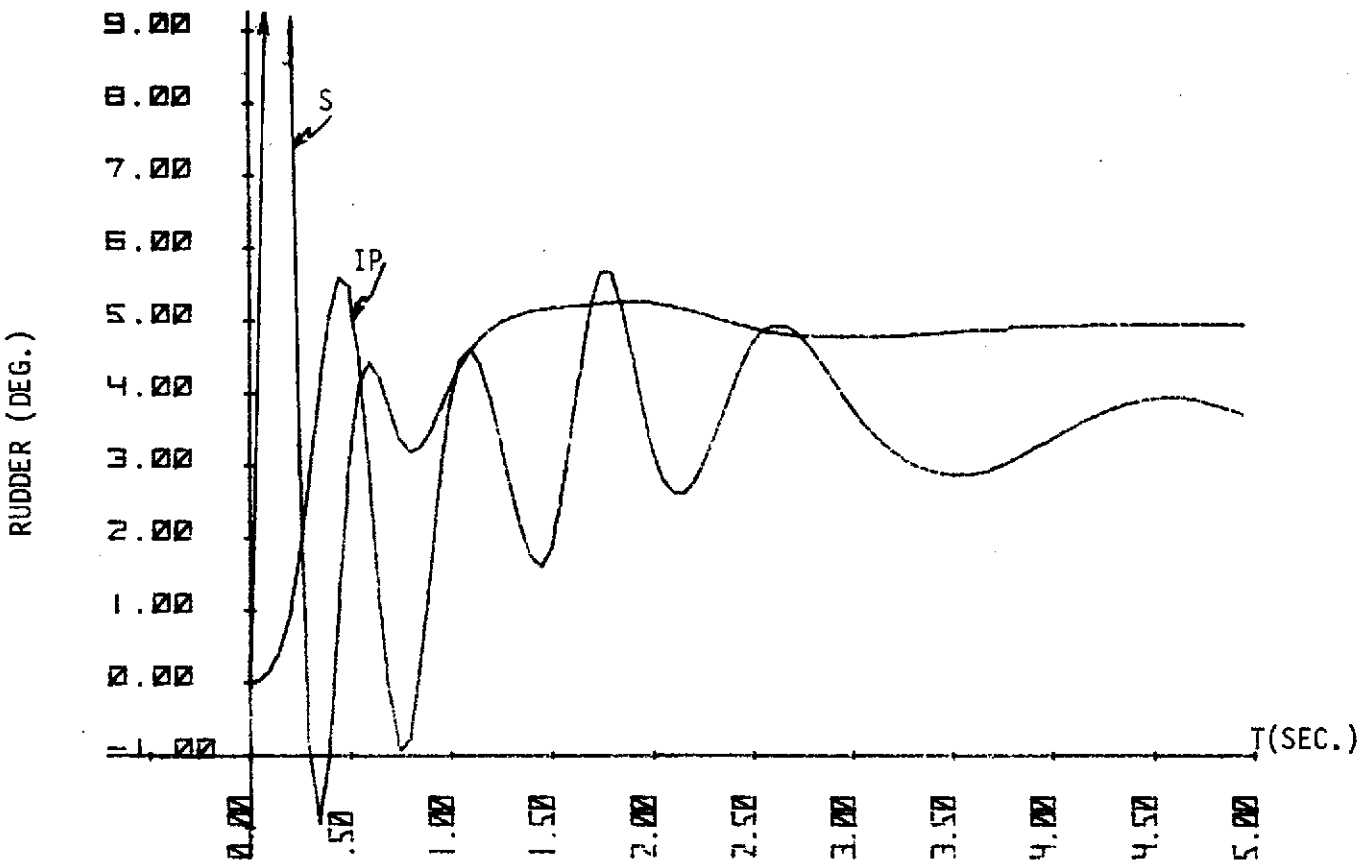

Flight Condition A ; $\delta_a^p = 0^o$, $\delta_r^p = 3^o$; $\delta^a(0) = 0^o$.

Figure A44.

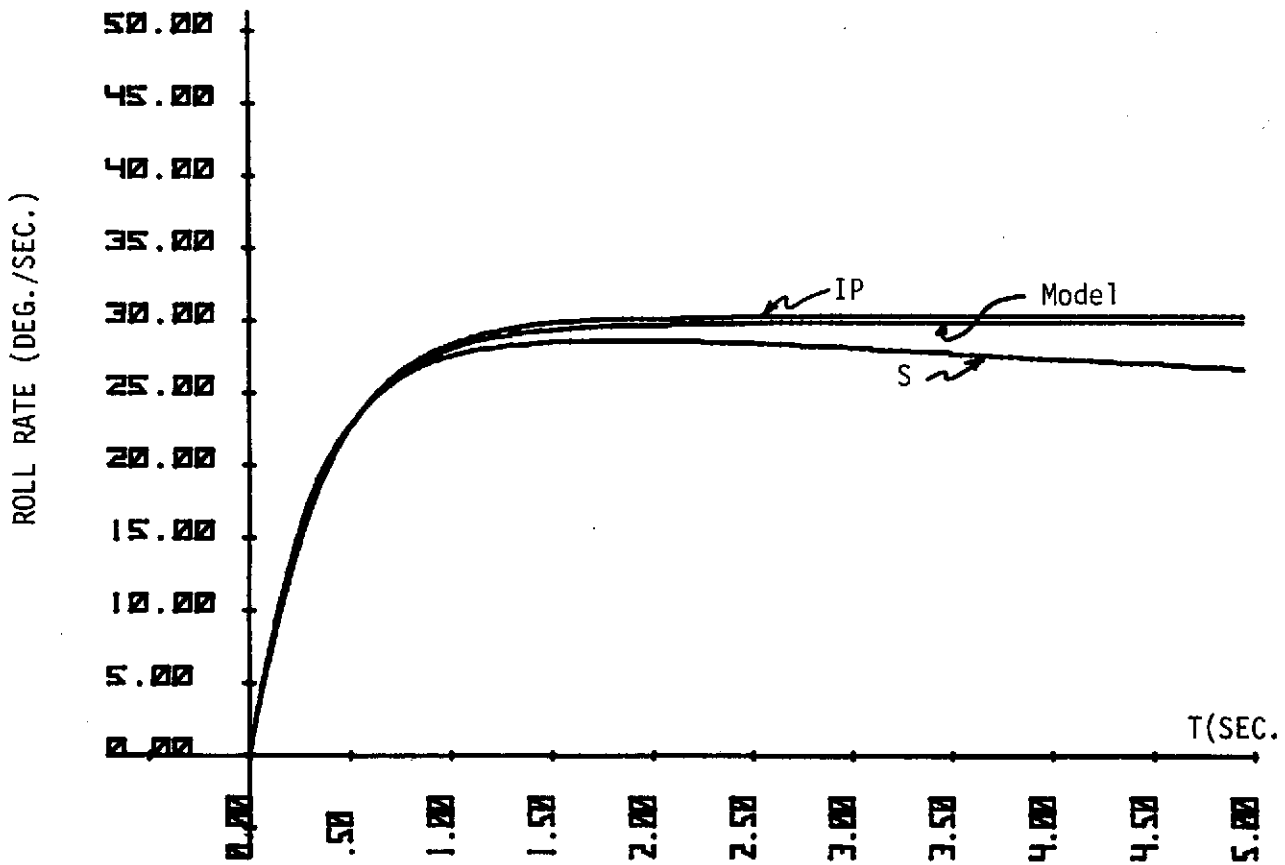

Flight Condition B; $\delta_a^p = 5°$, $\delta_r^p = 0°$; $\delta^a(0) = 0°$.

Figure A45.

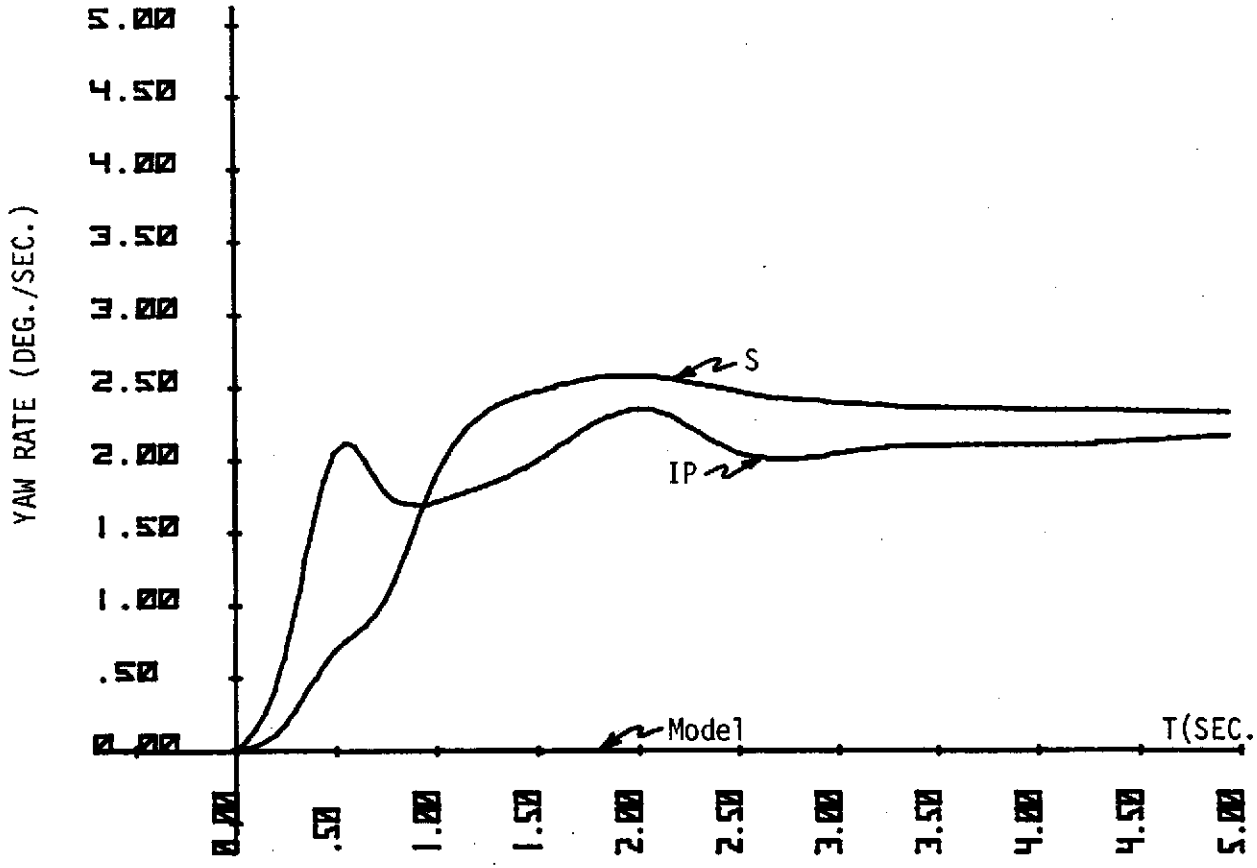

Flight Condition B; $\delta_a^p = 5°$, $\delta_r^p = 0°$; $\delta^a(0) = 0°$.
Figure A46.

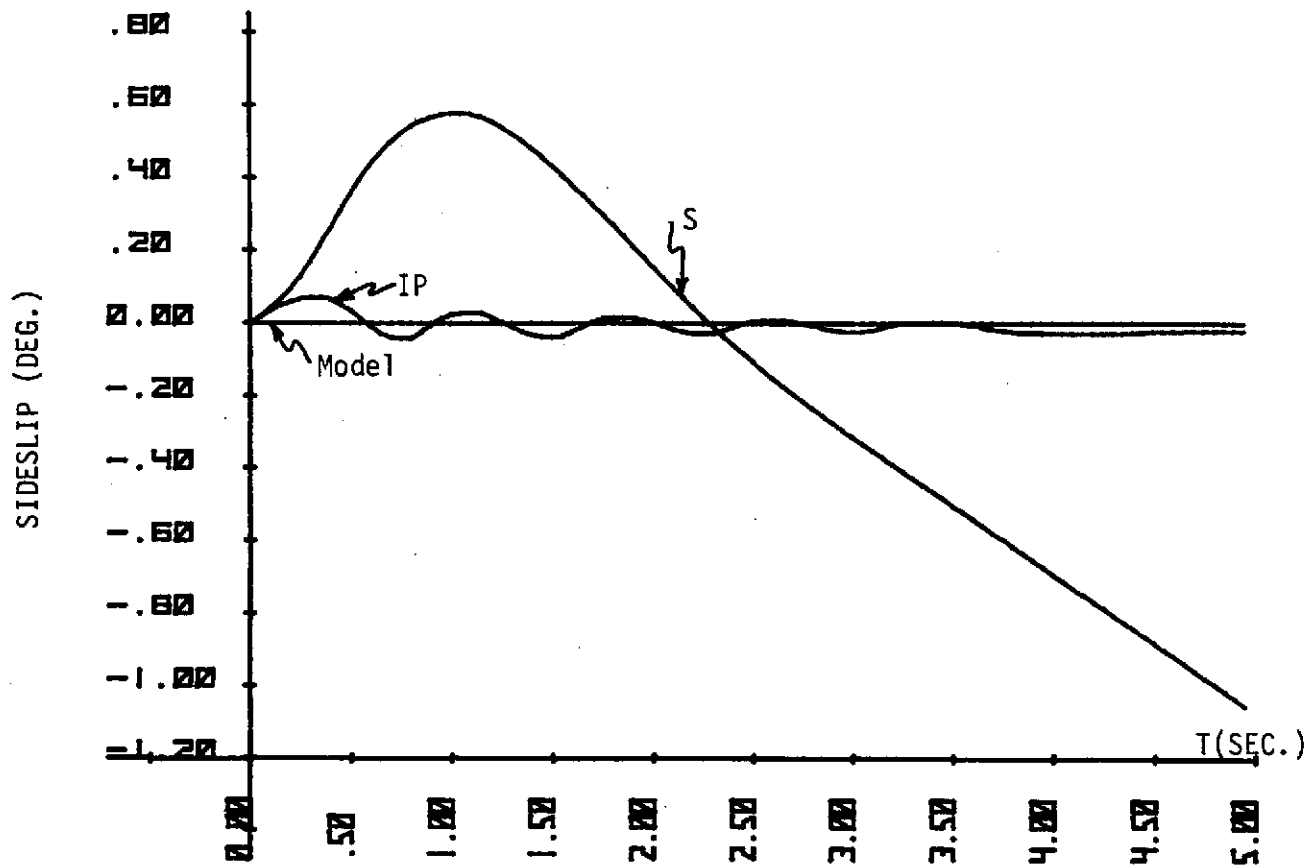

Flight Condition B; $\delta_a^p = 5°$, $\delta_r^p = 0°$; $\delta^a(0) = 0°$.

Figure A47.

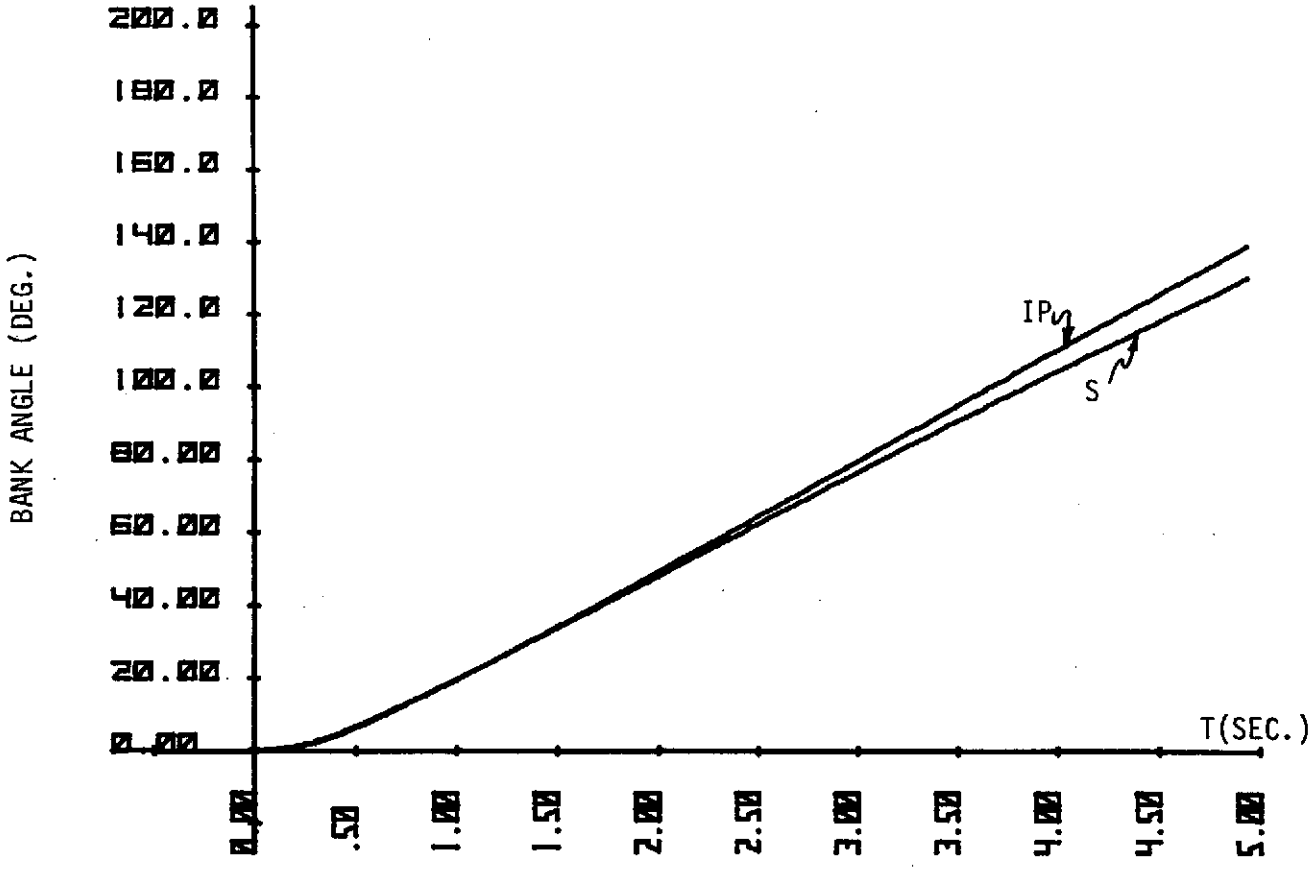

Flight Condition B; $\delta_a^p = 5°$, $\delta_r^p = 0°$; $\delta^a(0) = 0°$.

Figure A48.

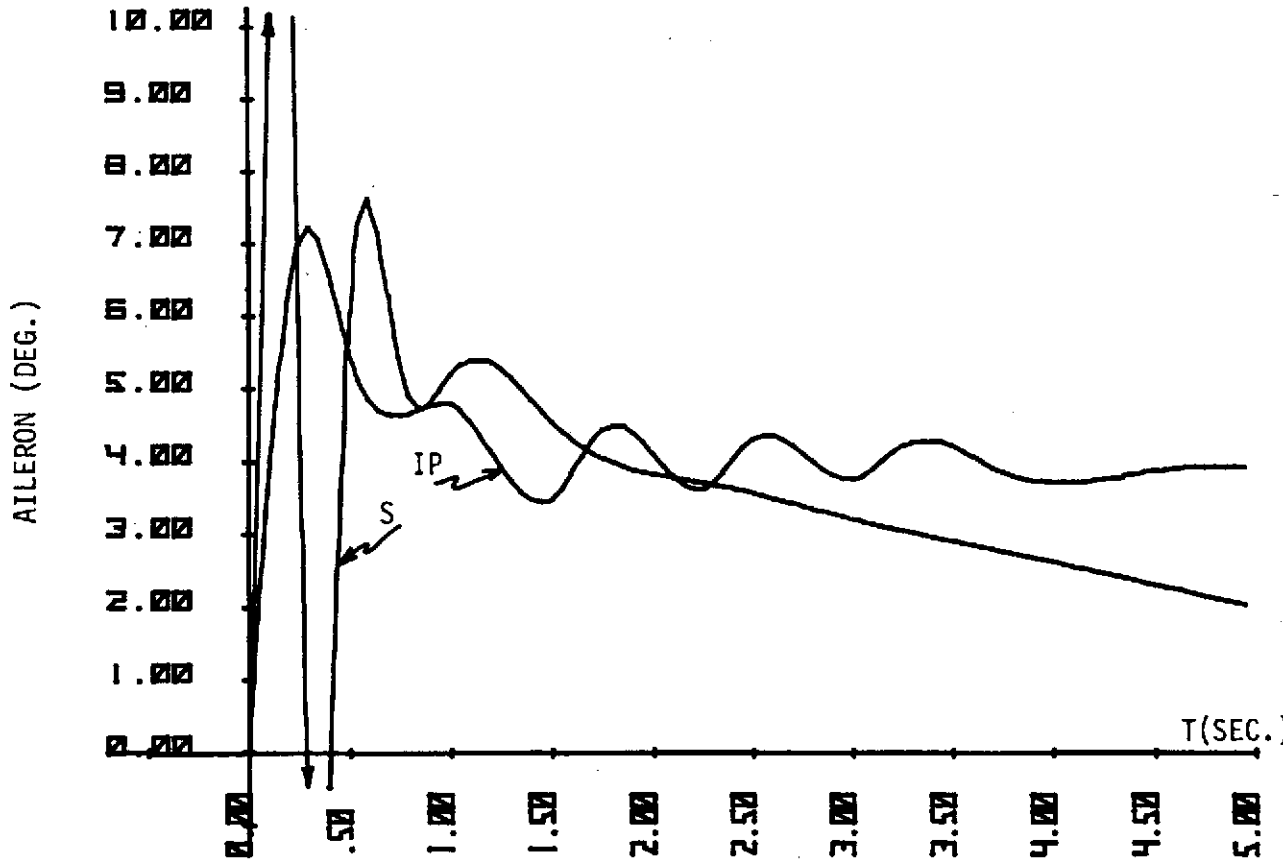

Flight Condition B; $\delta_a^p = 5°$, $\delta_r^p = 0°$; $\delta^a(0) = 0°$.

Figure A49.

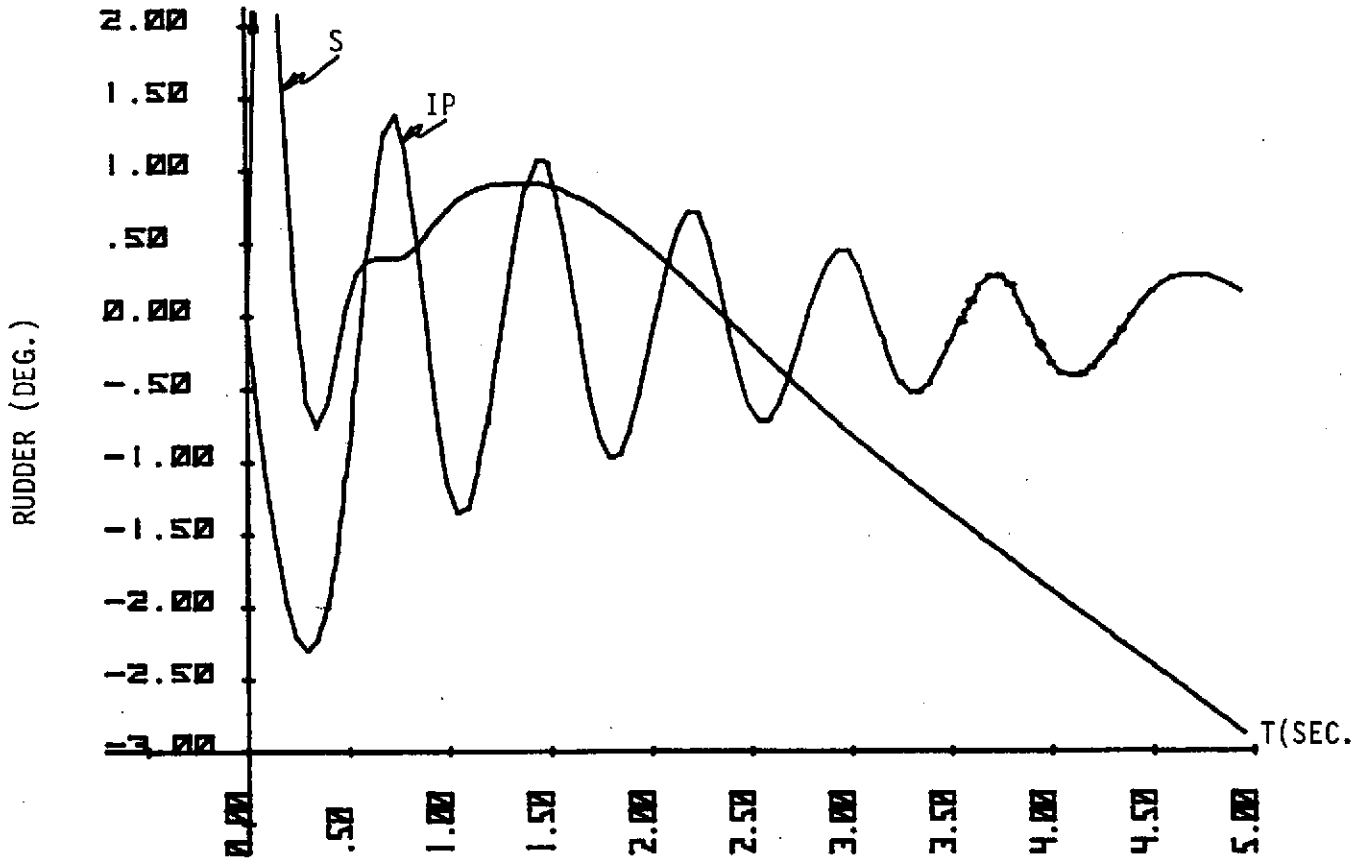

Flight Condition B; $\delta_a^p = 5°$, $\delta_r^p = 0°$; $\delta^a(0) = 0°$.

Figure A50.

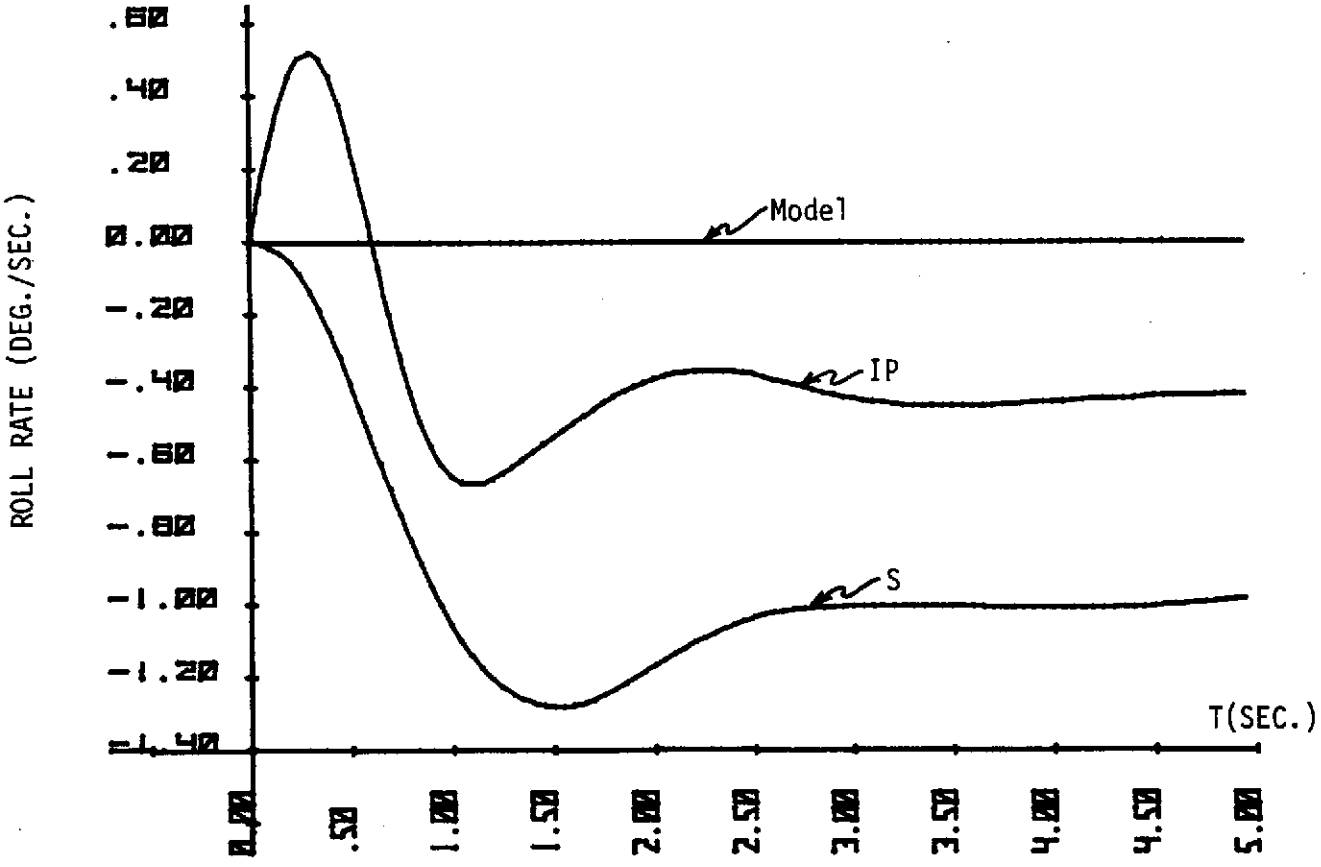

Flight Condition B; $\delta_a^p = 0°$, $\delta_r^p = 3°$; $\delta^a(0) = 0°$.

Figure A51.

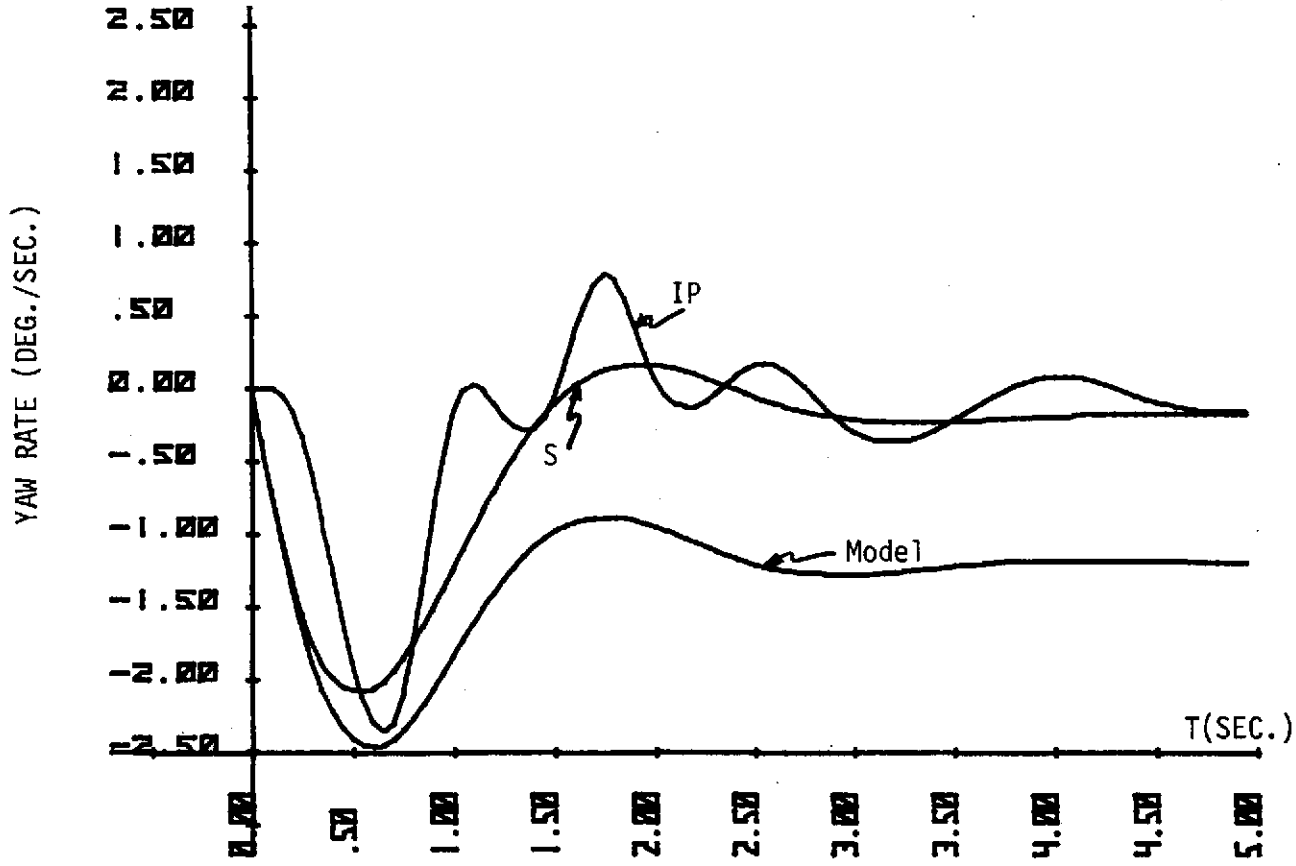

Flight Condition B; $\delta_a^p = 0°$, $\delta_r^p = 3°$; $\delta^a(0) = 0°$.

Figure A52.

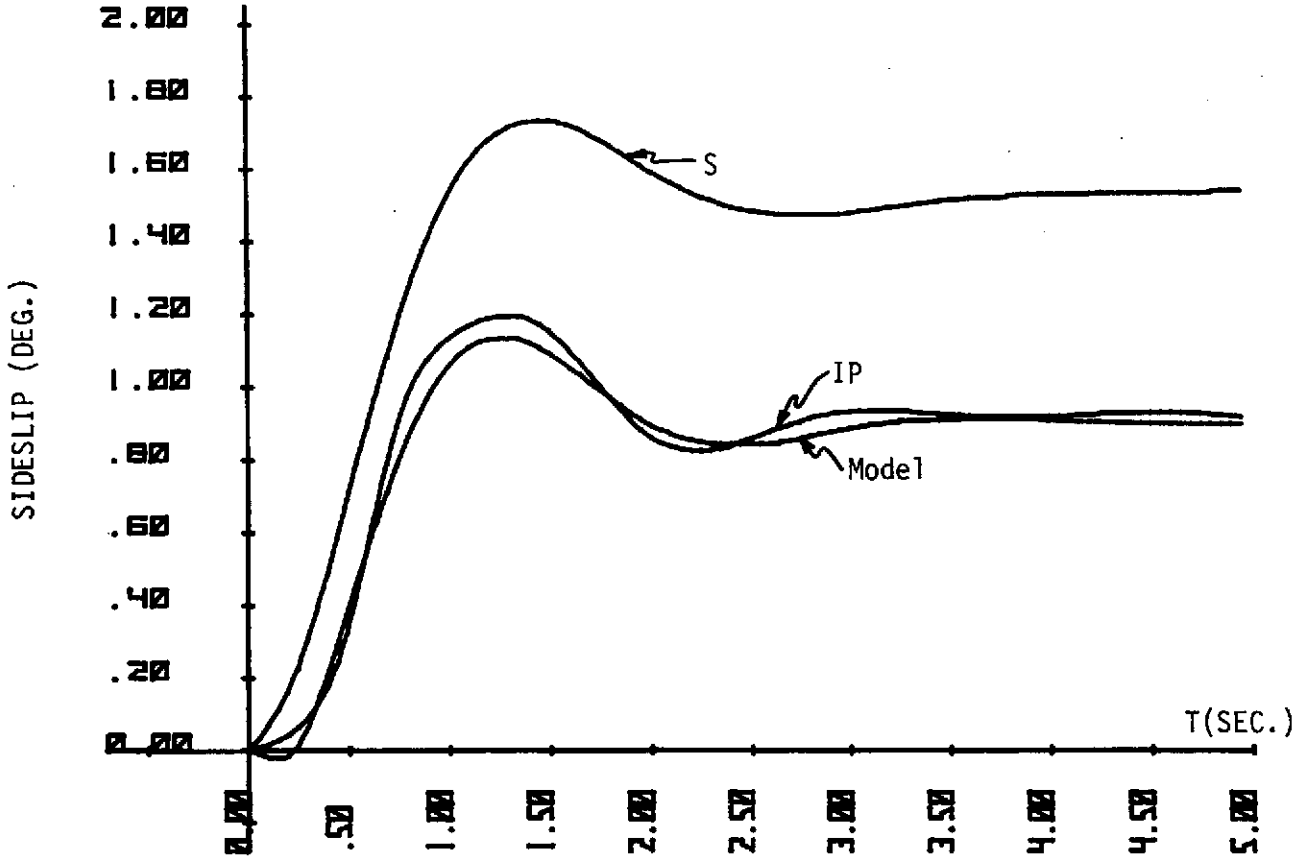

Flight Condition B; $\delta_a^p = 0°$, $\delta_r^p = 3°$; $\delta^a(0) = 0°$.

Figure A53.

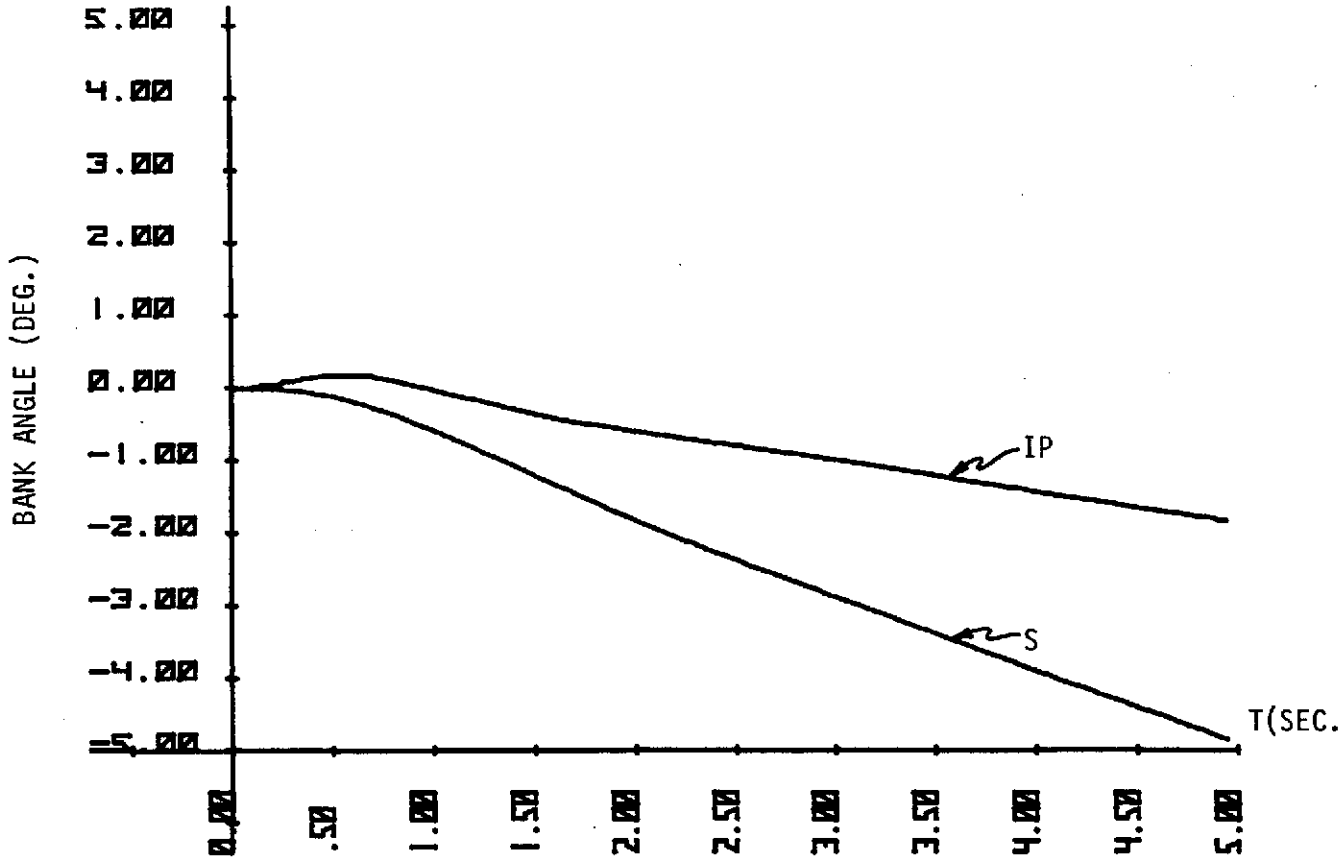

Flight Condition B; $\delta_a^p = 0°$, $\delta_r^p = 3°$; $\delta^a(0) = 0°$.
Figure A54.

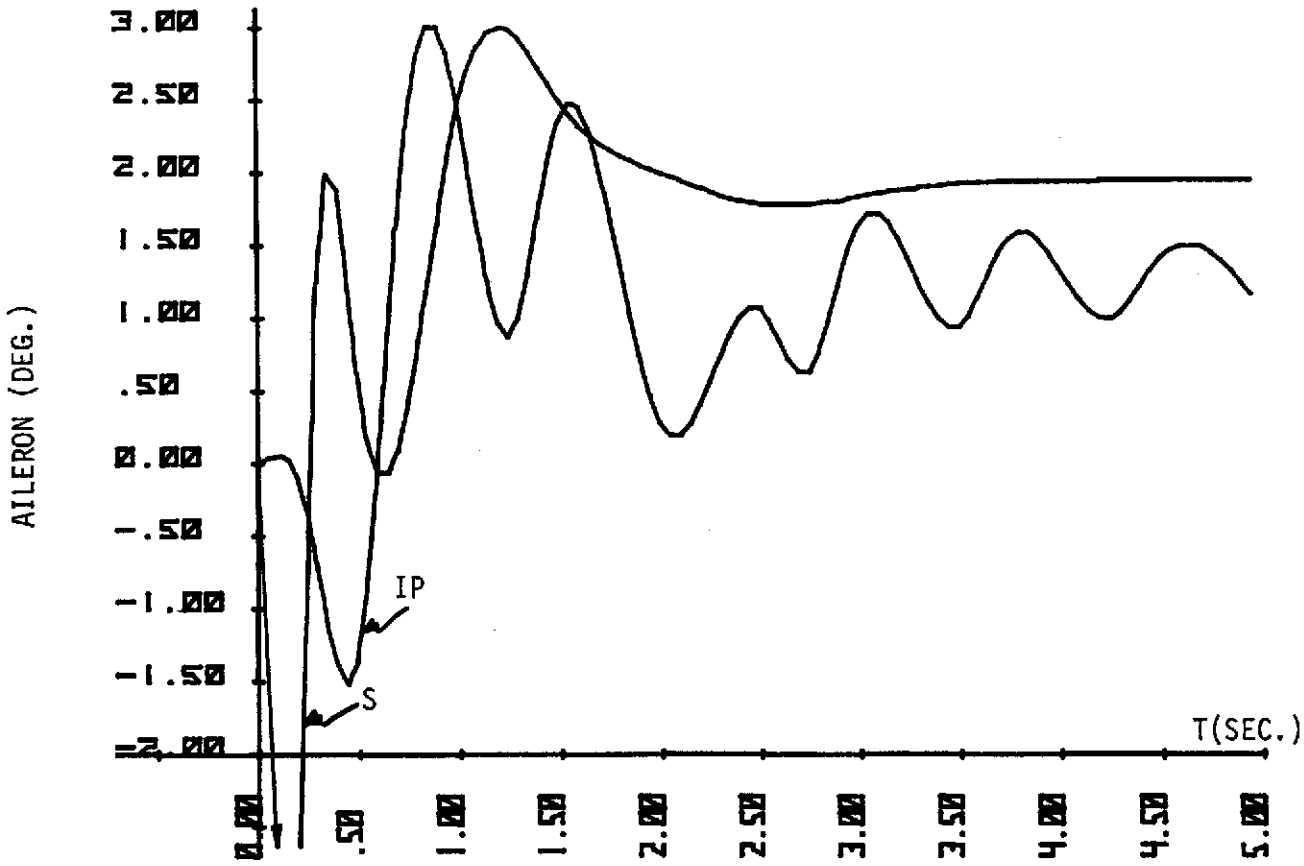

Flight Condition B; $\delta_a^p = 0°$, $\delta_r^p = 3°$; $\delta^a(0) = 0°$.
Figure A55.

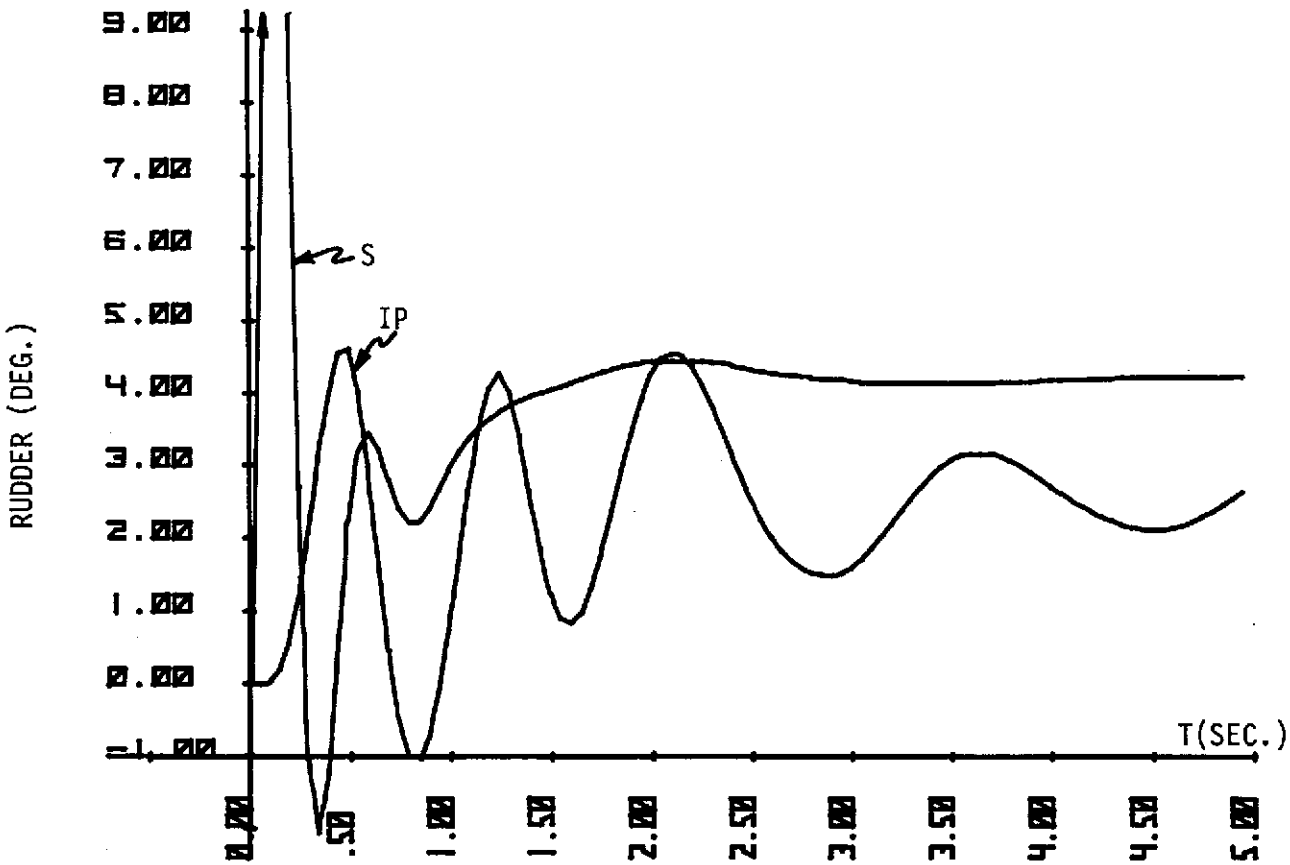

Flight Condition B; $\delta_a^p = 0°$, $\delta_r^p = 3°$; $\delta^a(0) = 0°$.

Figure A56.

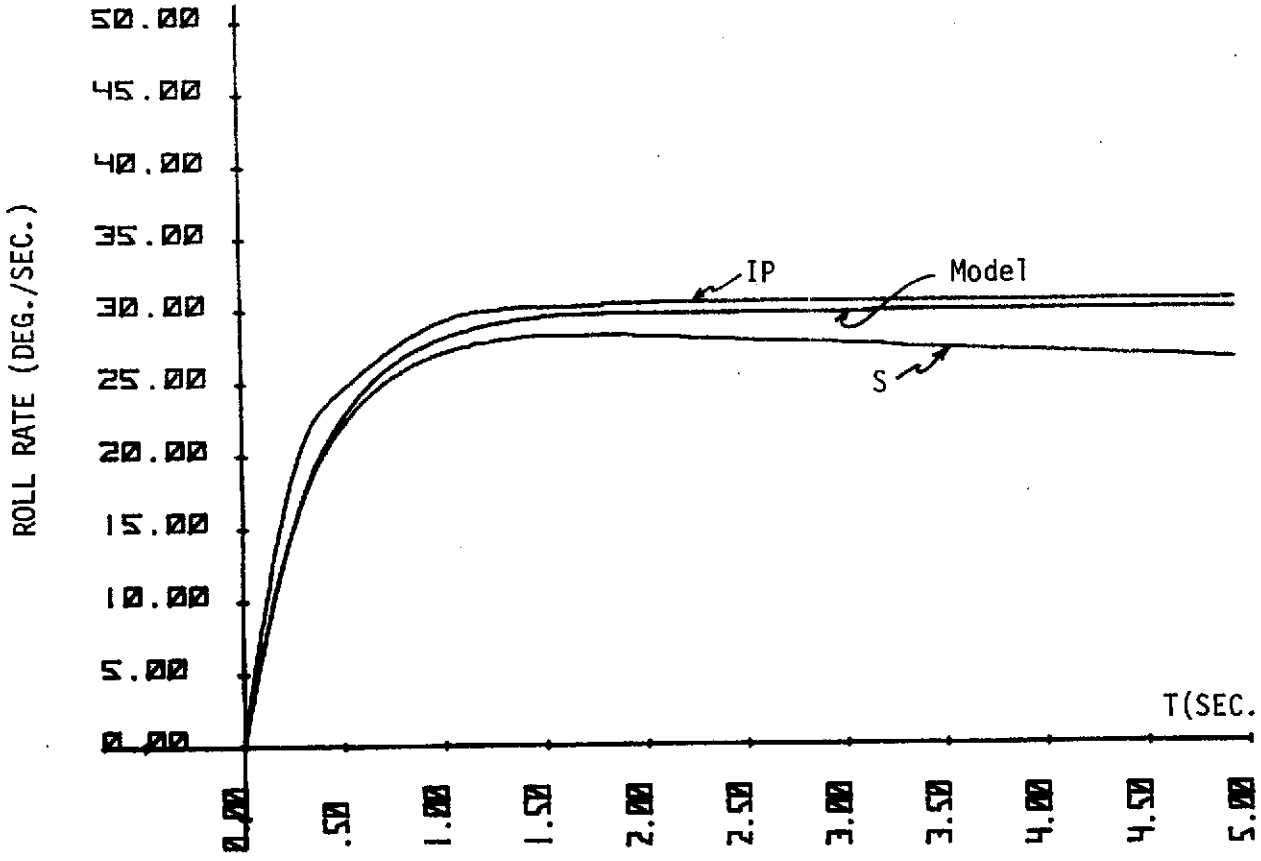

Flight Condition C; $\delta_a^p = 5°$, $\delta_r^p = 0°$, $\delta^a(0) = 0°$.
Figure A57.

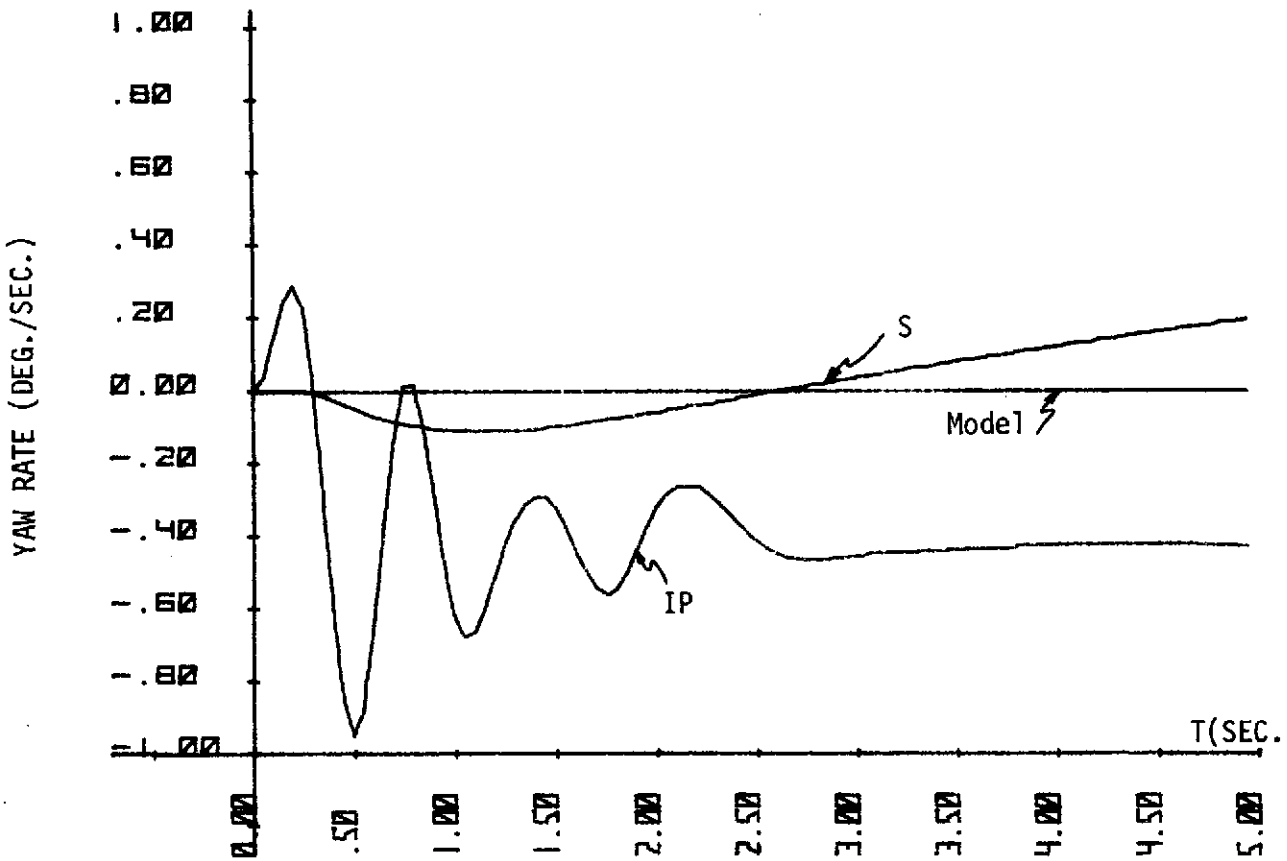

Flight Condition C; $\delta_a^p = 5°$, $\delta_r^p = 0°$; $\delta^a(0) = 0°$.

Figure A58.

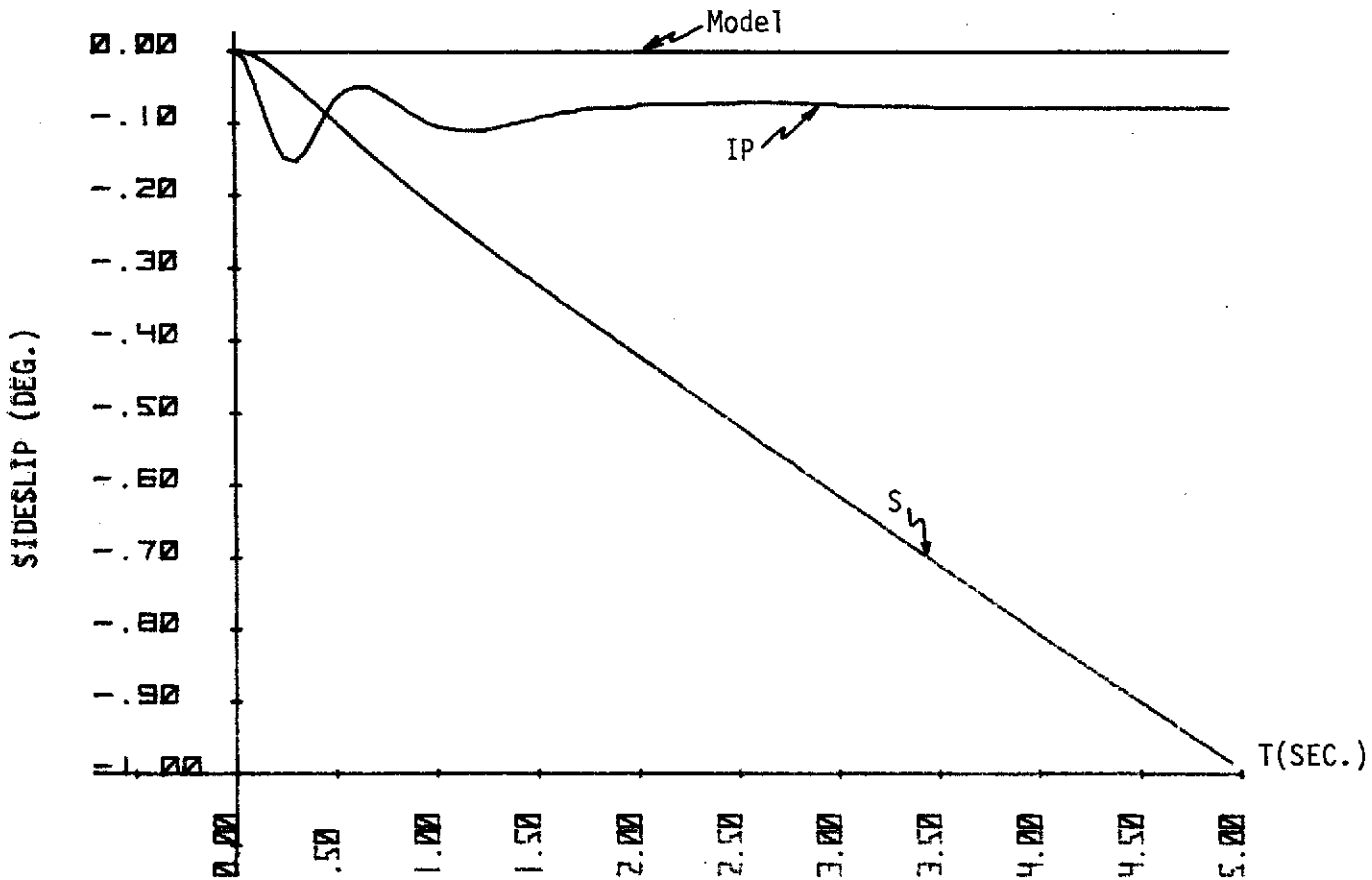

Flight Condition C; $\delta_a^p = 5°$, $\delta_r^p = 0°$; $\delta^a(0) = 0°$.

Figure A59.

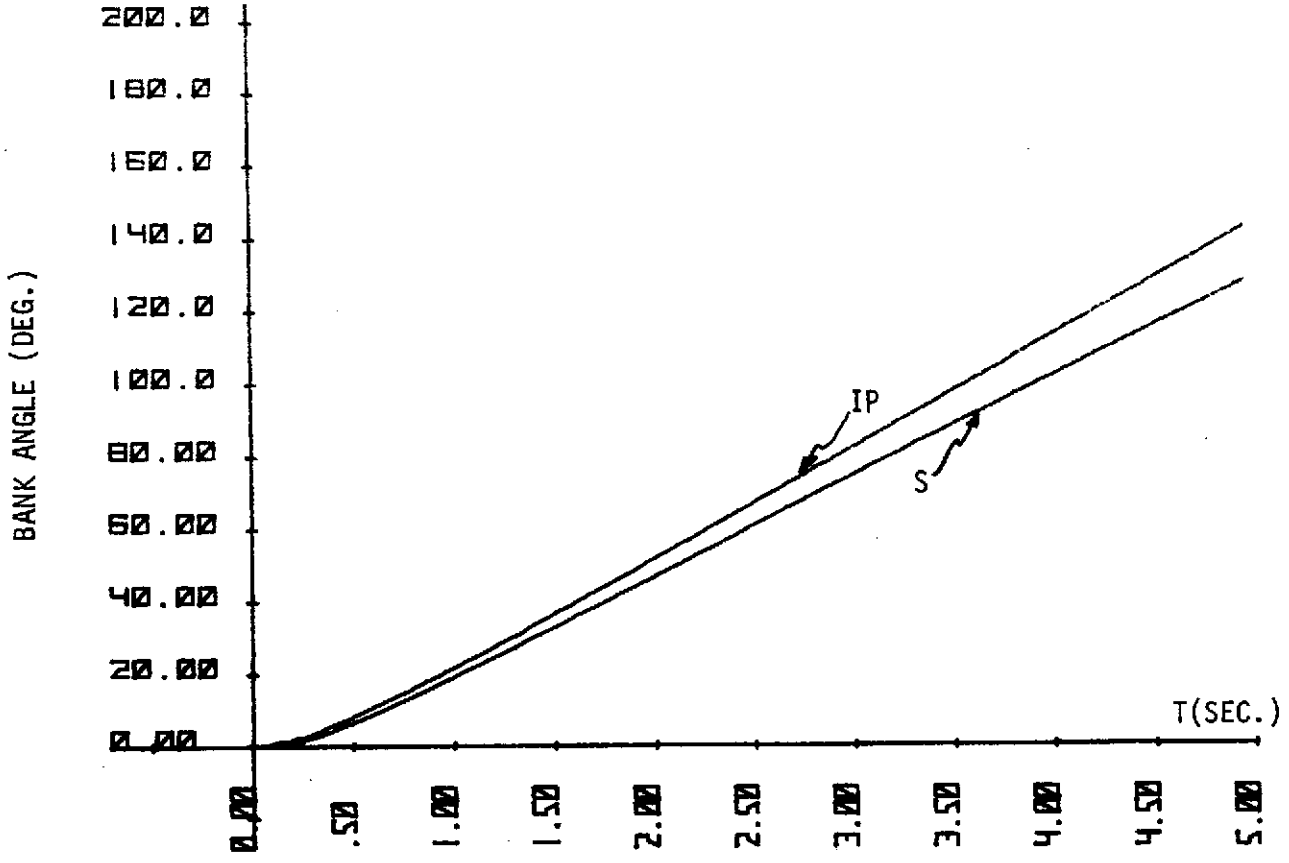

Flight Condition C; $\delta_a^p = 5°$, $\delta_r^p = 0°$; $\delta^a(0) = 0°$.
Figure A60.

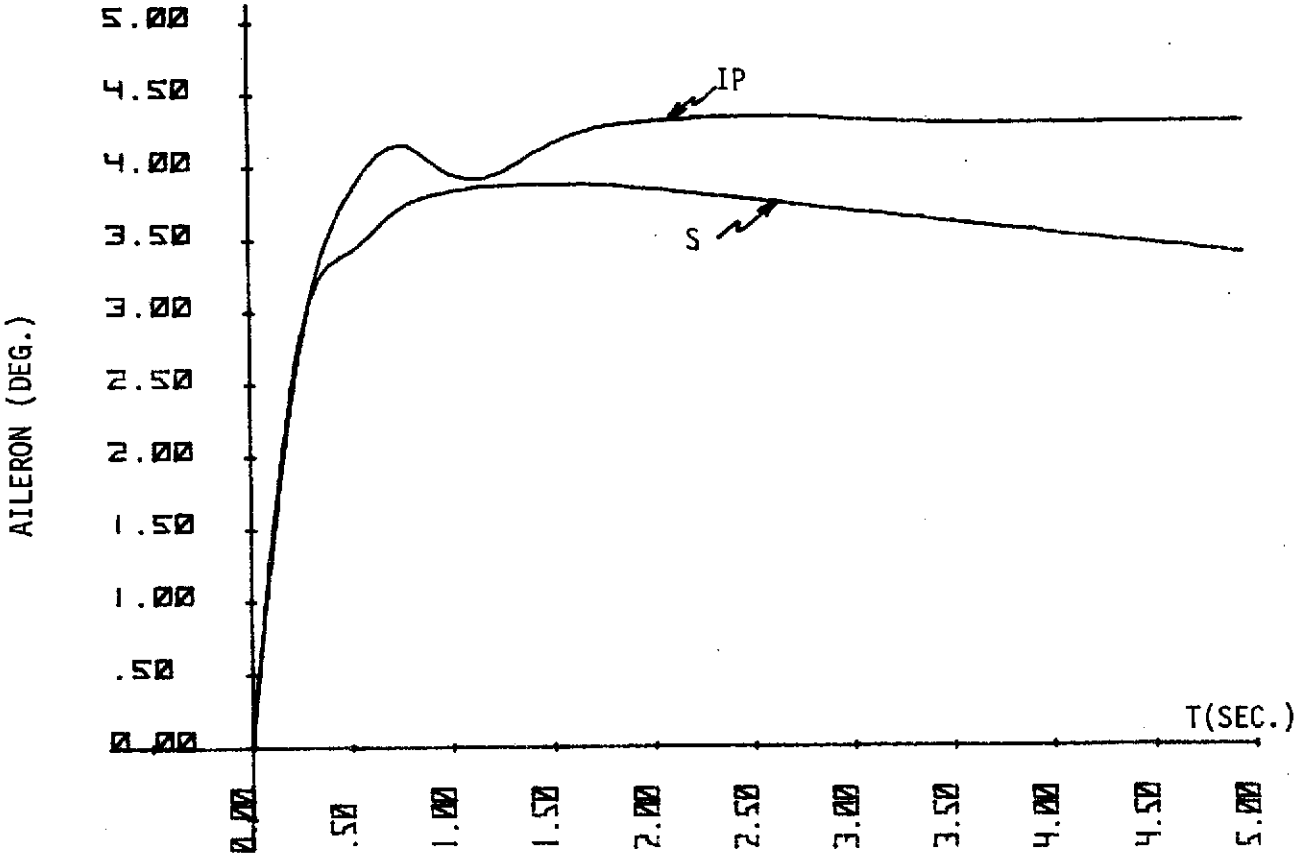

Flight Condition C; $\delta_a^p = 5°$, $\delta_r^p = 3°$; $\delta^a(0) = 0°$.

Figure A61.

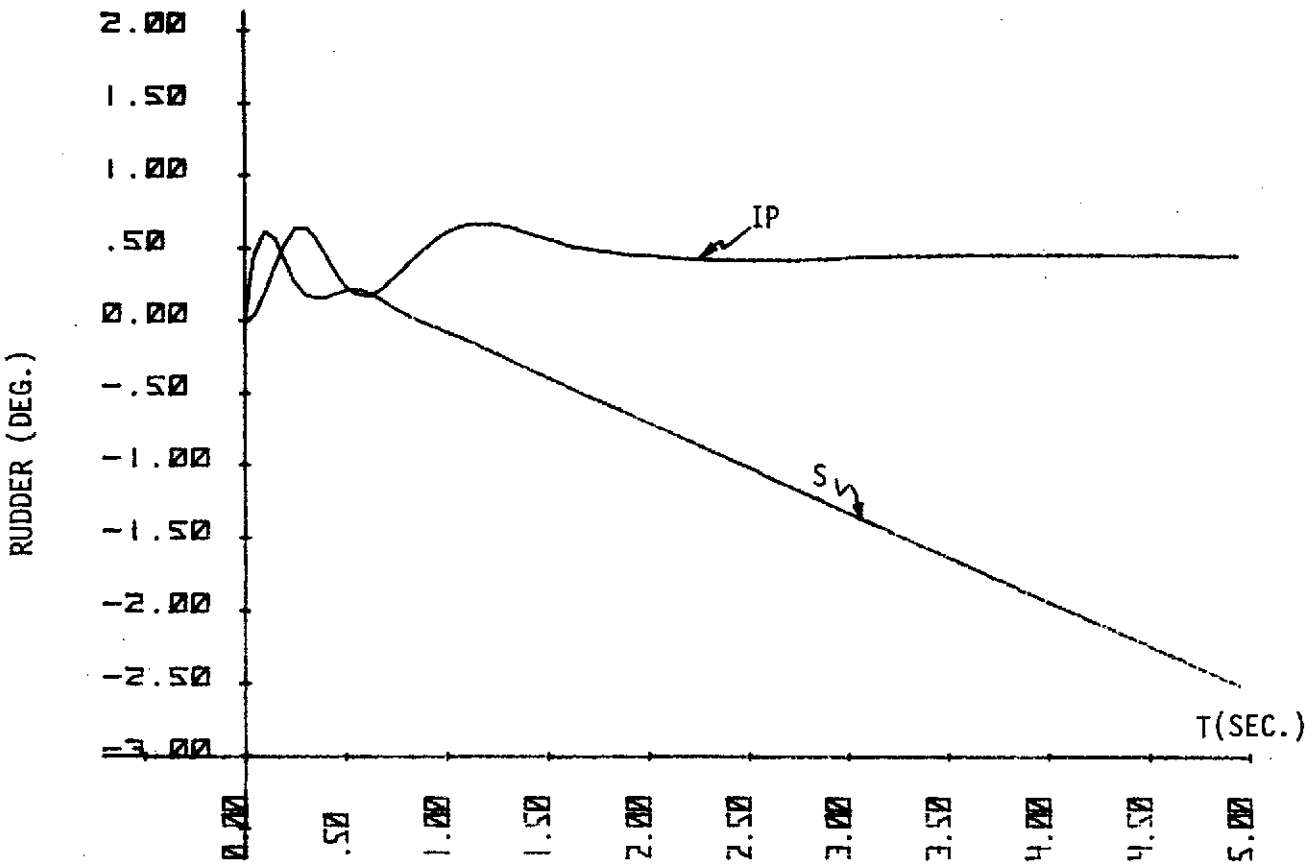

Flight Condition C; $\delta_a^p = 5°$, $\delta_r^p = 0°$; $\delta^a(0) = 0°$.

Figure A62.

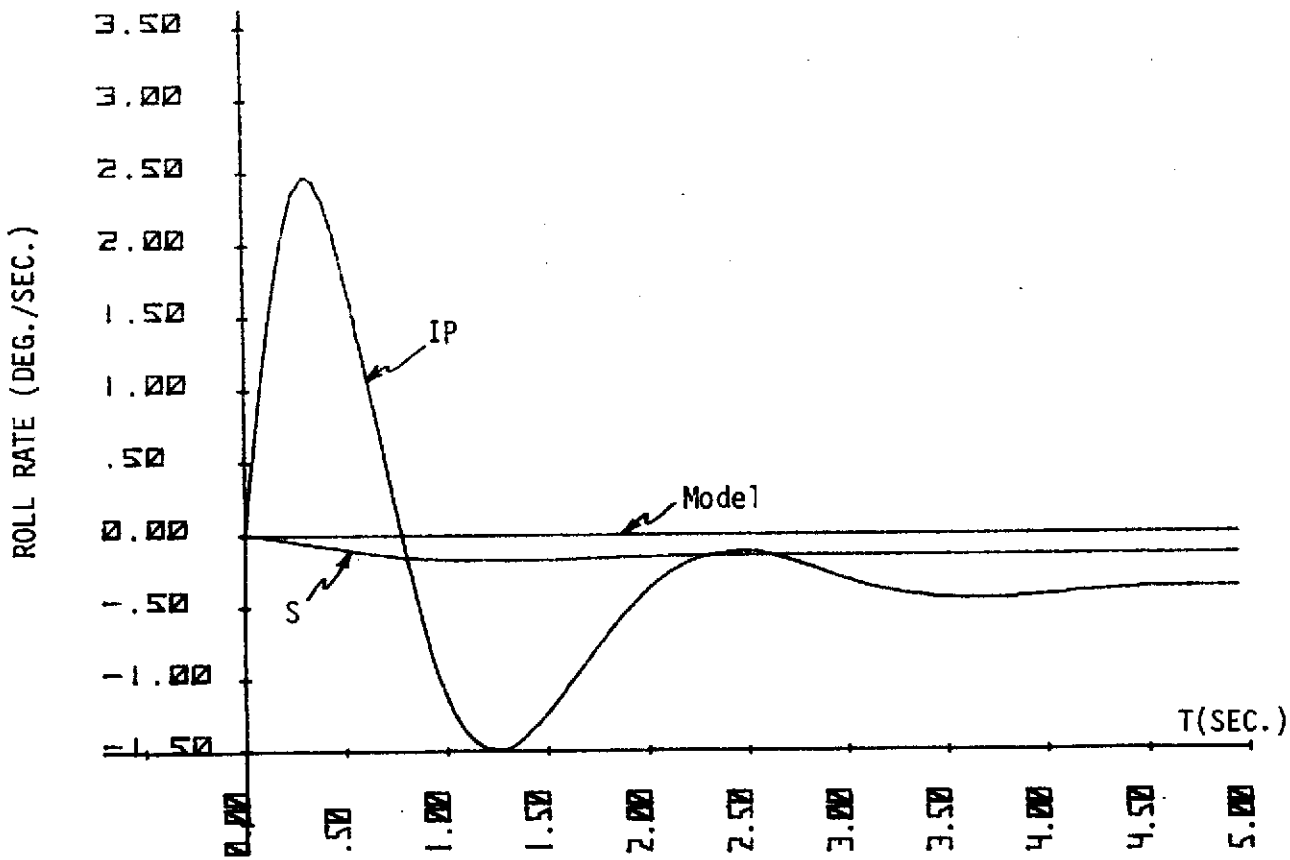

Flight Condition C; $\delta_a^p = 0°$, $\delta_r^p = 3°$; $\delta^a(0) = 0°$.

Figure A63.

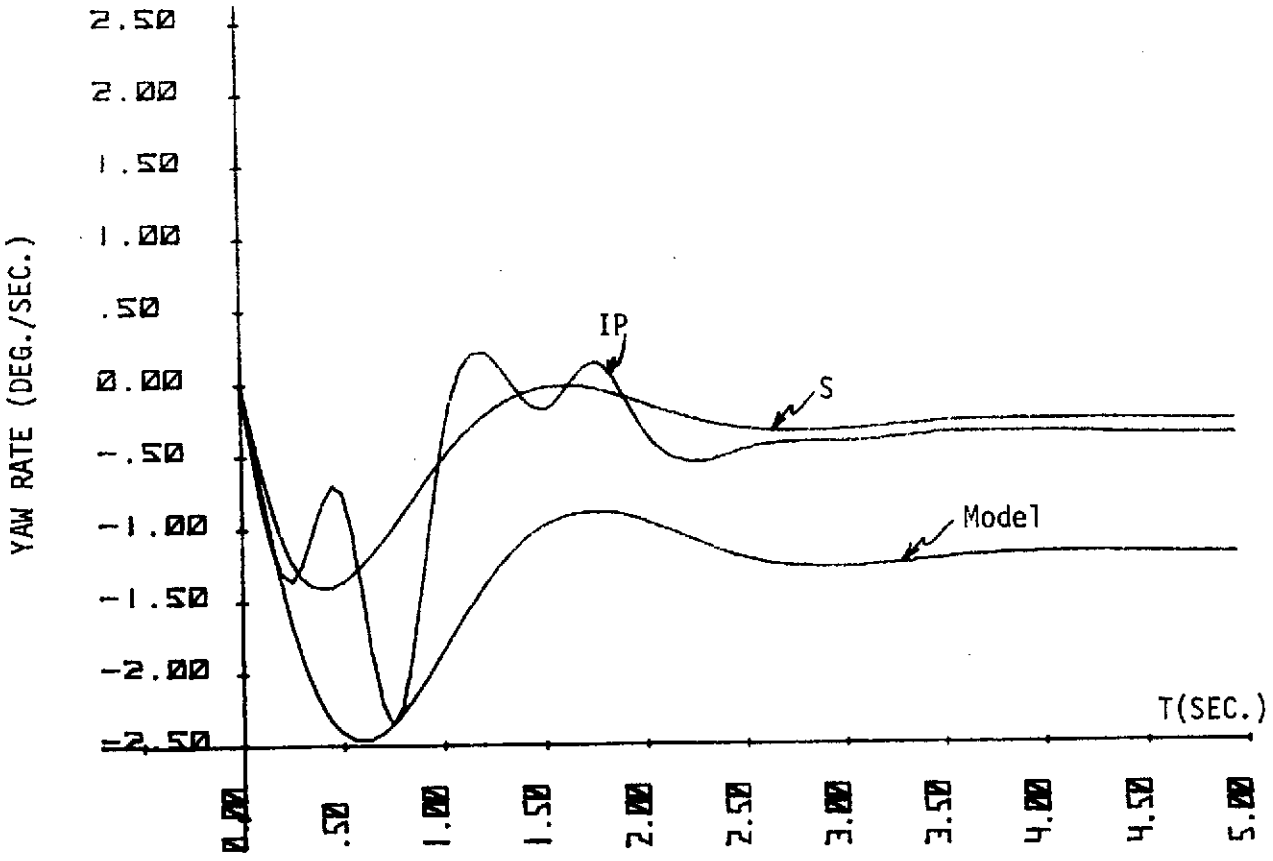

Flight Condition C; $\delta_a^p = 0°$, $\delta_r^p = 3°$; $\delta^a(0) = 0°$.

Figure A64.

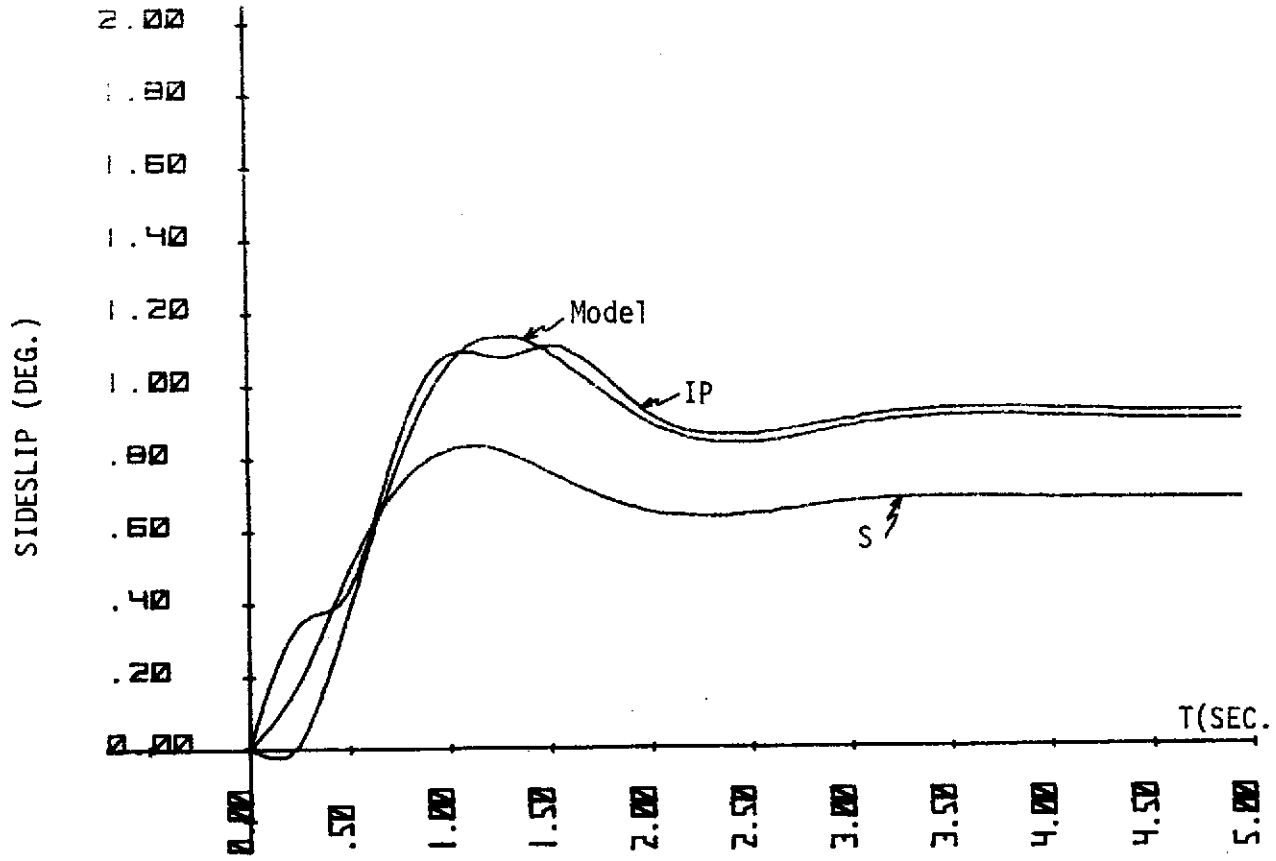

Flight Condition C; $\delta_a^p = 0°$, $\delta_r^p = 3°$; $\delta^a(0) = 0°$.

Figure A65.

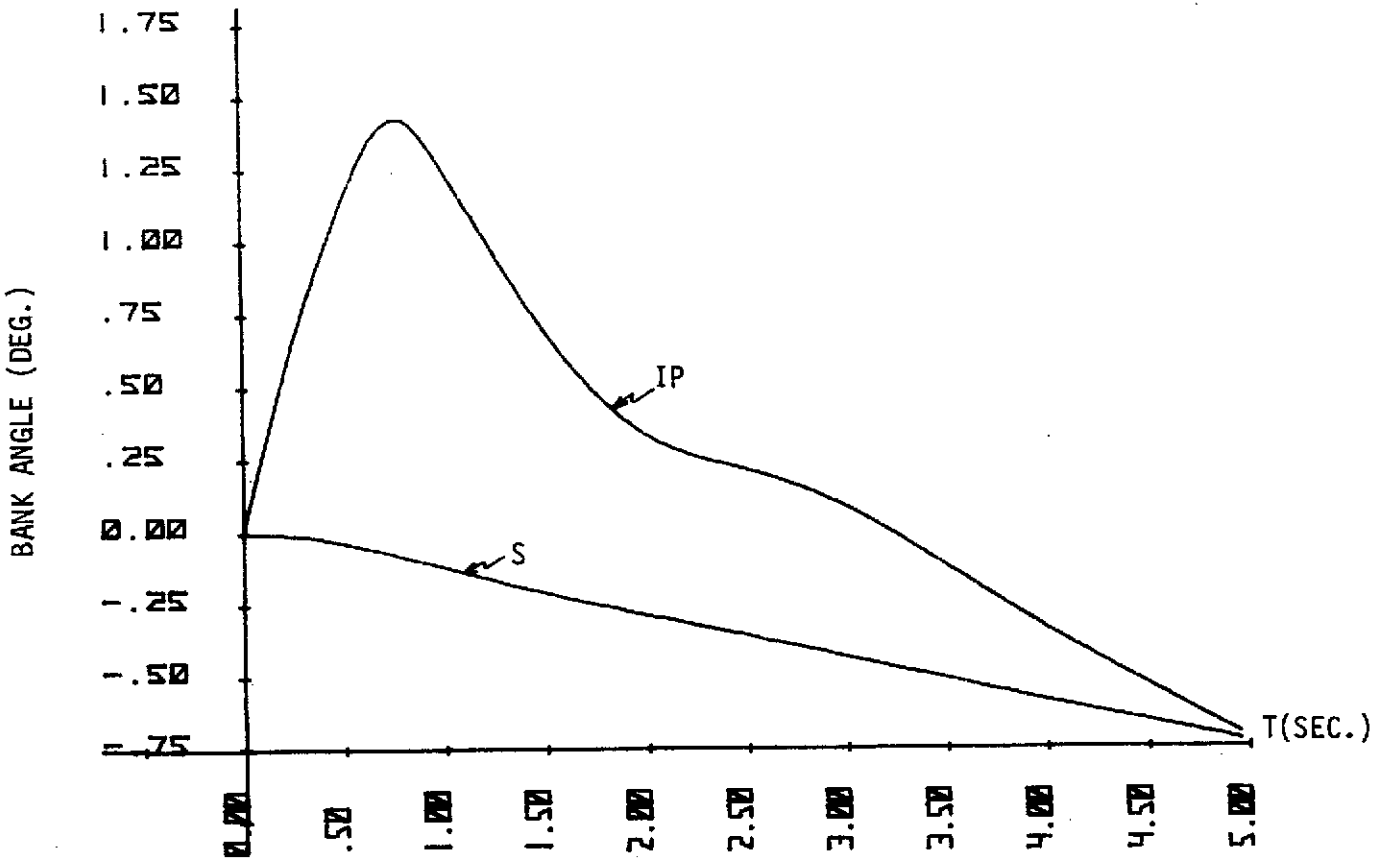

Flight Condition C; $\delta_a^p = 0°$, $\delta_r^p = 3°$; $\delta^a(0) = 0°$.

Figure A66.

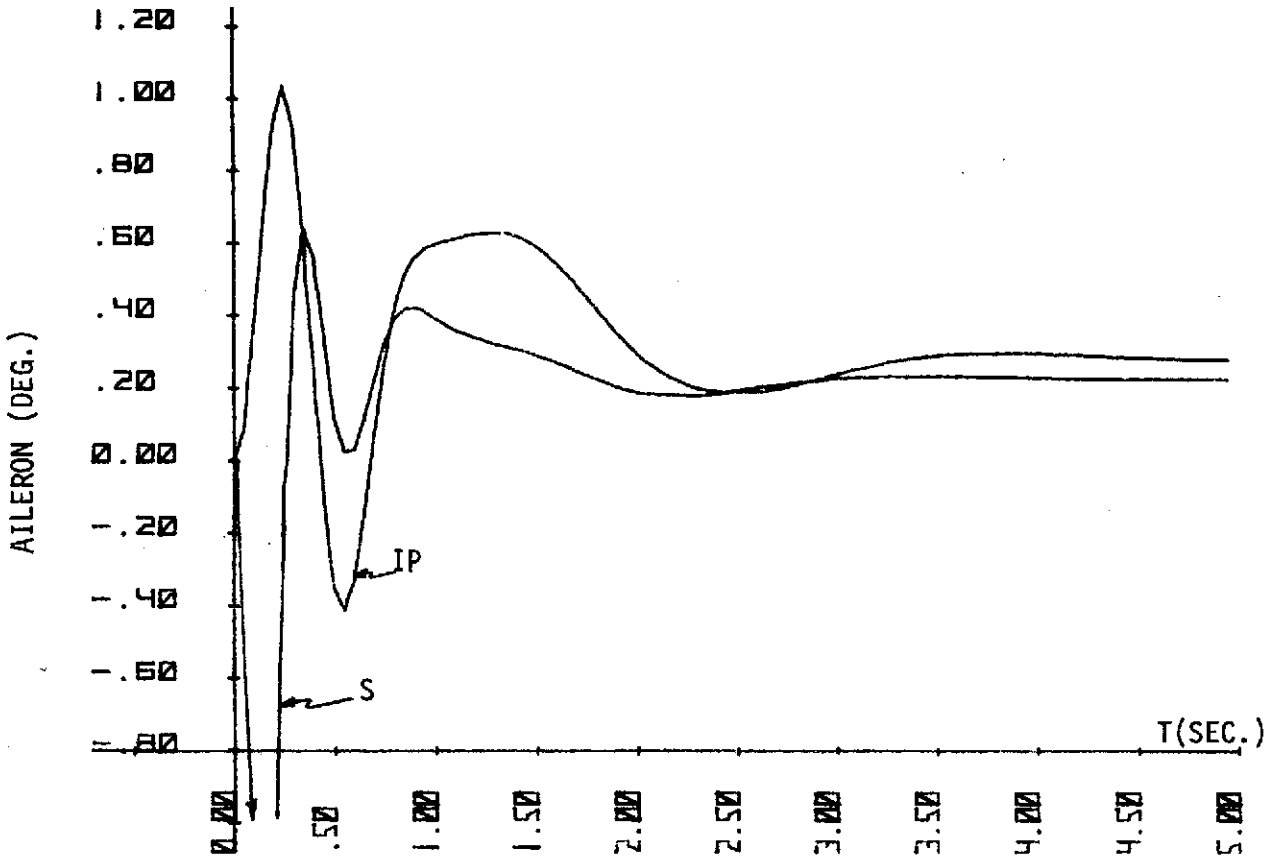

Flight Condition C; $\delta_a^p = 0°$, $\delta_r^p = 3°$; $\delta^a(0) = 0°$.
Figure A67.

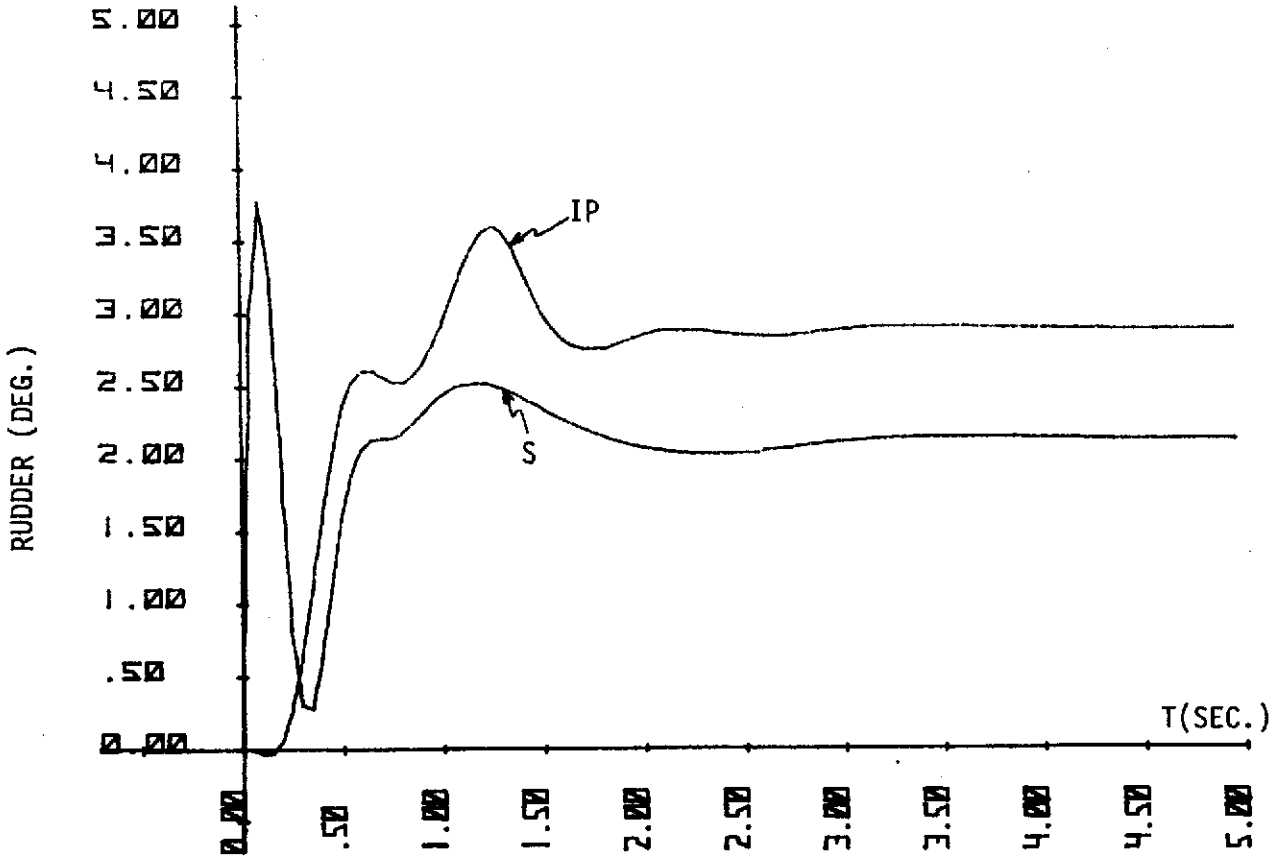

Flight Condition C; $\delta_a^p = 0°$, $\delta_r^p = 3°$; $\delta^a(0) = 0°$.
Figure A68.

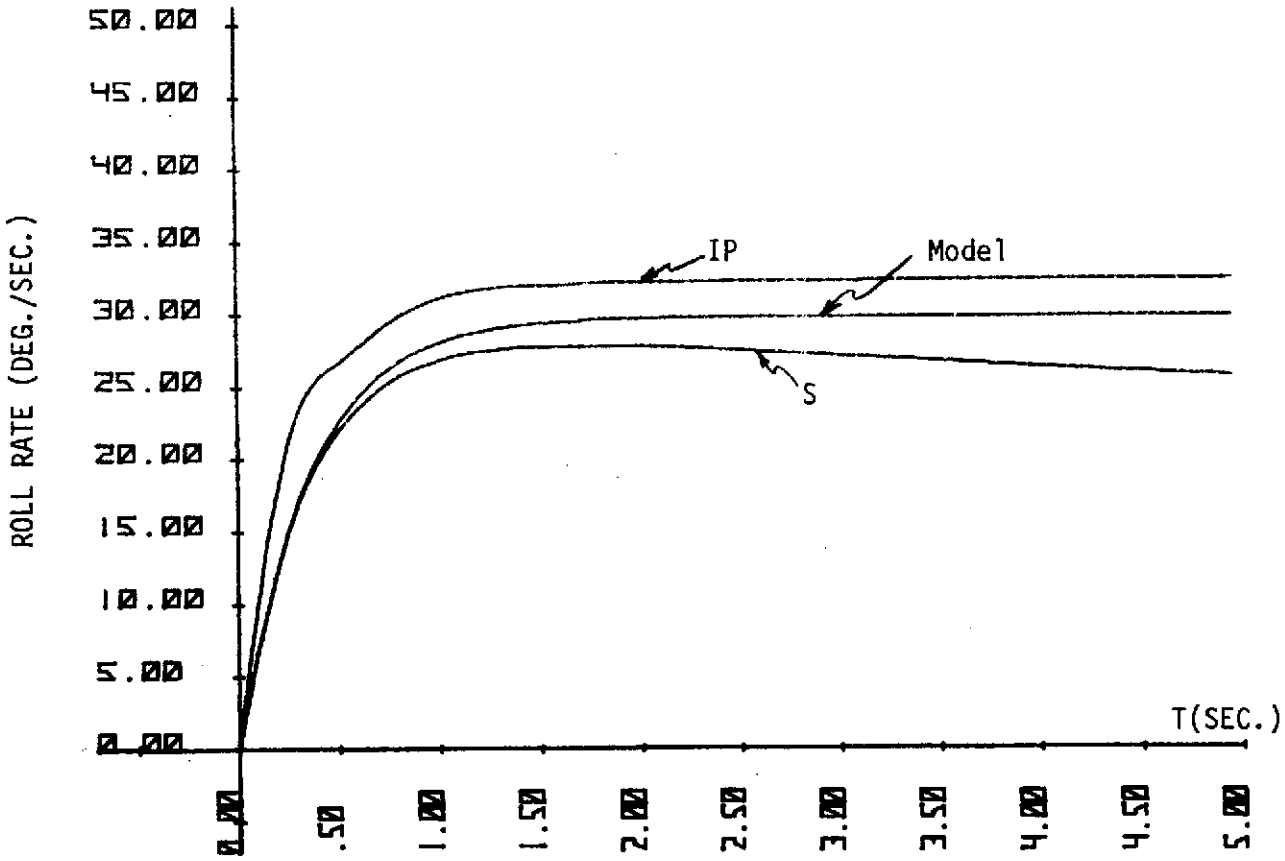

Flight Condition D; $\delta_a^p = 5°$, $\delta_r^p = 0°$; $\delta^a(0) = 0°$.
Figure A69.

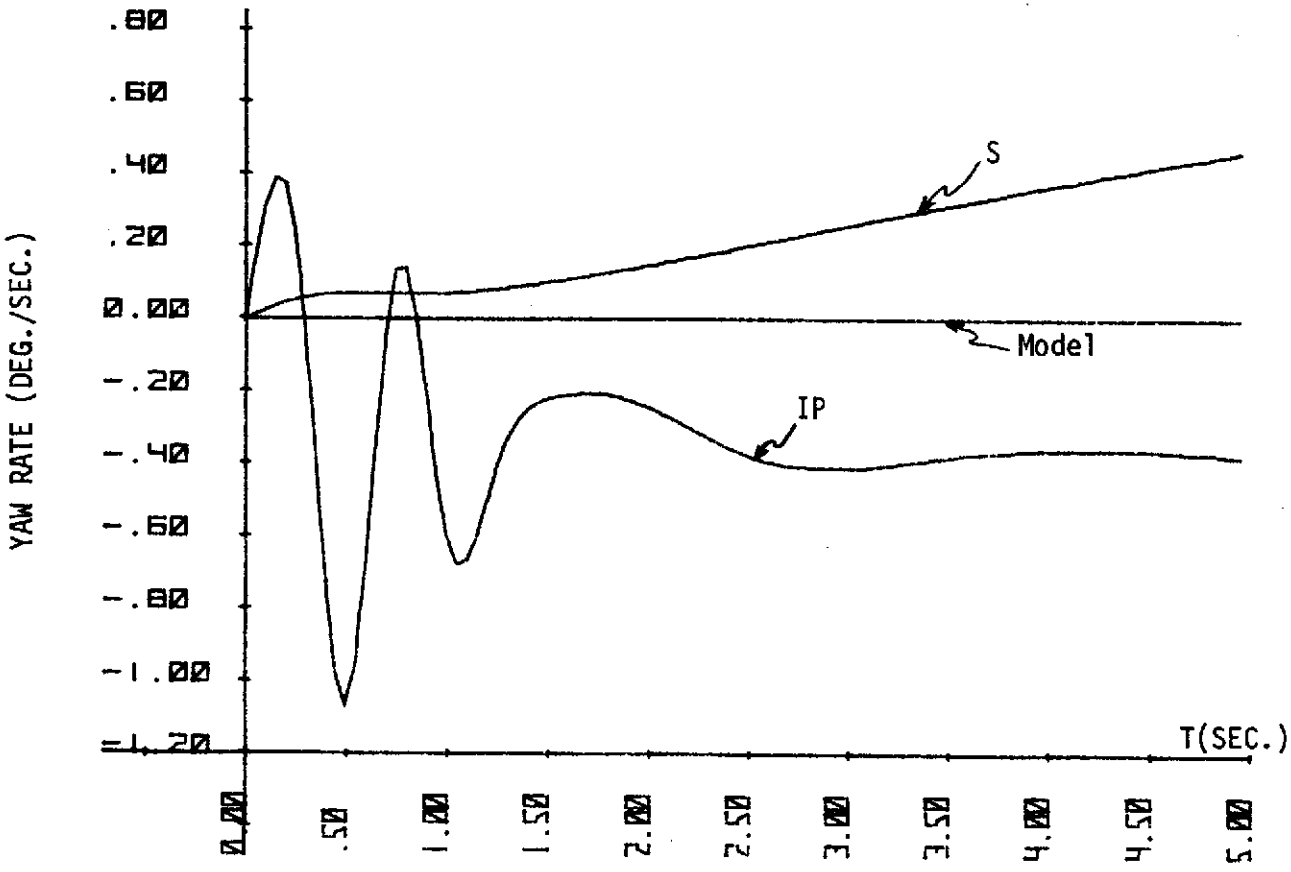

Flight Condition D; $\delta_a^p = 5°$, $\delta_r^p = 0°$; $\delta^a(0) = 0°$.
Figure A70.

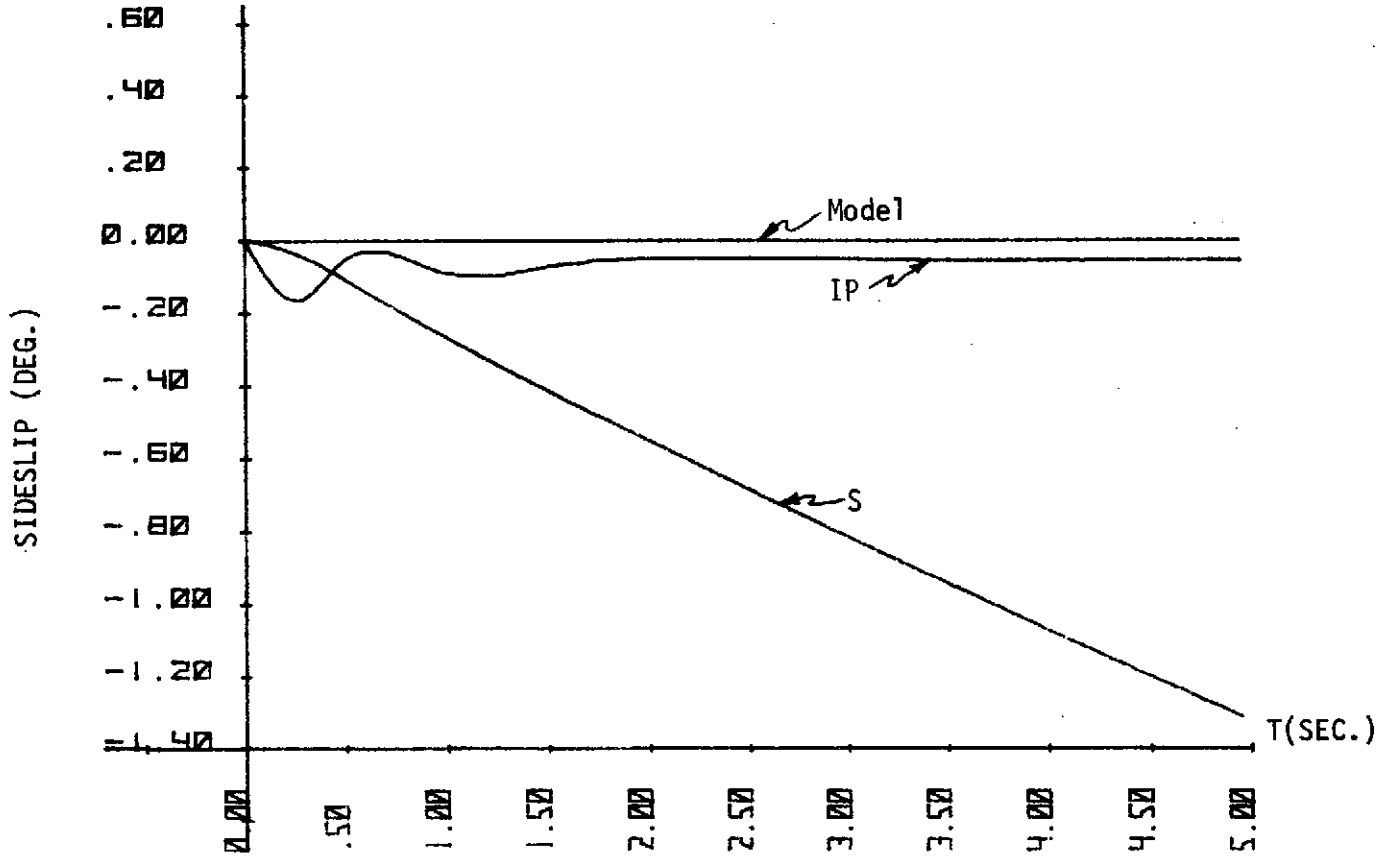

Flight Condition D; $\delta_a^p = 5°$, $\delta_r^p = 0°$, $\delta^a(0) = 0°$.

Figure A71.

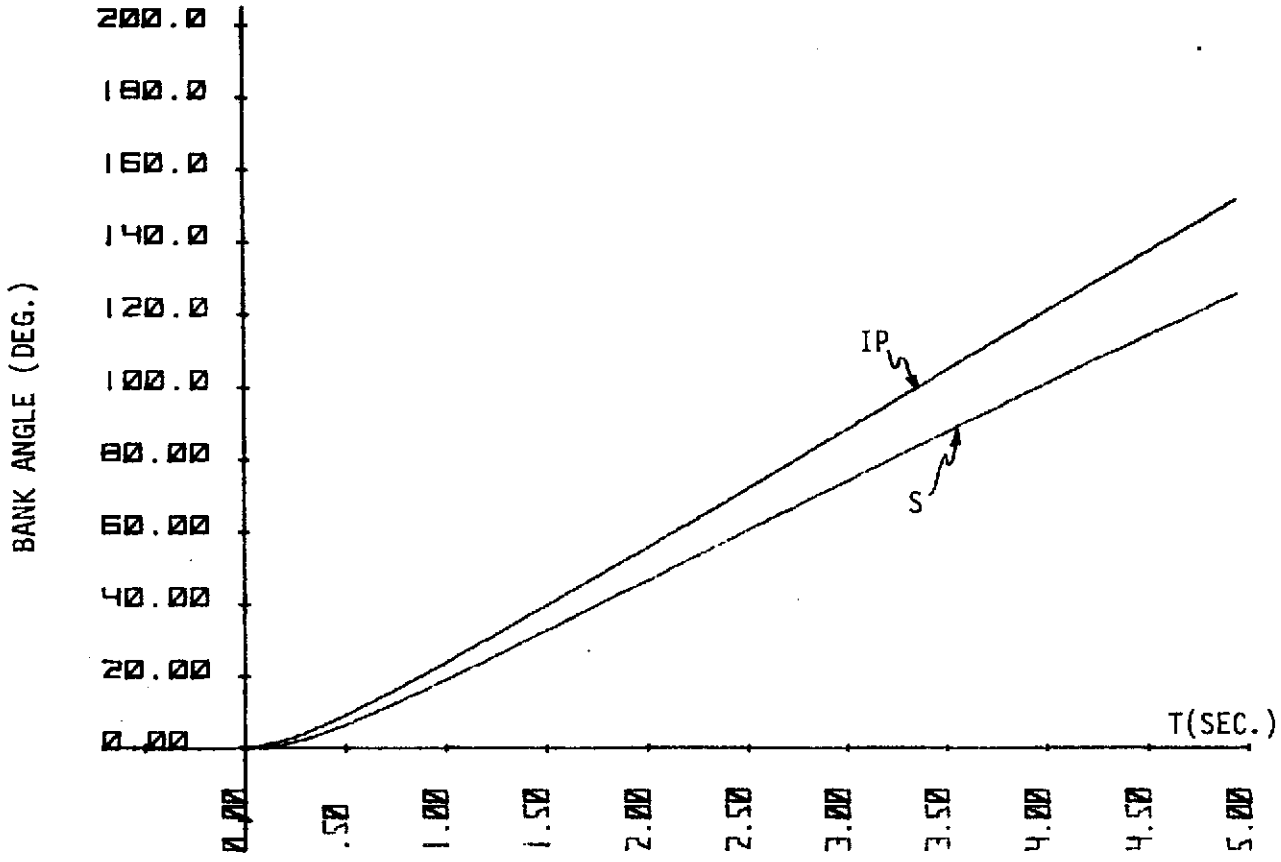

Flight Condition D; $\delta_a^p = 5°$, $\delta_r^p = 0°$; $\delta^a(0) = 0°$.

Figure A72.

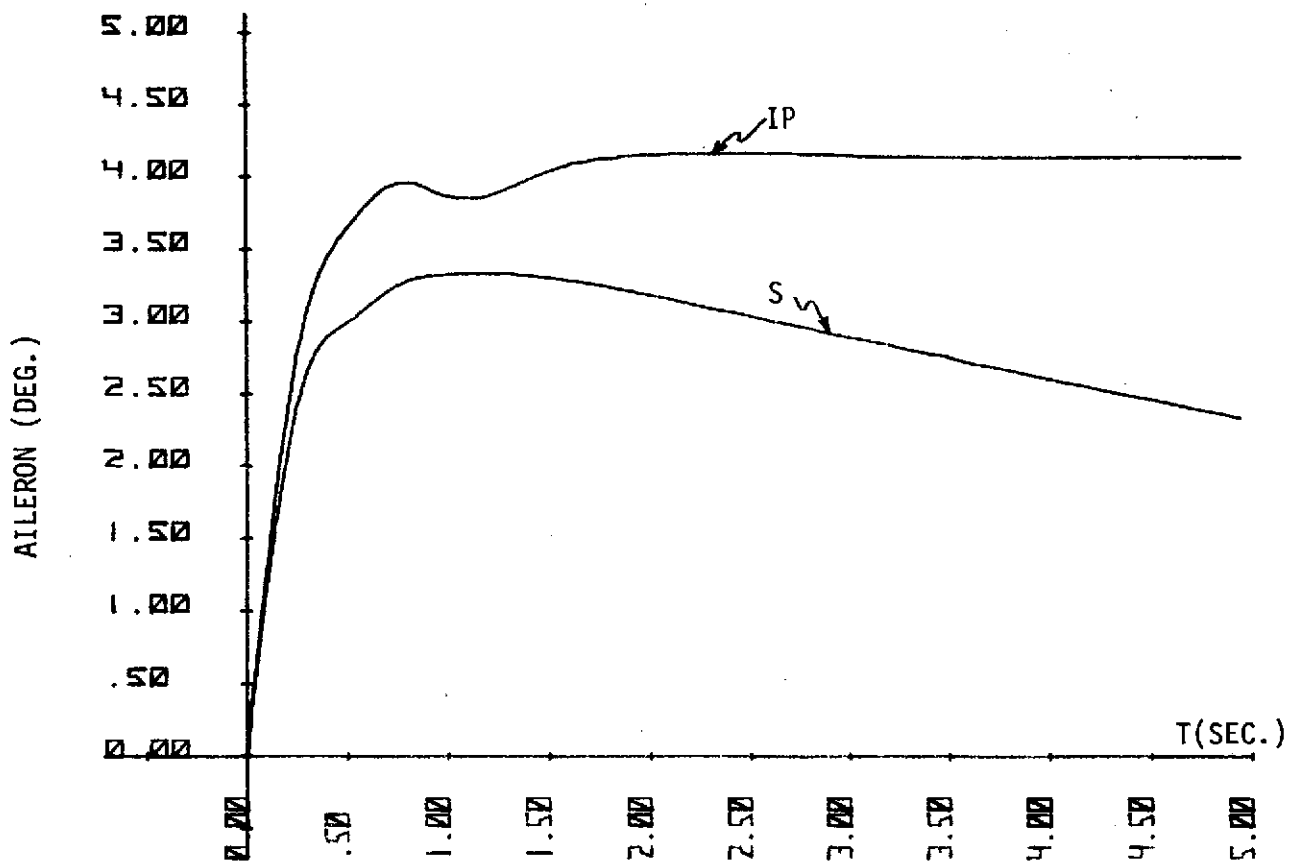

Flight Condition D; $\delta_a^p = 5°$, $\delta_r^p = 0°$; $\delta^a(0) = 0°$.

Figure A73.

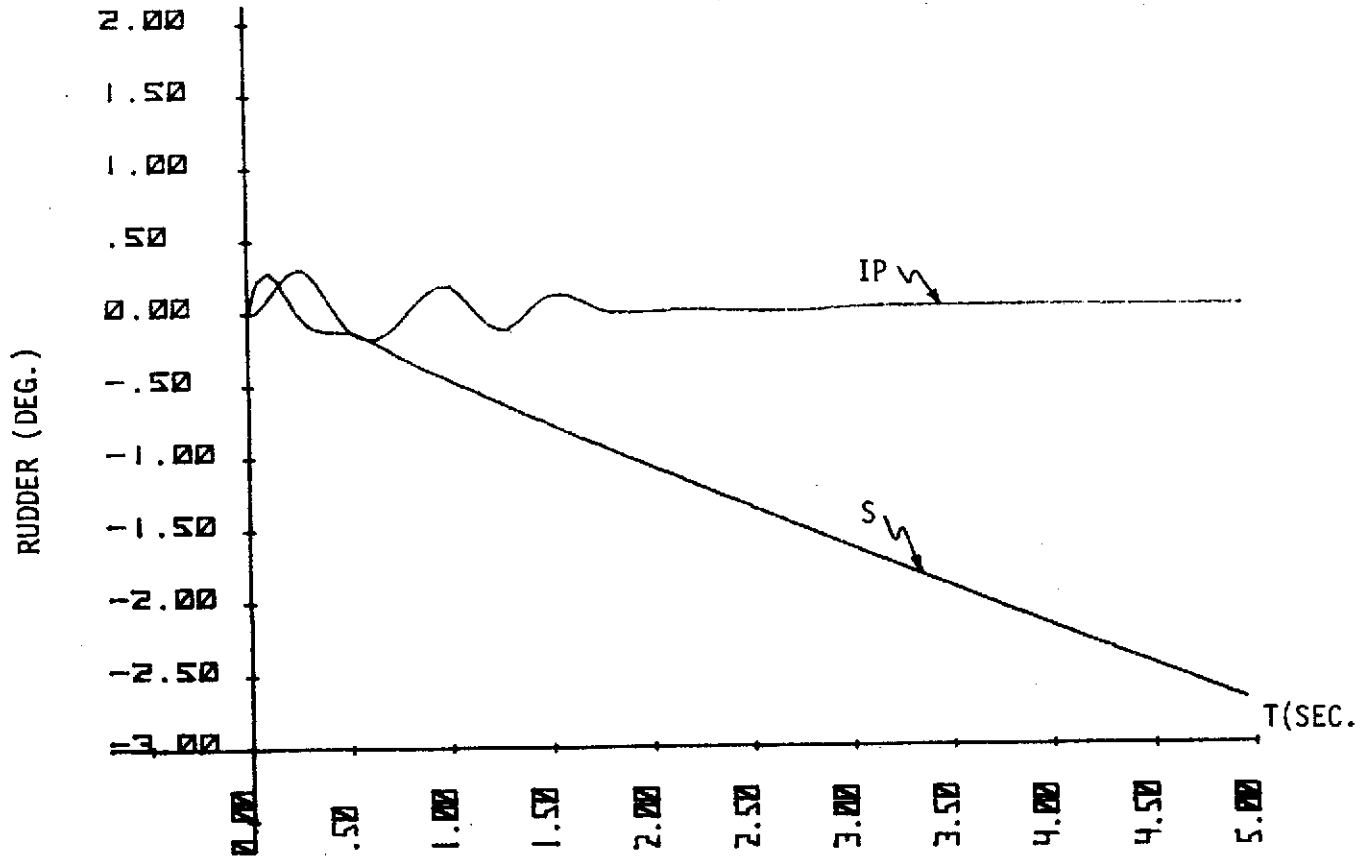

Flight Condition D; $\delta_a^p = 5°$, $\delta_r^p = 0°$; $\delta^a(0) = 0°$.

Figure A74.

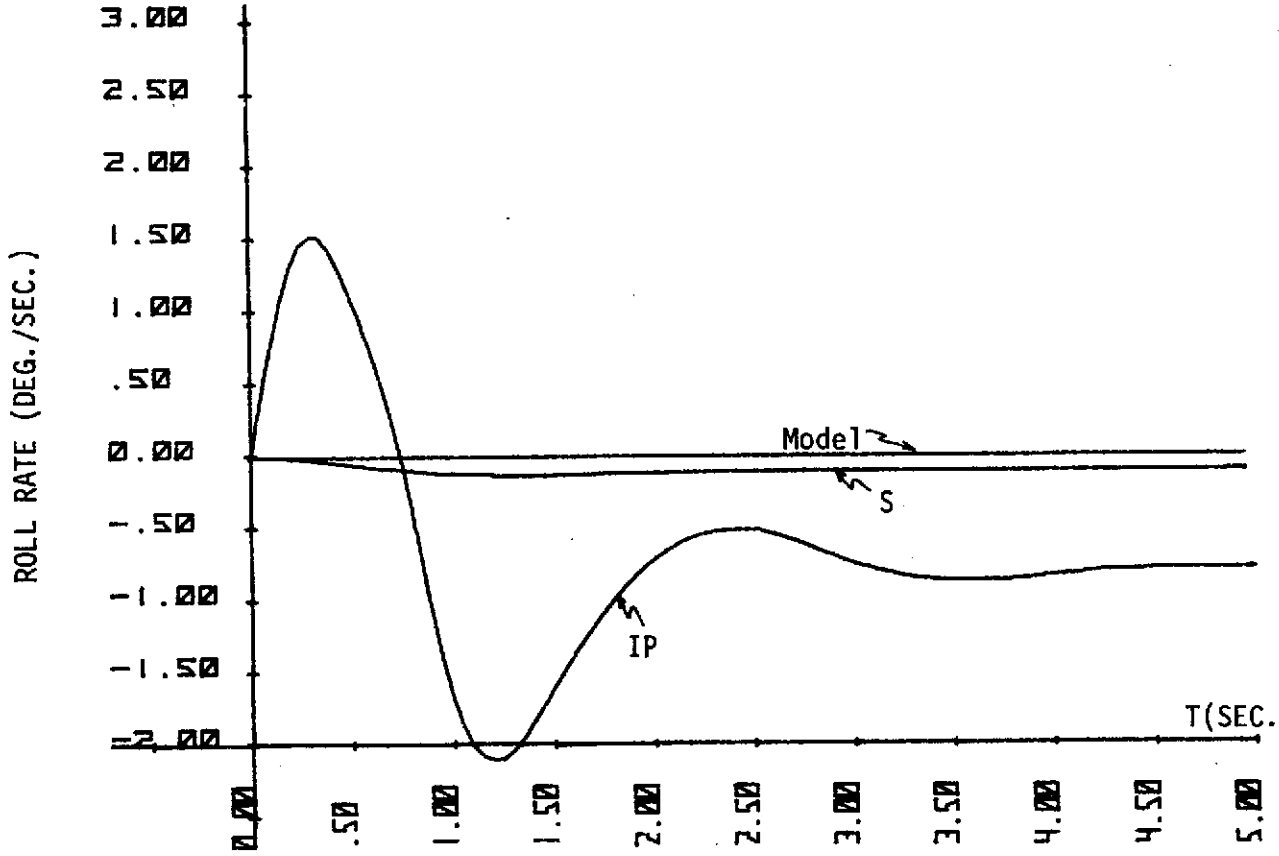

Flight Condition D ; $\delta_a^p = 0°$, $\delta_r^p = 3°$; $\delta^a(0) = 0°$.

Figure A75.

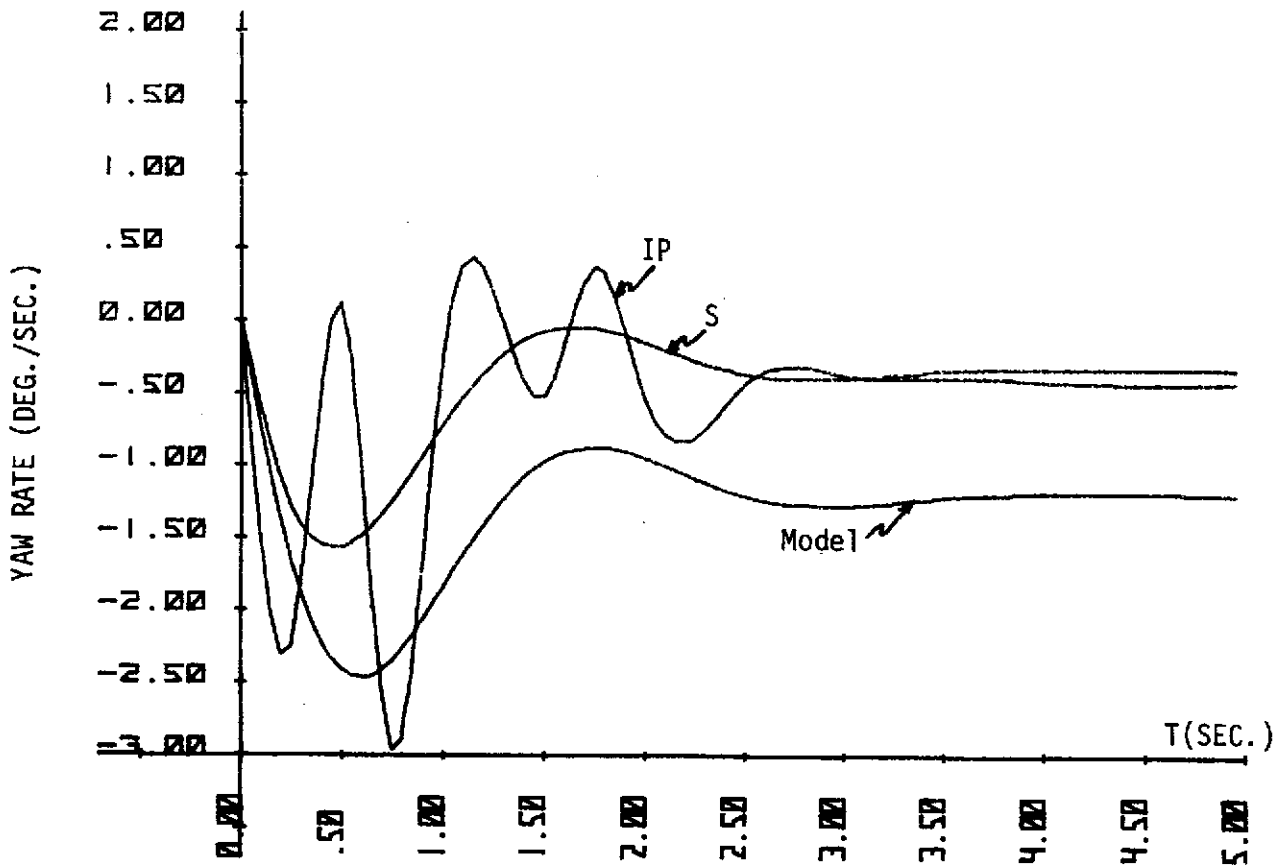

Flight Condition D ; $\delta_a^p = 0°$, $\delta_r^p = 3°$; $\delta^a(0) = 0°$.

Figure A76.

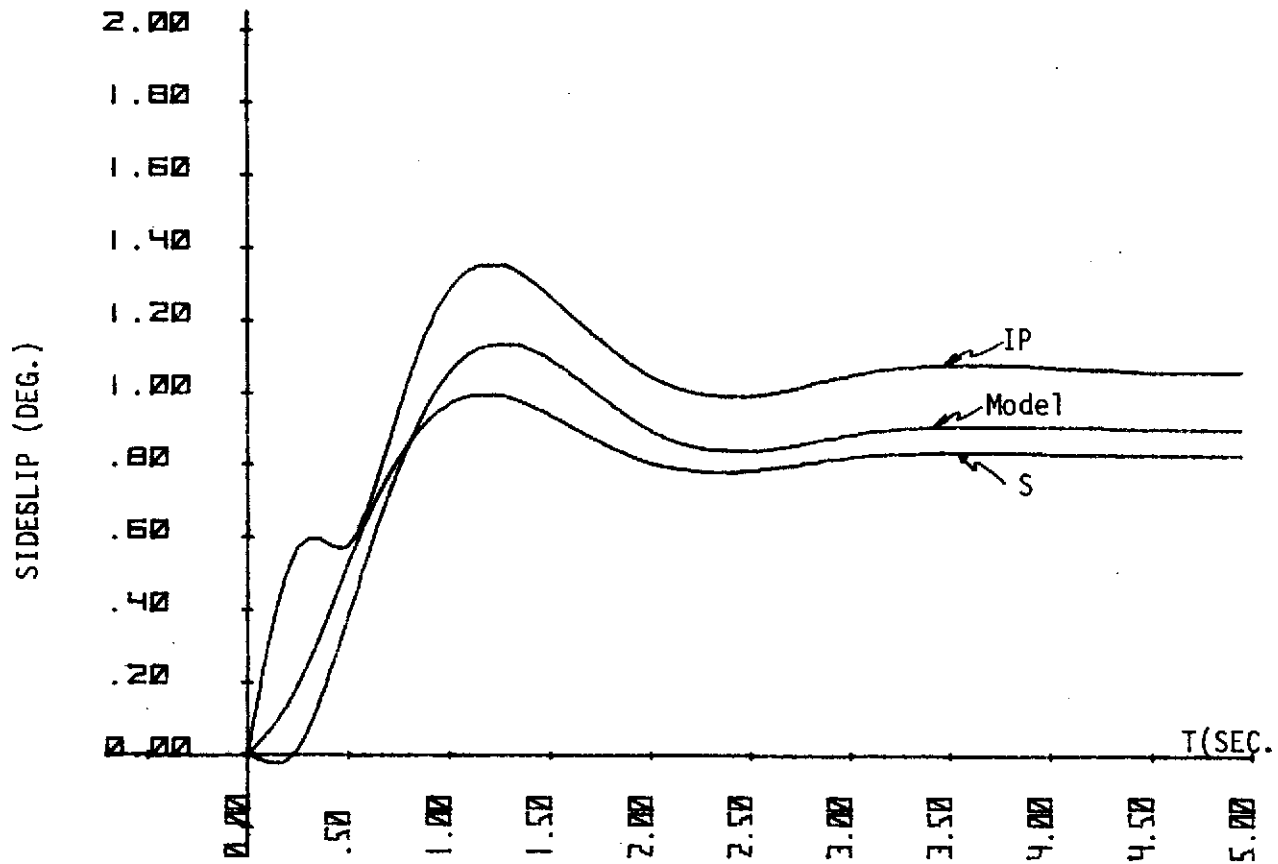

Flight Condition D ; $\delta_a^p = 0°$, $\delta_r^p = 3°$; $\delta^a(0) = 0°$.

Figure A77.

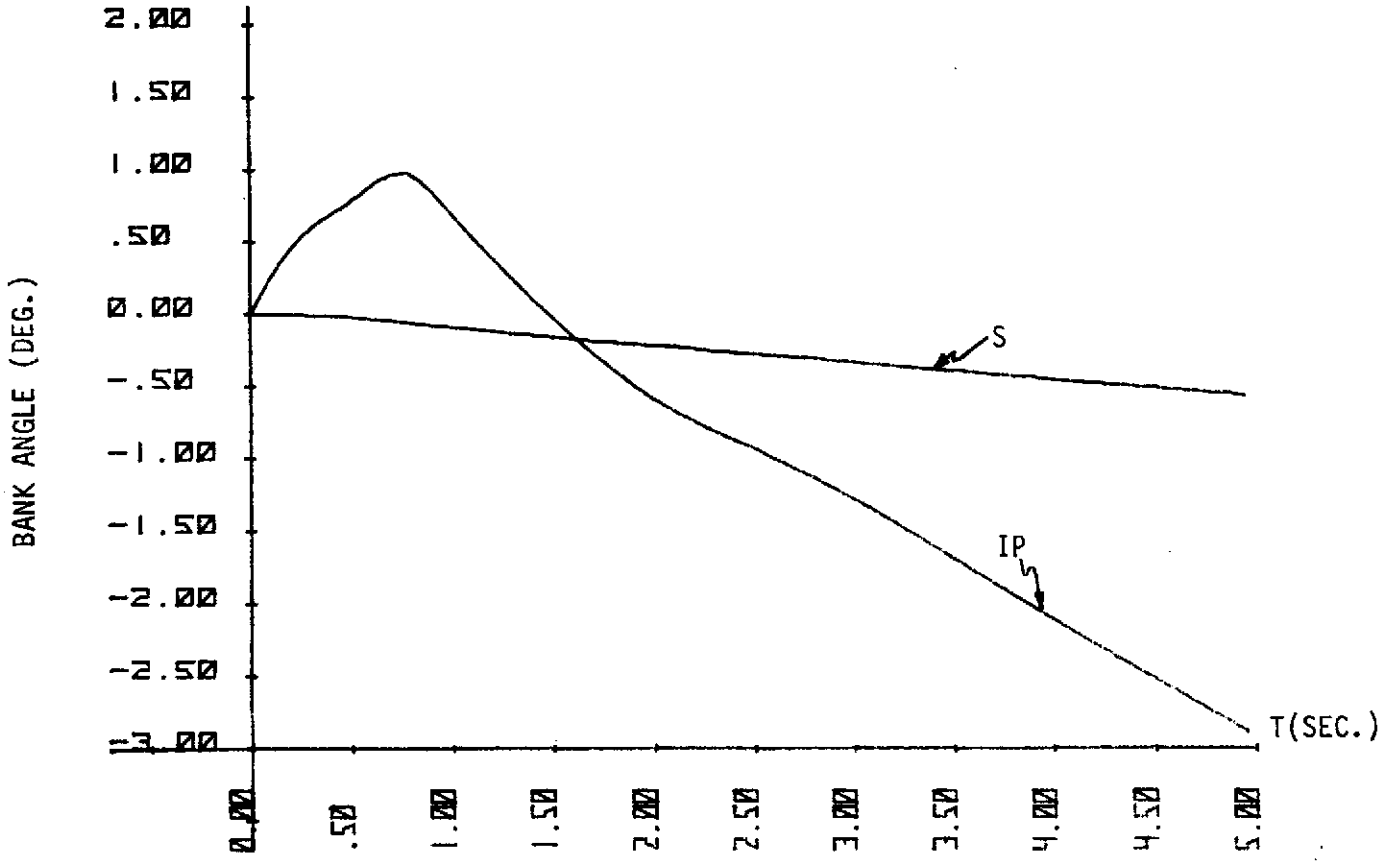

Flight Condition D; $\delta_a^p = 0°$, $\delta_r^p = 3°$; $\delta^a(0) = 0°$.

Figure A78.

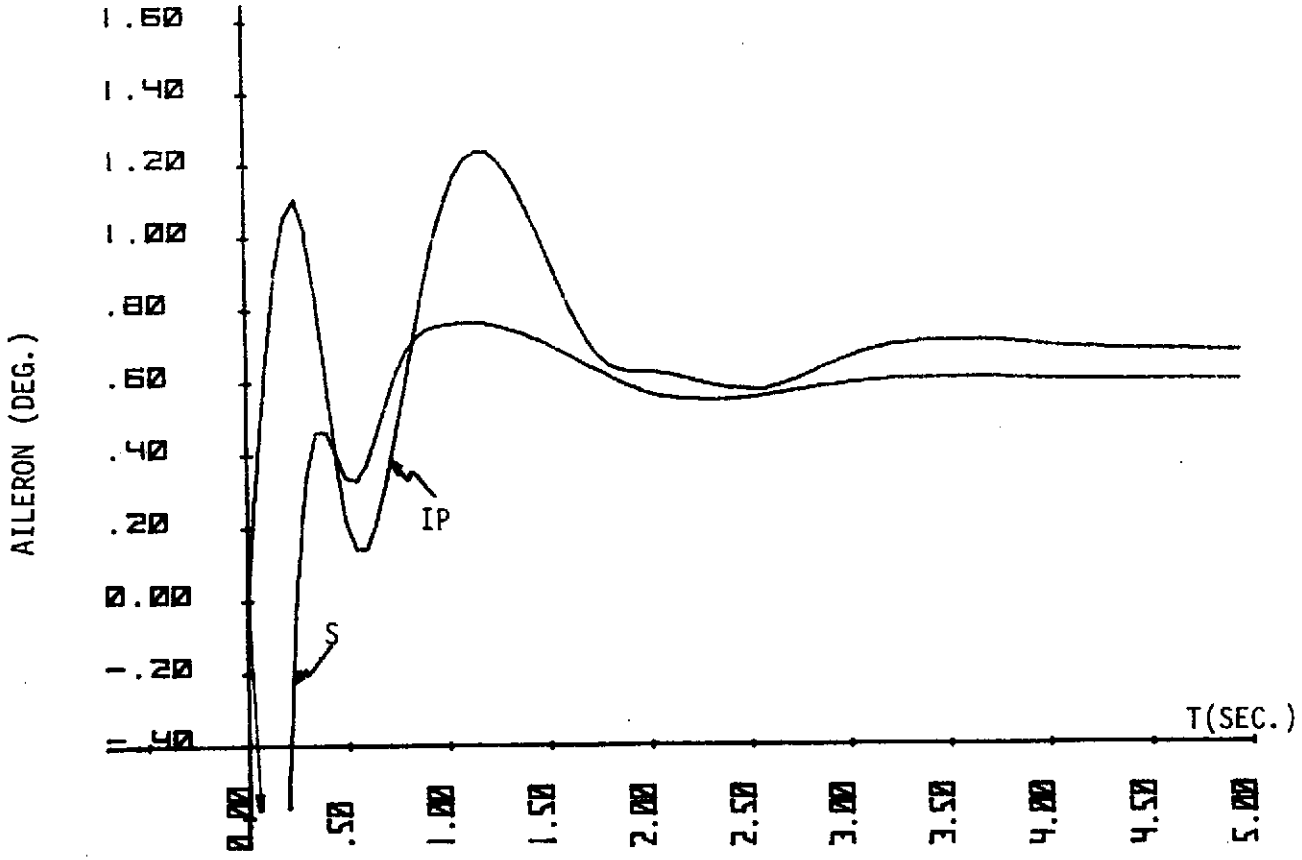

Flight Condition D; $\delta_a^p = 0°$, $\delta_r^p = 3°$; $\delta^a(0) = 0°$.

Figure A79.

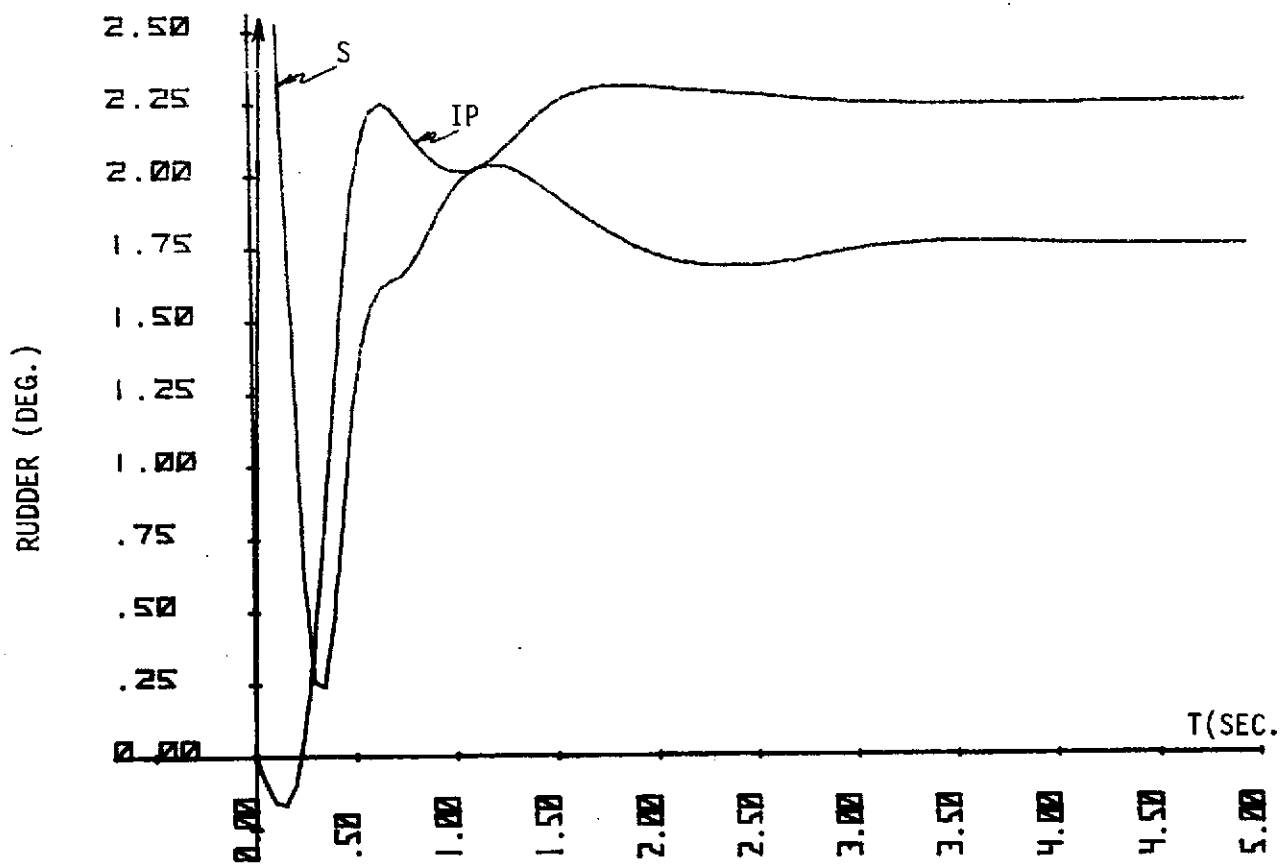

Flight Condition D; $\delta_a^p = 0°$, $\delta_r^p = 3°$; $\delta^a(0) = 0°$.
Figure A80.

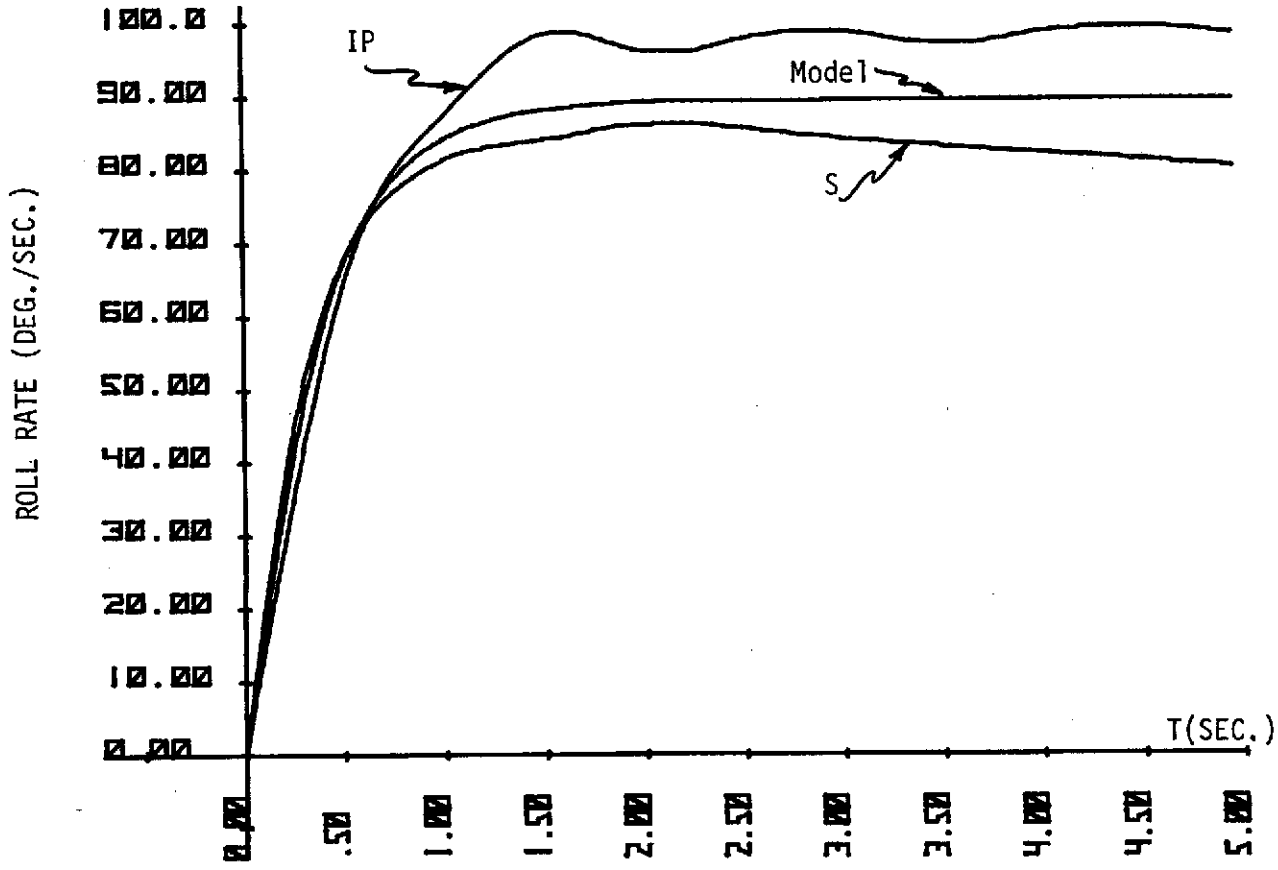

Flight Condition A; $\delta_a^p = 15°$, $\delta_r^p = 0°$; $\delta^a(0) = 0°$;
Rate and Magnitude Constrained.
Figure A81.

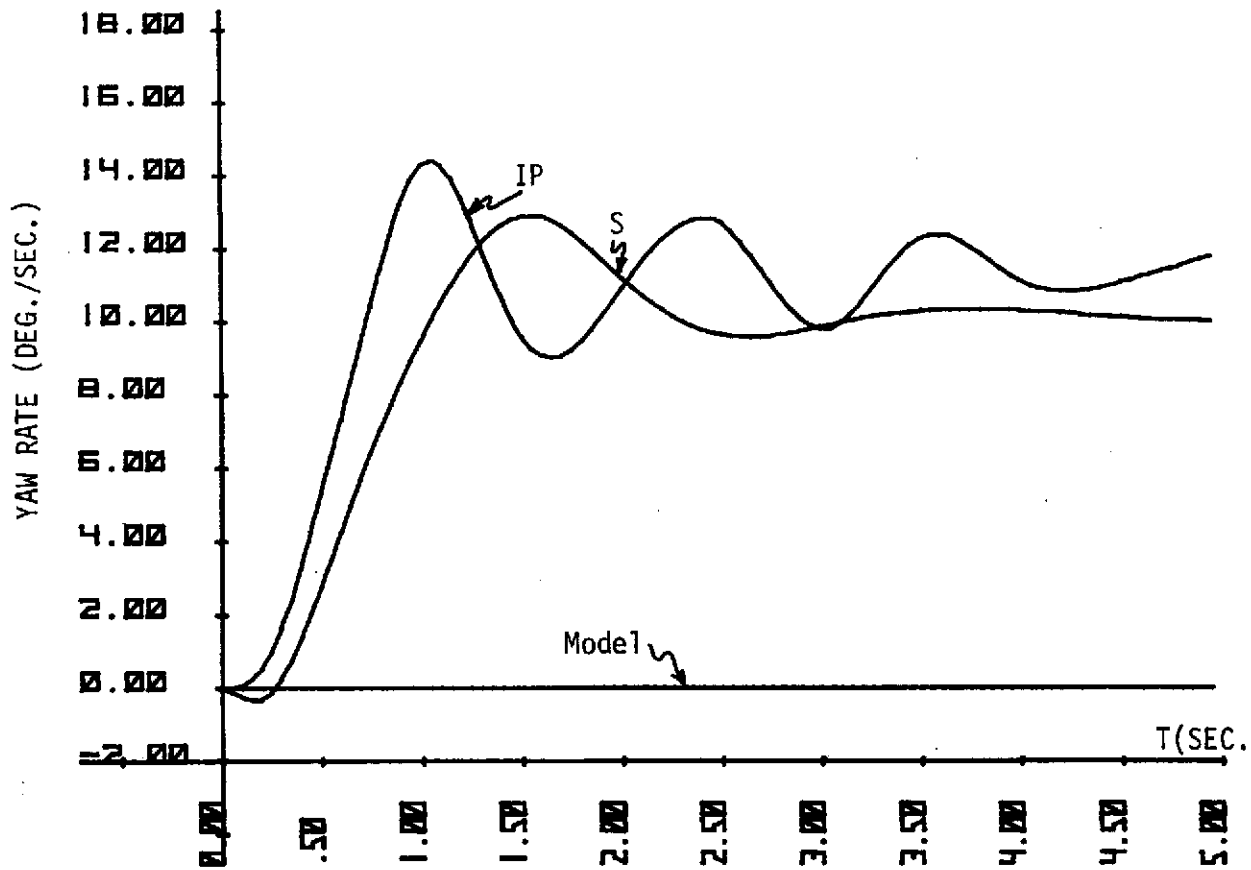

Flight Condition A; $\delta_a^p = 15°$, $\delta_r^p = 0°$; $\delta^a(0) = 0°$;

Rate and Magnitude Constrained.

Figure A82.

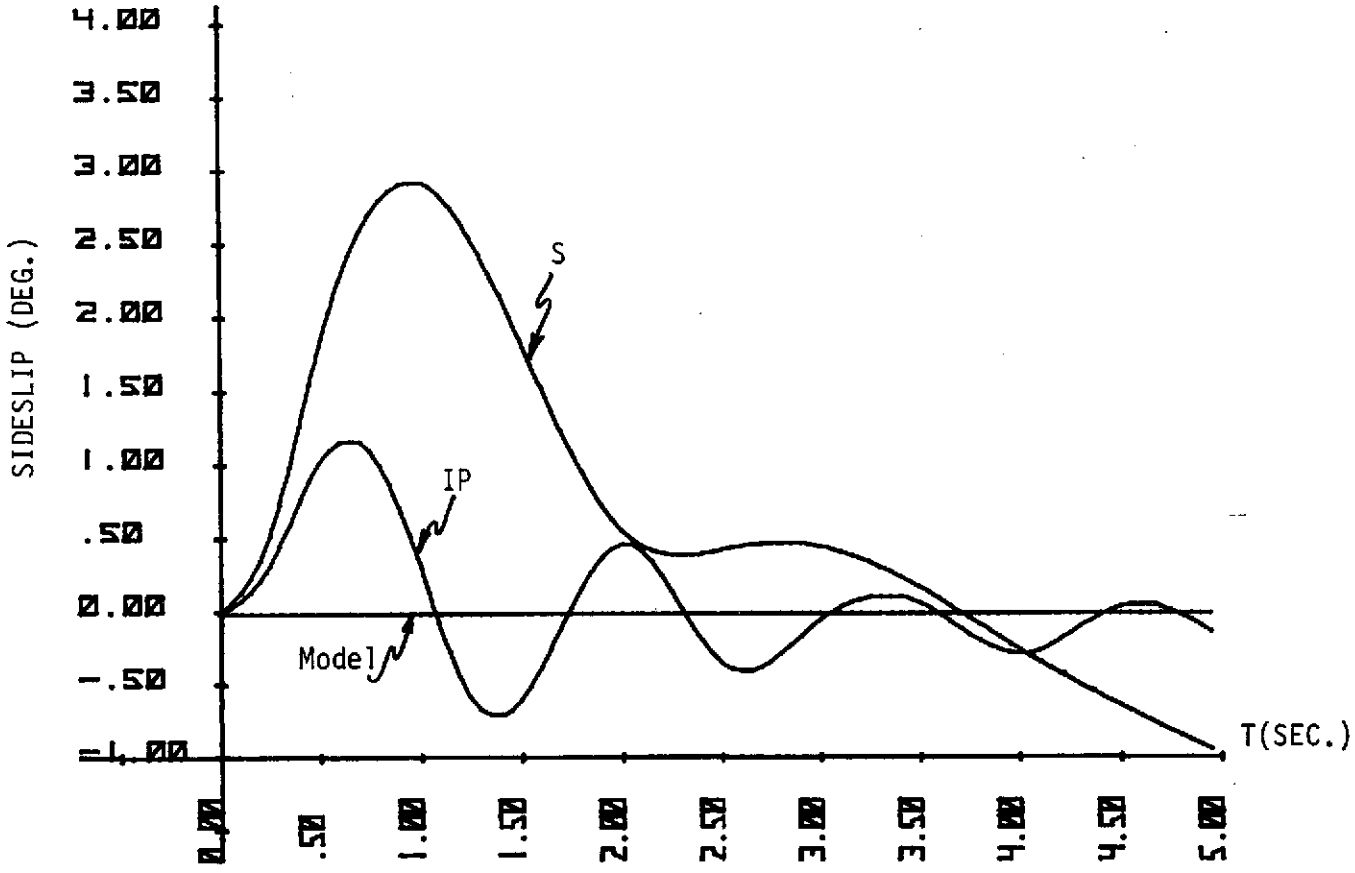

Flight Condition A; $\delta_a^p = 15°$, $\delta_r^p = 0°$; $\delta^a(0) = 0°$;

Rate and Magnitude Constrained.

Figure A83.

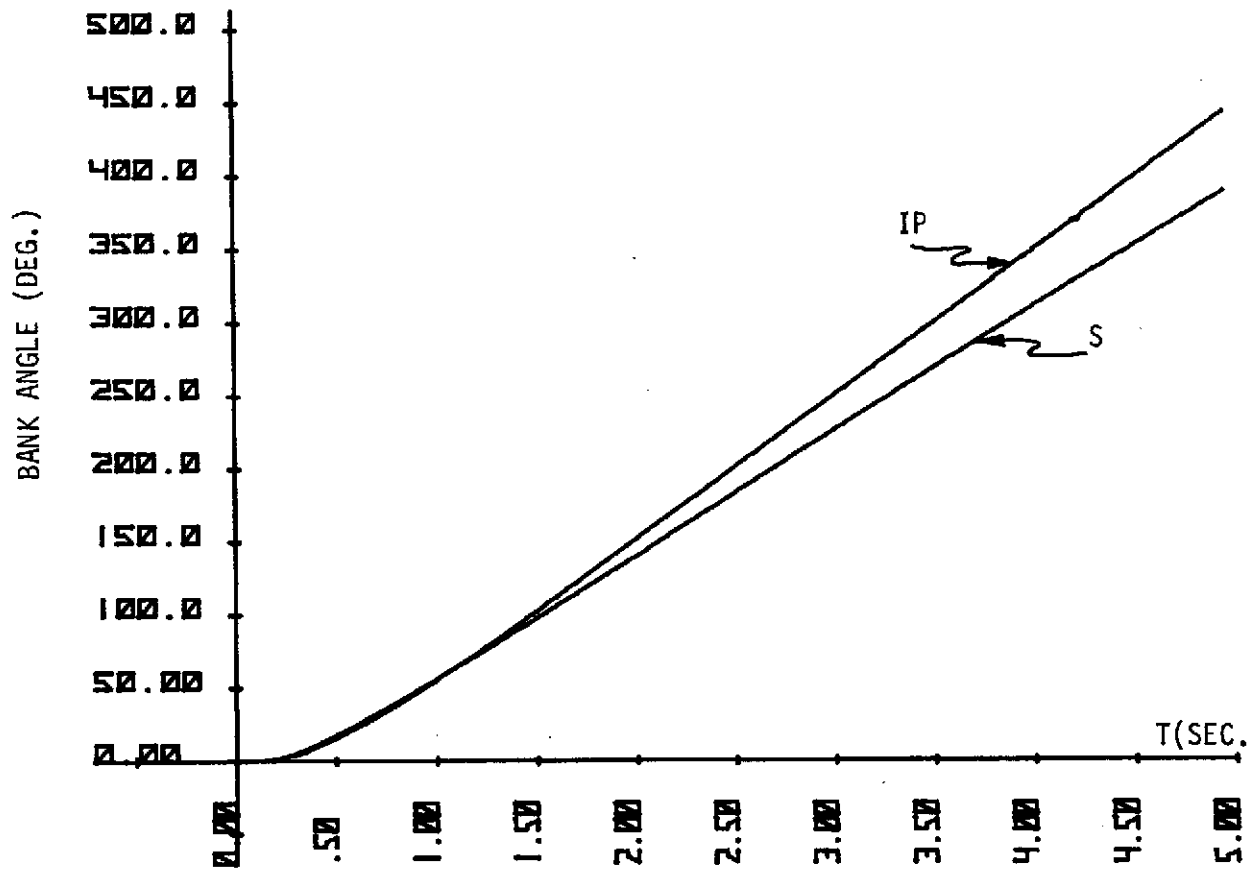

Flight Condition A; $\delta_a^p = 15°$, $\delta_r^p = 0°$; $\delta^a(0) = 0°$;
Rate and Magnitude Constrained.
Figure A84.

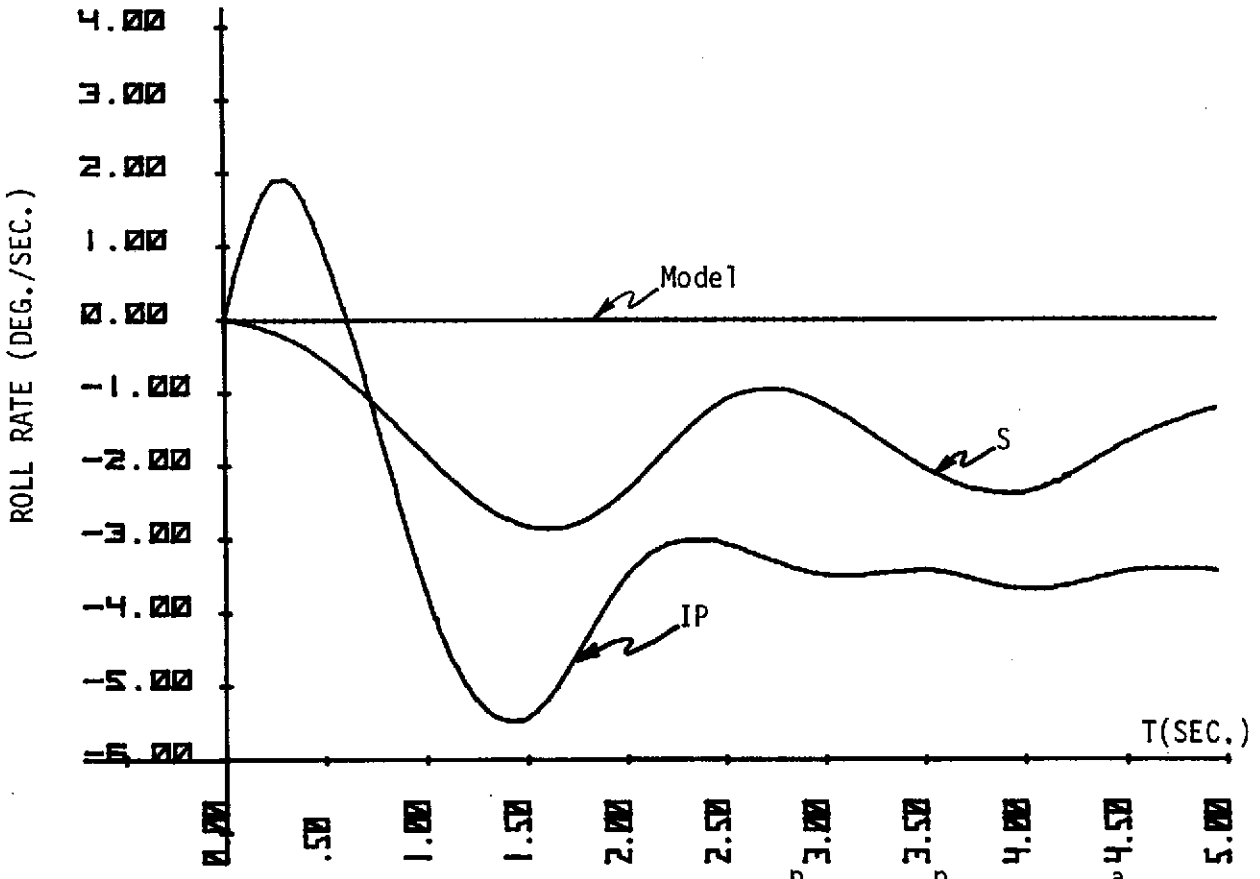

Flight Condition A; $\delta_a^p = 0°$, $\delta_r^p = 4.5°$; $\delta^a(0) = 0°$;
Rate and Magnitude Constrained.
Figure A85.

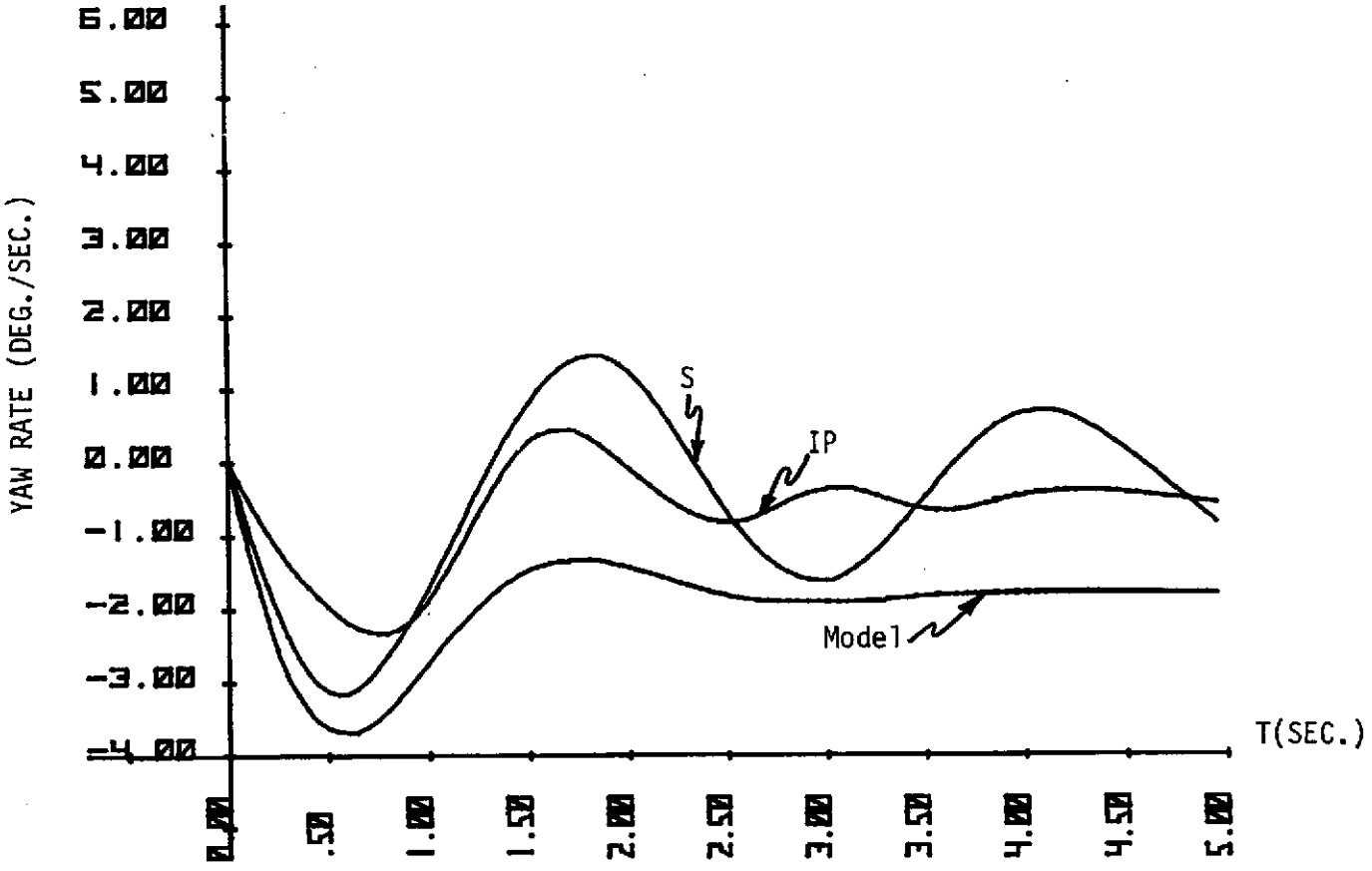

Flight Condition A; $\delta_a^p = 0°$, $\delta_r^p = 4.5°$; $\delta^a(0) = 0°$;

Rate and Magnitude Constrained.

Figure A86.

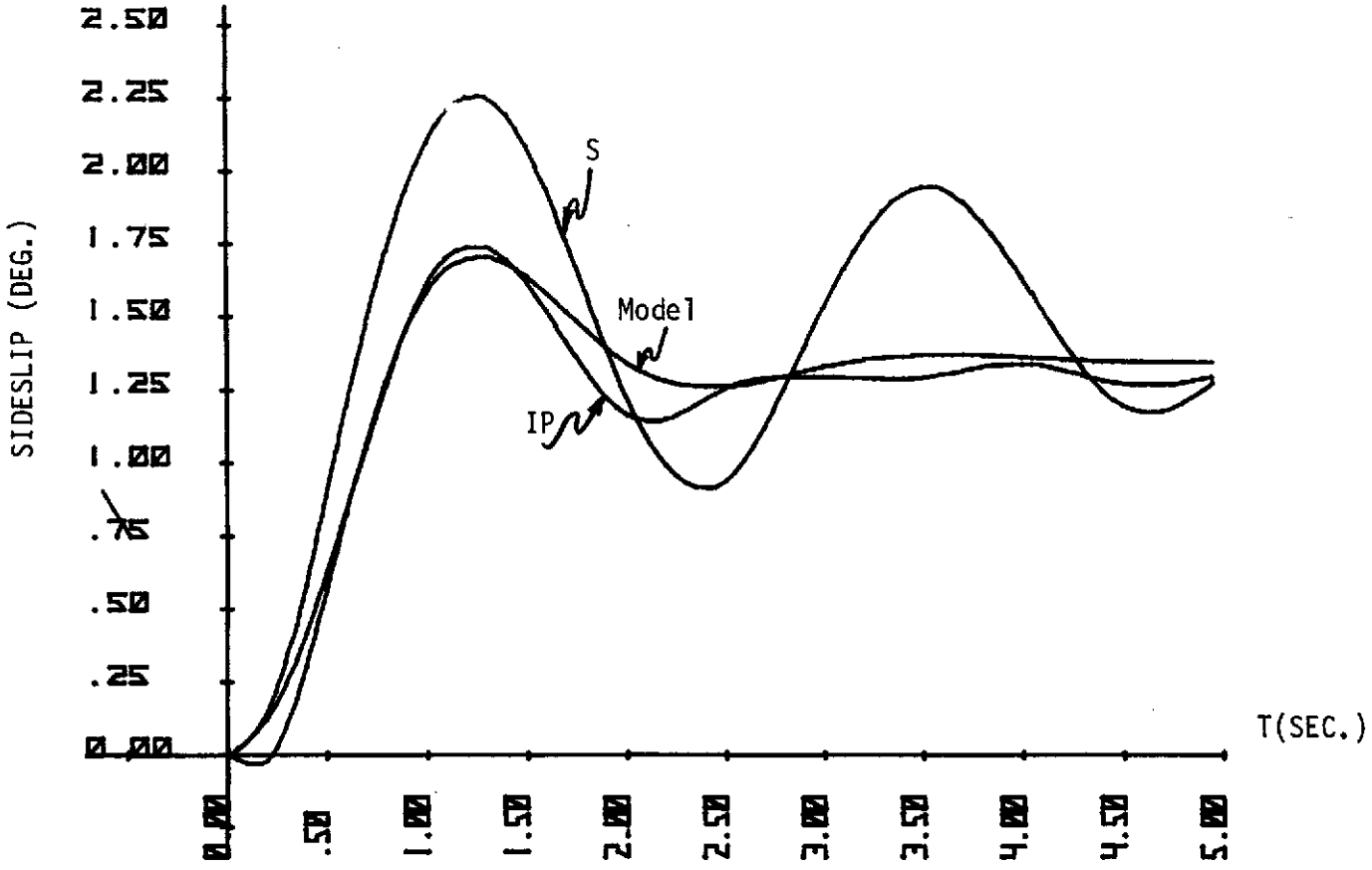

Flight Condition A; $\delta_a^p = 0°$, $\delta_r^p = 4.5°$; $\delta^a(0) = 0°$;
Rate and Magnitude Constrained.
Figure A87.

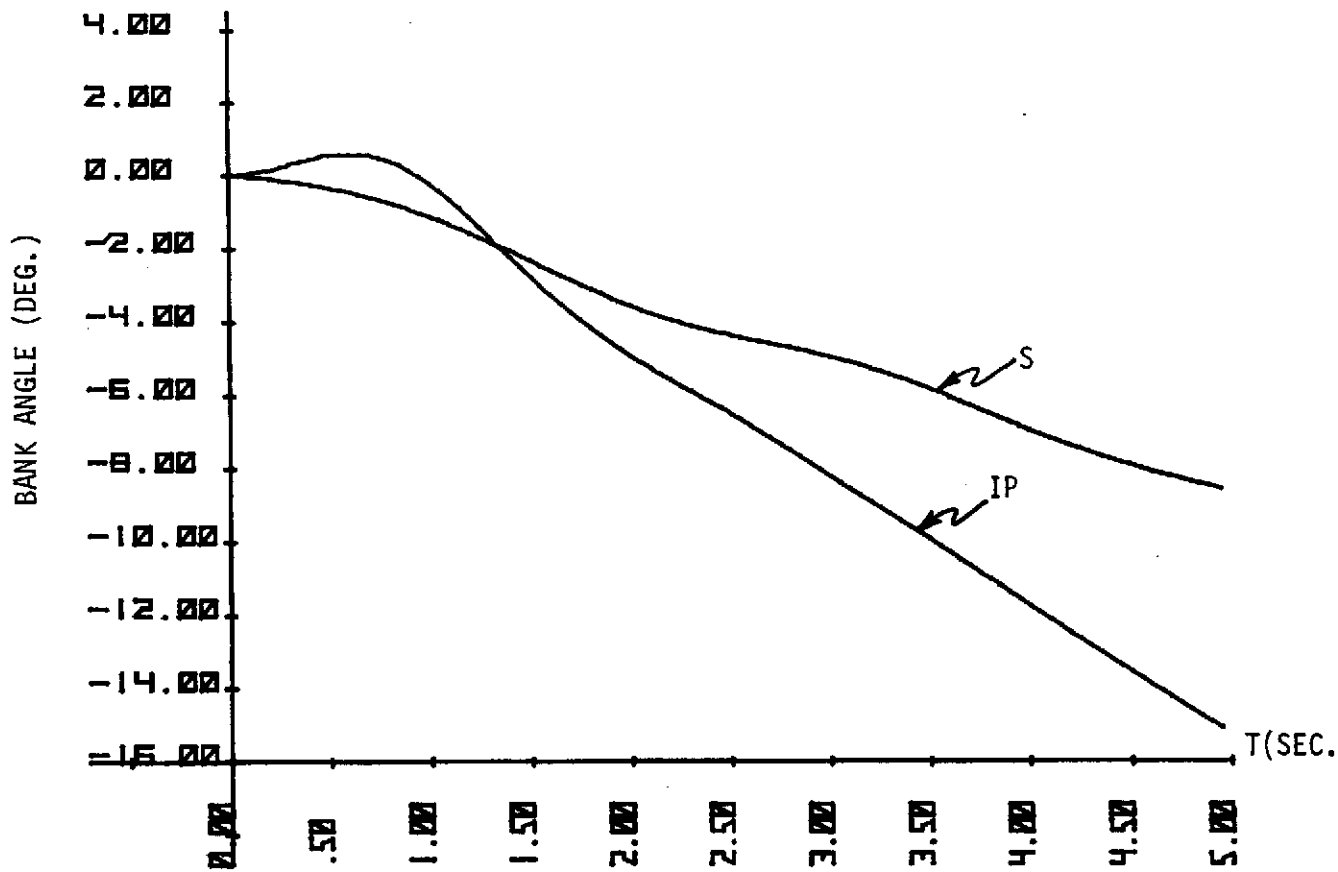

Flight Condition A; $\delta_a^p = 0°$, $\delta_r^p = 4.5°$; $\delta^a(0) = 0°$;
Rate and Magnitude Constrained.
Figure A88.

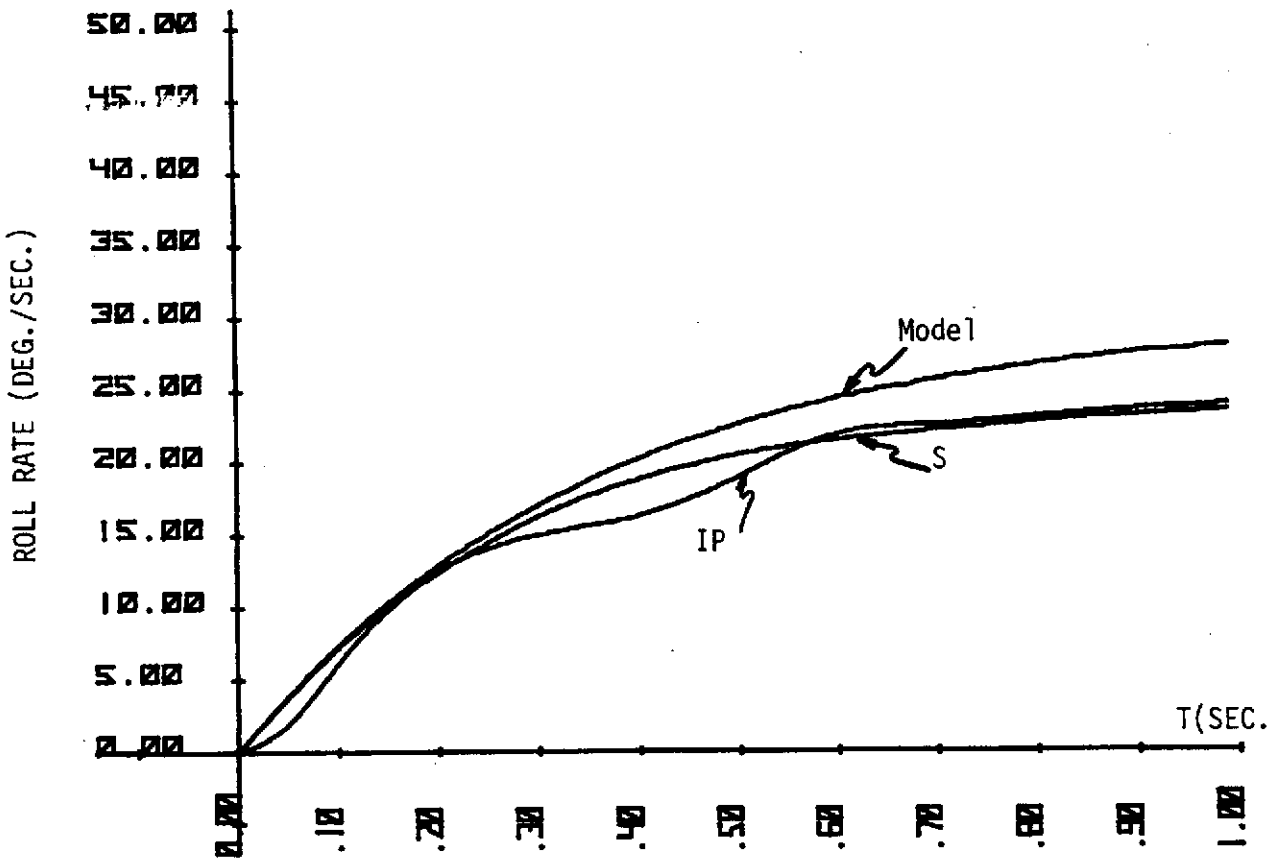

Flight Condition A; $\delta_a^p = 5°$, $\delta_r^p = 0°$; $\delta^a(0) = 0°$;

Rate and Magnitude Constrained

$\Delta\alpha = -8°/sec.$

Figure A89.

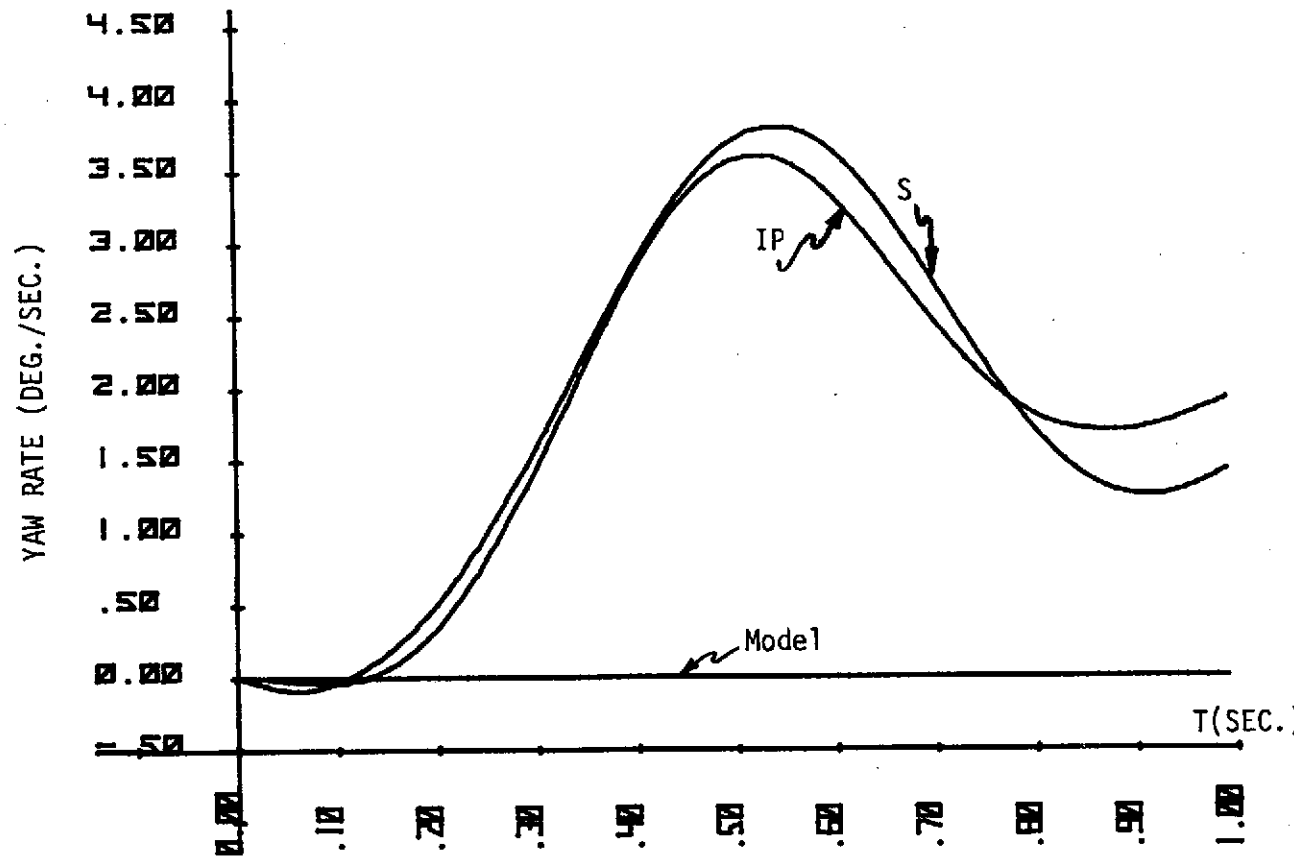

Flight Condition A; $\delta_a^p = 5°$, $\delta_r^p = 0°$; $\delta^a(0) = 0°$;

Rate and Magnitude Constrained

$\Delta\alpha = -8°/sec.$

Figure A90.

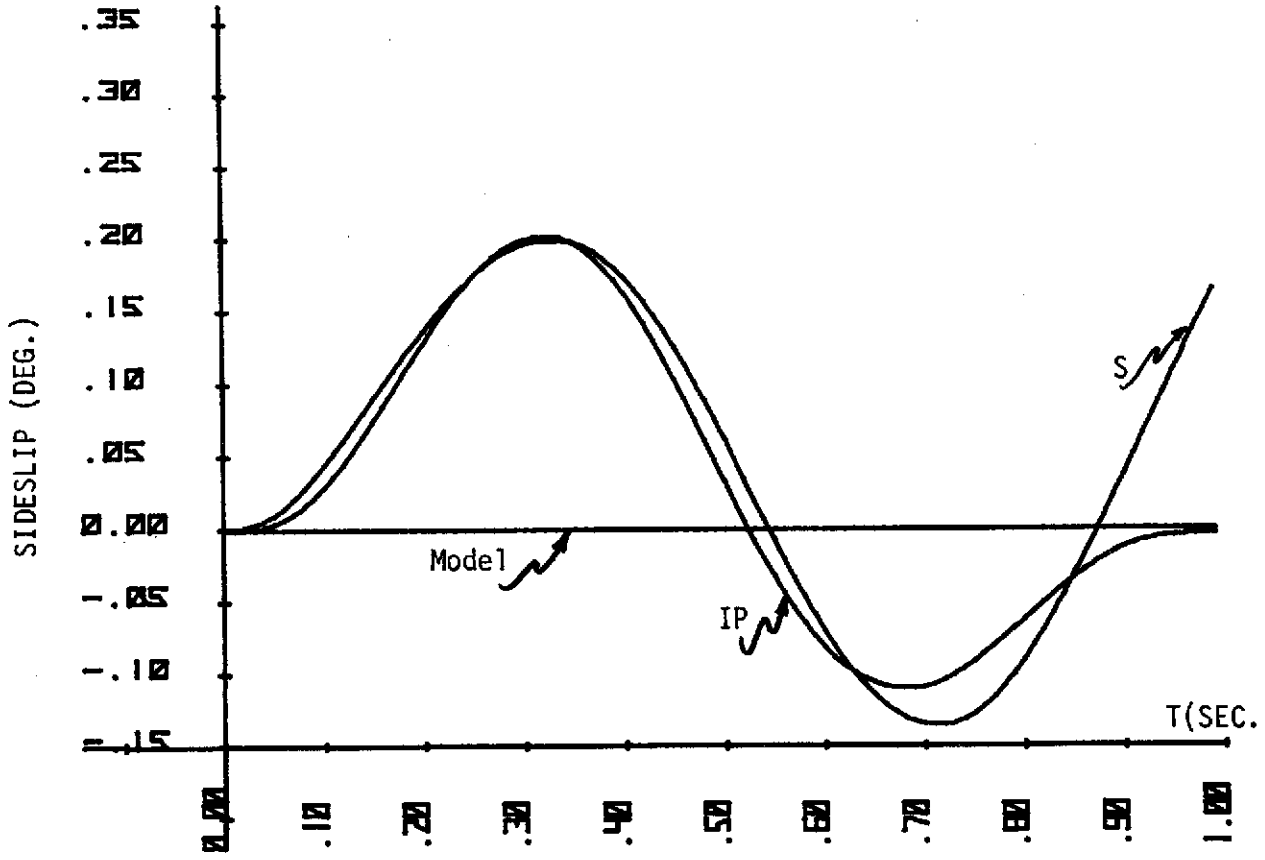

Flight Condition A; $\delta_a^p = 5°$, $\delta_r^p = 0°$; $\delta^a(0) = 0°$;

Rate and Magnitude Constrained

$\Delta\alpha = -8°/sec.$

Figure A91.

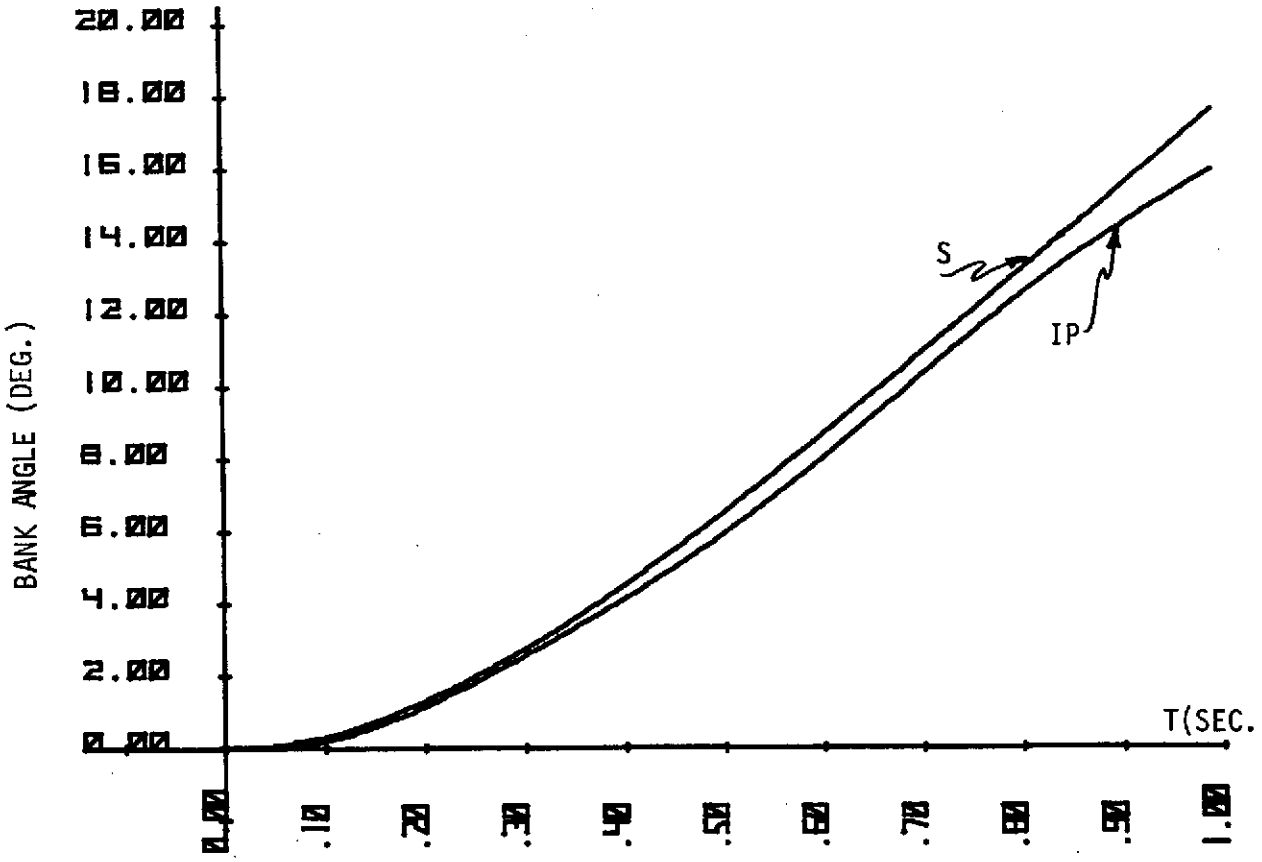

Flight Condition A; $\delta_a^p = 5°$, $\delta_r^p = 0°$; $\delta^a(0) = 0°$;

Rate and Magnitude Constrained

$\Delta\alpha = -8°/sec.$

Figure A92.

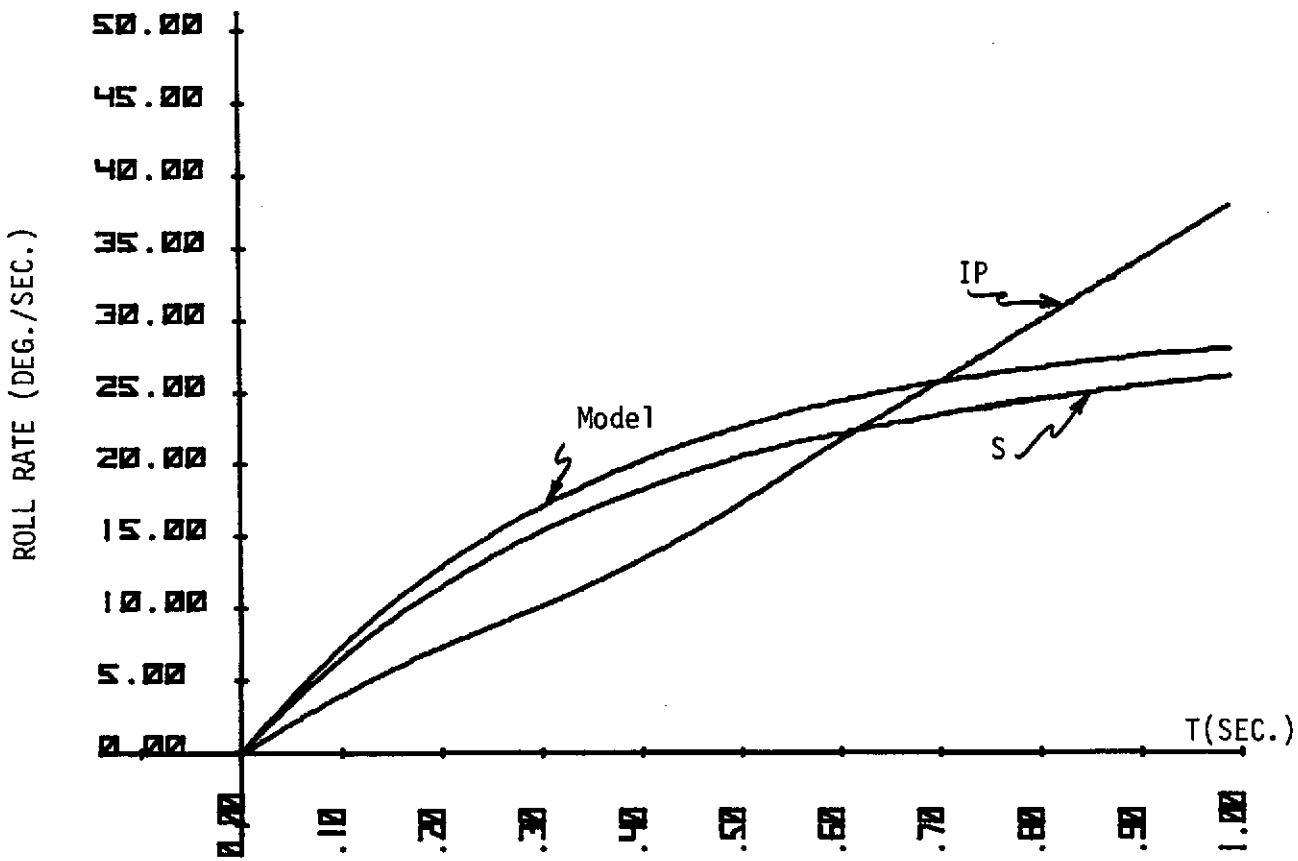

Flight Condition A; $\delta_a^p = 5°$, $\delta_r^p = 0°$; $\delta^a(0) = 0°$;

Rate and Magnitude Constrained

$\Delta\alpha = 8°/sec.$

Figure A93.

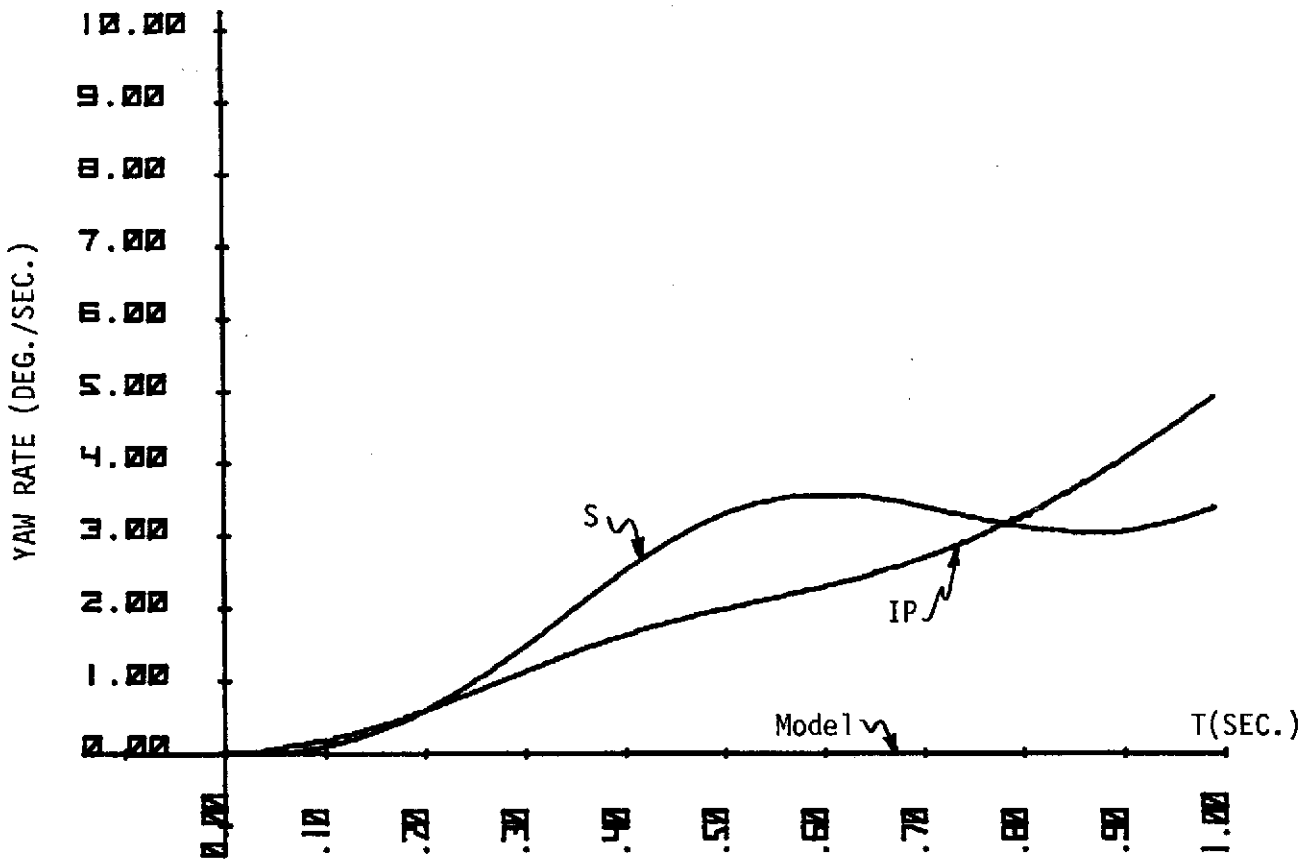

Flight Condition A; $\delta_a^p = 5°$, $\delta_r^p = 0°$; $\delta^a(0) = 0°$;

Rate and Magnitude Constrained

$\Delta\alpha = 8°/sec.$

Figure A94.

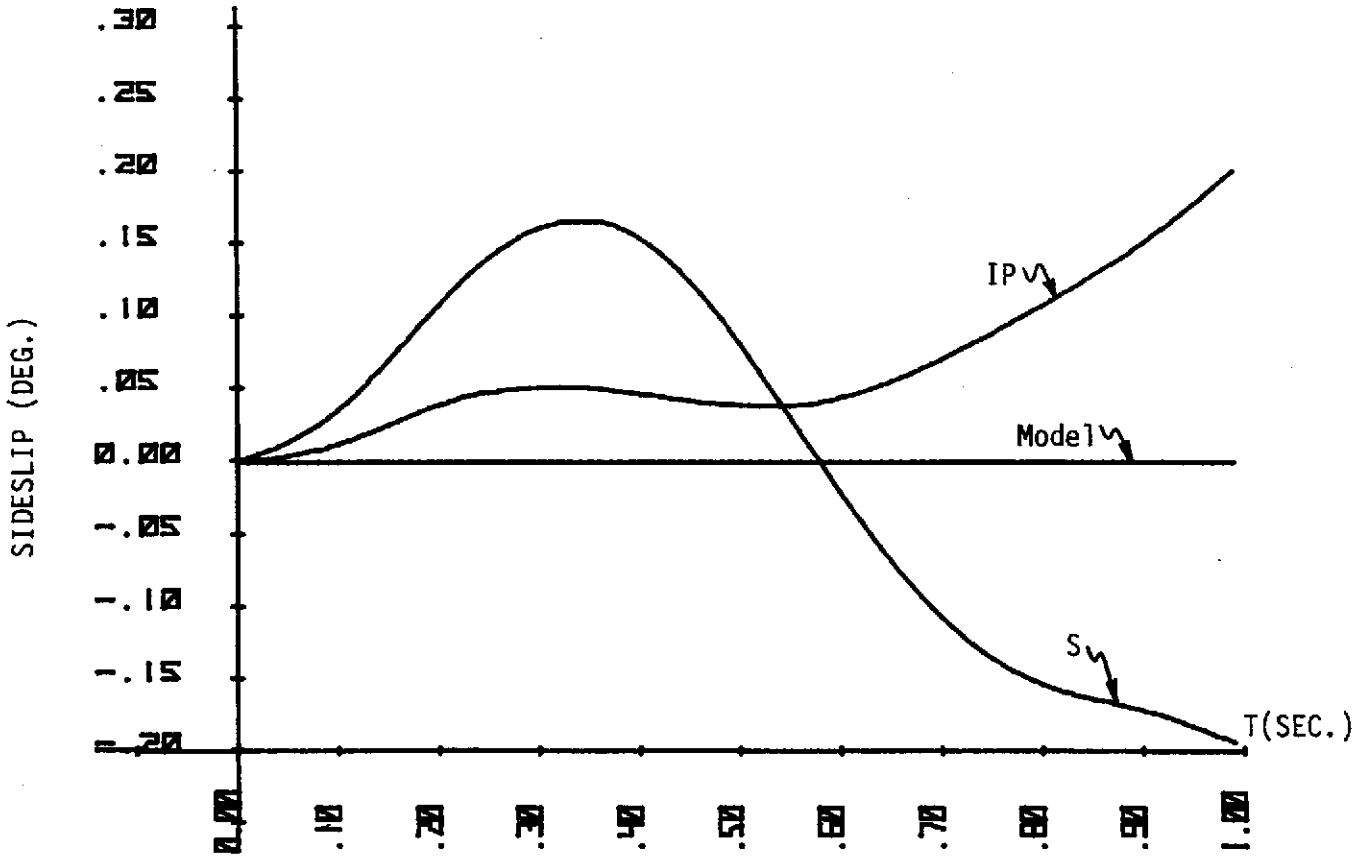

Flight Condition A; $\delta_a^p = 5°$, $\delta_r^p = 0°$; $\delta^a(0) = 0°$;

Rate and Magnitude Constrained

$\Delta\alpha = 8°/sec.$

Figure A95.

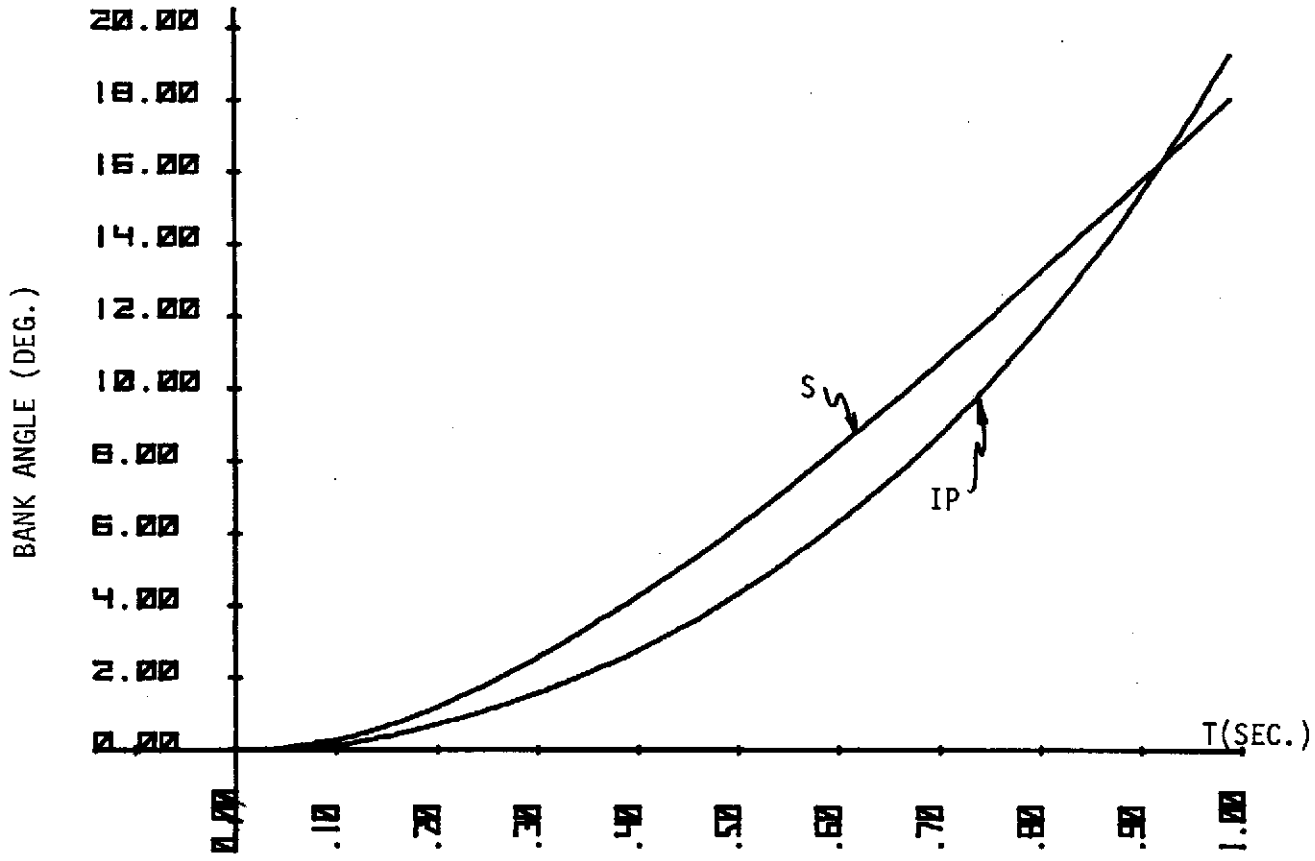

Flight Condition A; $\delta_a^p = 5°$, $\delta_r^p = 0°$; $\delta^a(0) = 0°$;

Rate and Magnitude Constrained

$\Delta\alpha = 8°/sec.$

Figure A96.

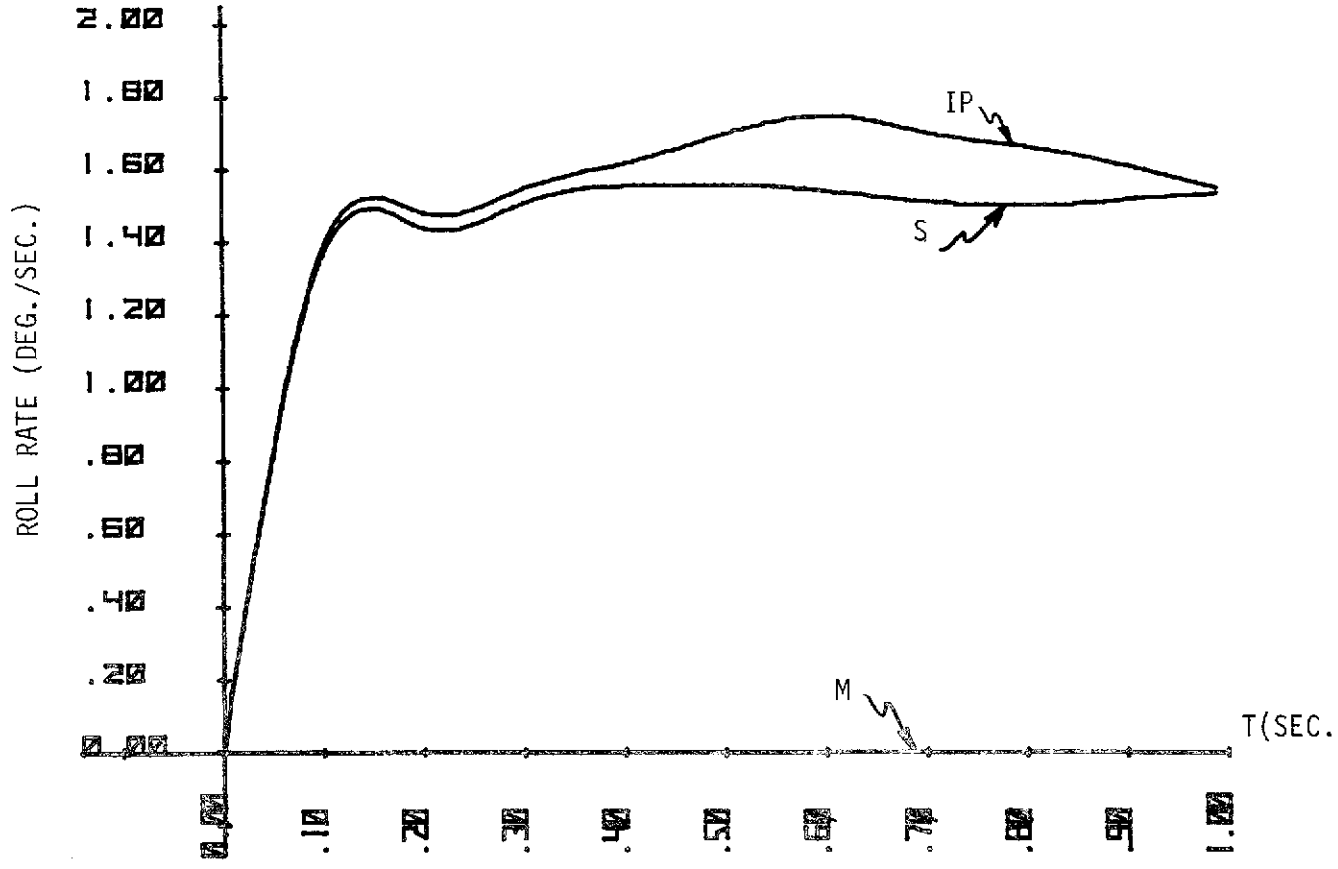

Flight Condition A; $\delta_a^p = 0°$, $\delta_r^p = 3°$; $\delta^a(0) = 0°$;

Rate and Magnitude Constrained

$\Delta\alpha = -8°/sec.$

Figure A97.

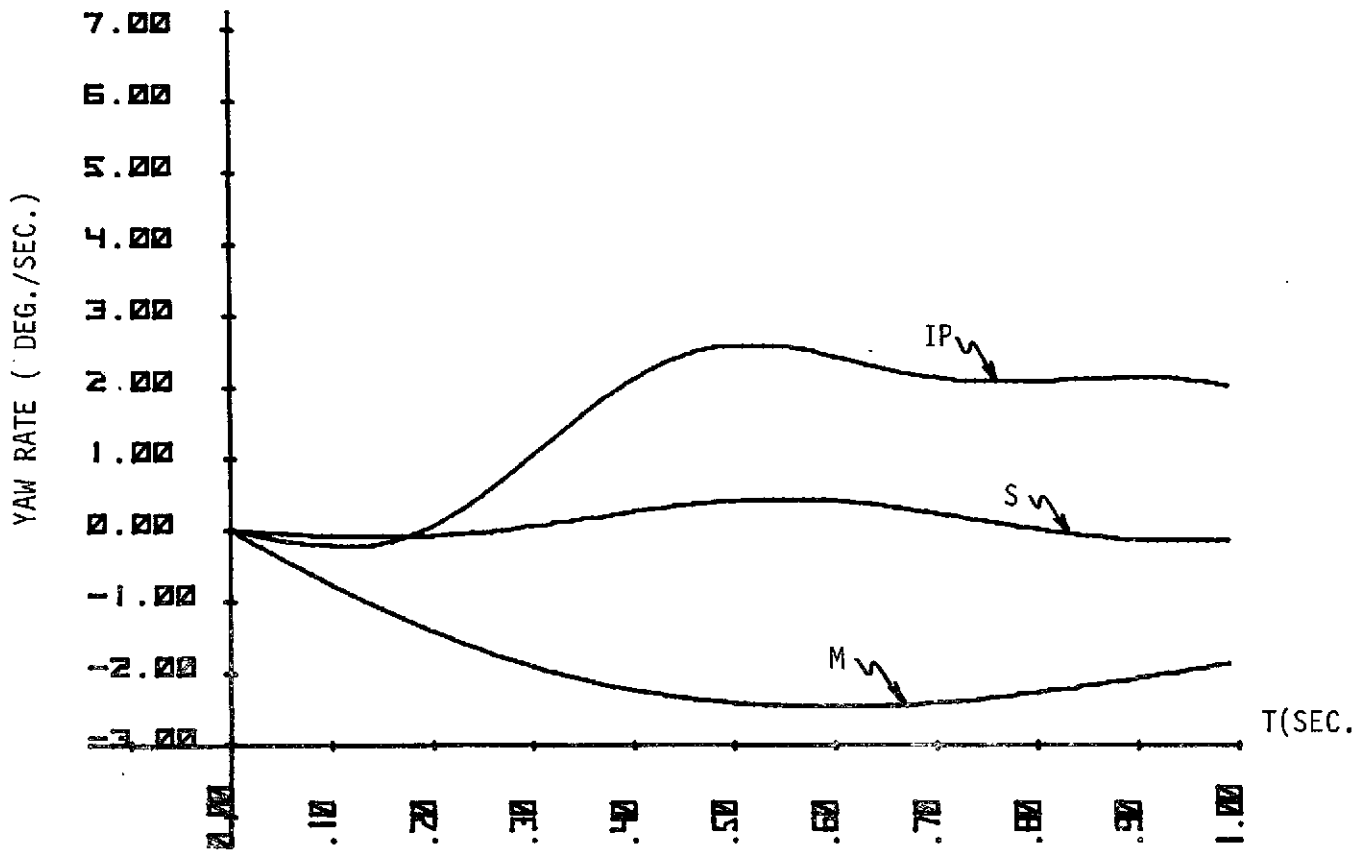

Flight Condition A; $\delta_a^p = 0°$, $\delta_r^p = 3°$; $\delta^a(0) = 0°$;

Rate and Magnitude Constrained

$\Delta\alpha = -8°/sec.$

Figure A 98.

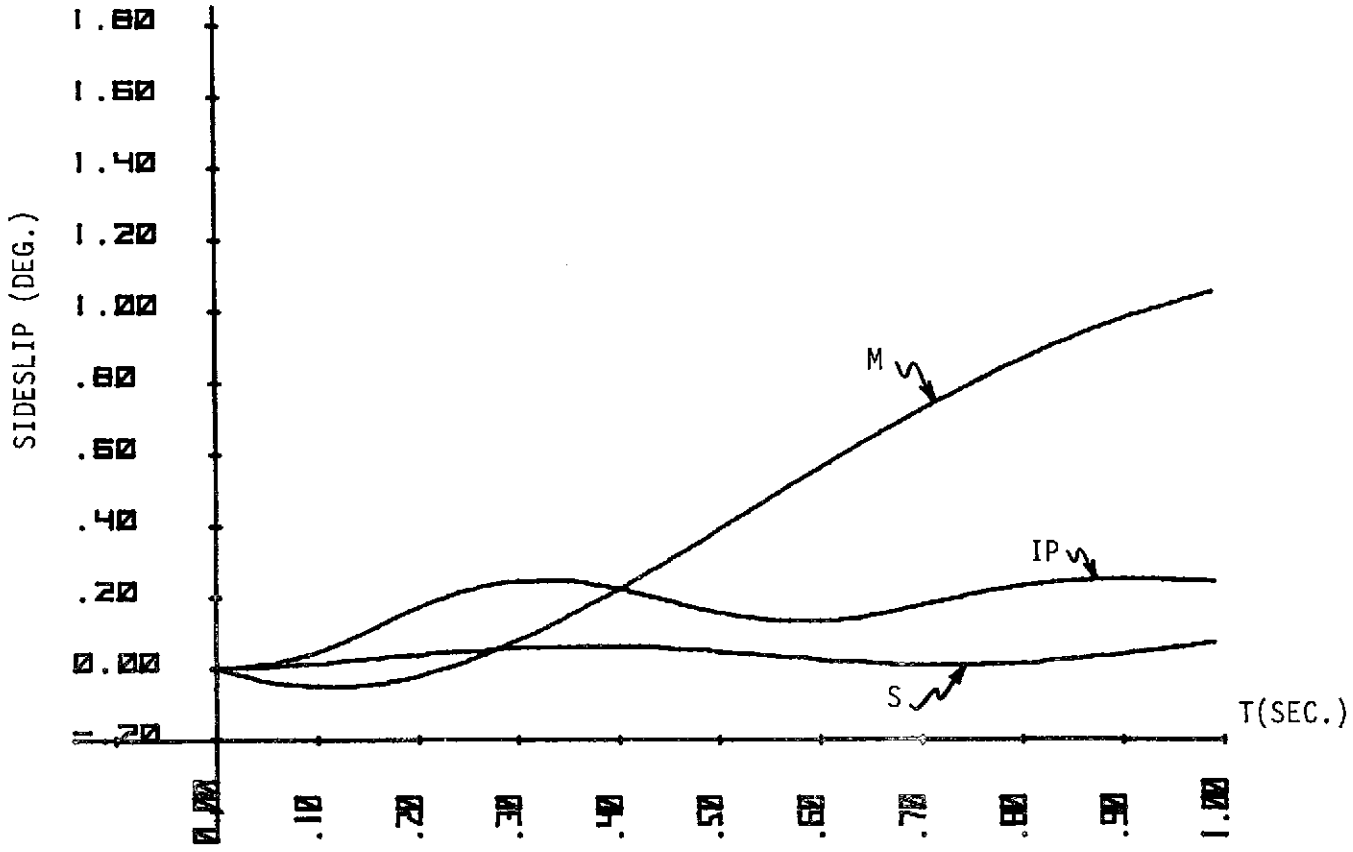

Flight Condition A; $\delta_a^p = 0°$, $\delta_r^p = 3°$; $\delta^a(0) = 0°$;
Rate and Magnitude Constrained
$\Delta\alpha = -8°/sec.$
Figure A 99

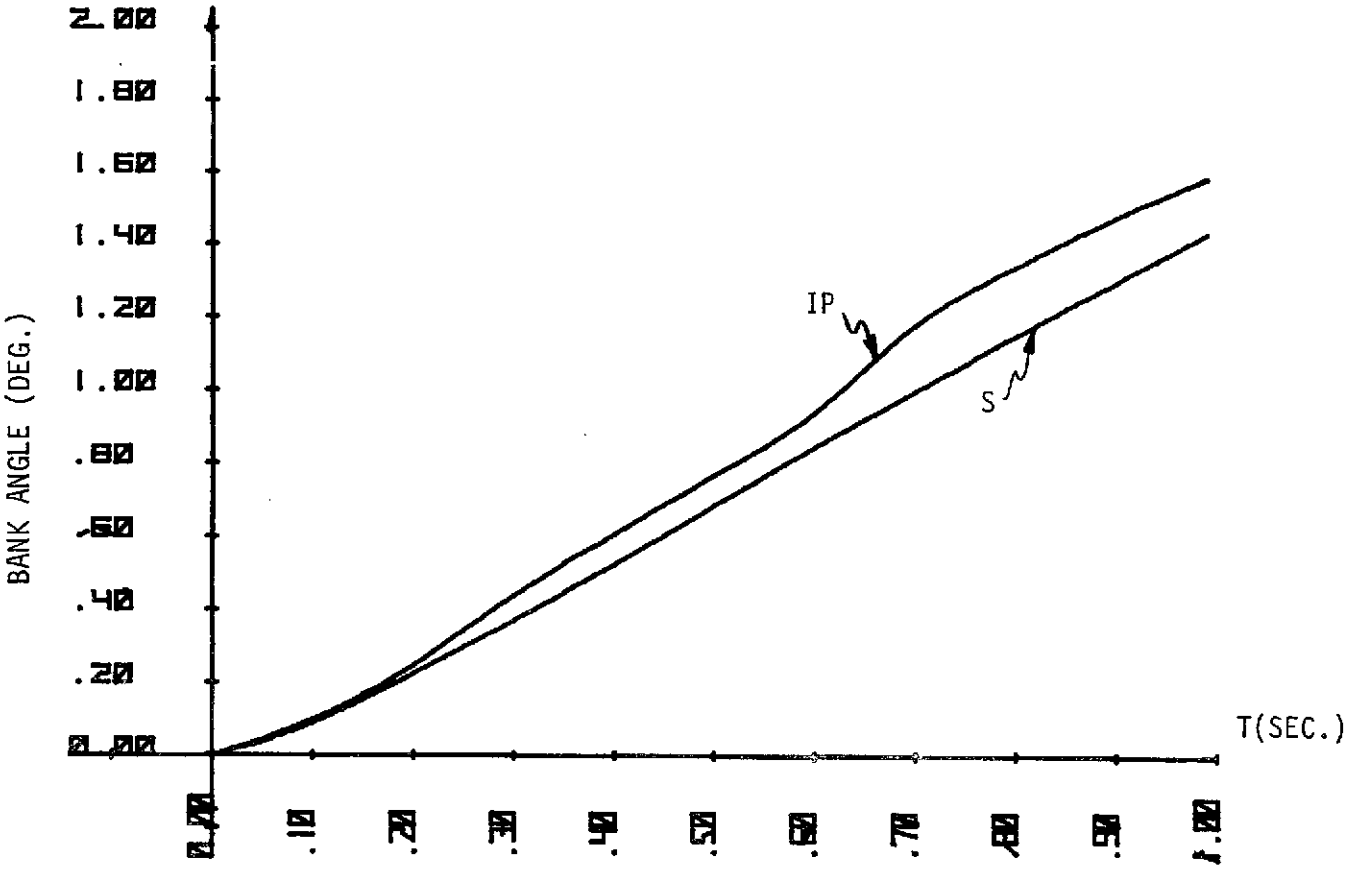

Flight Condition A; $\delta_a^p = 0°$, $\delta_r^p = 3°$; $\delta^a(0) = 0°$;

Rate and Magnitude Constrained

$\Delta\alpha = -8°/sec.$

Figure A 100.

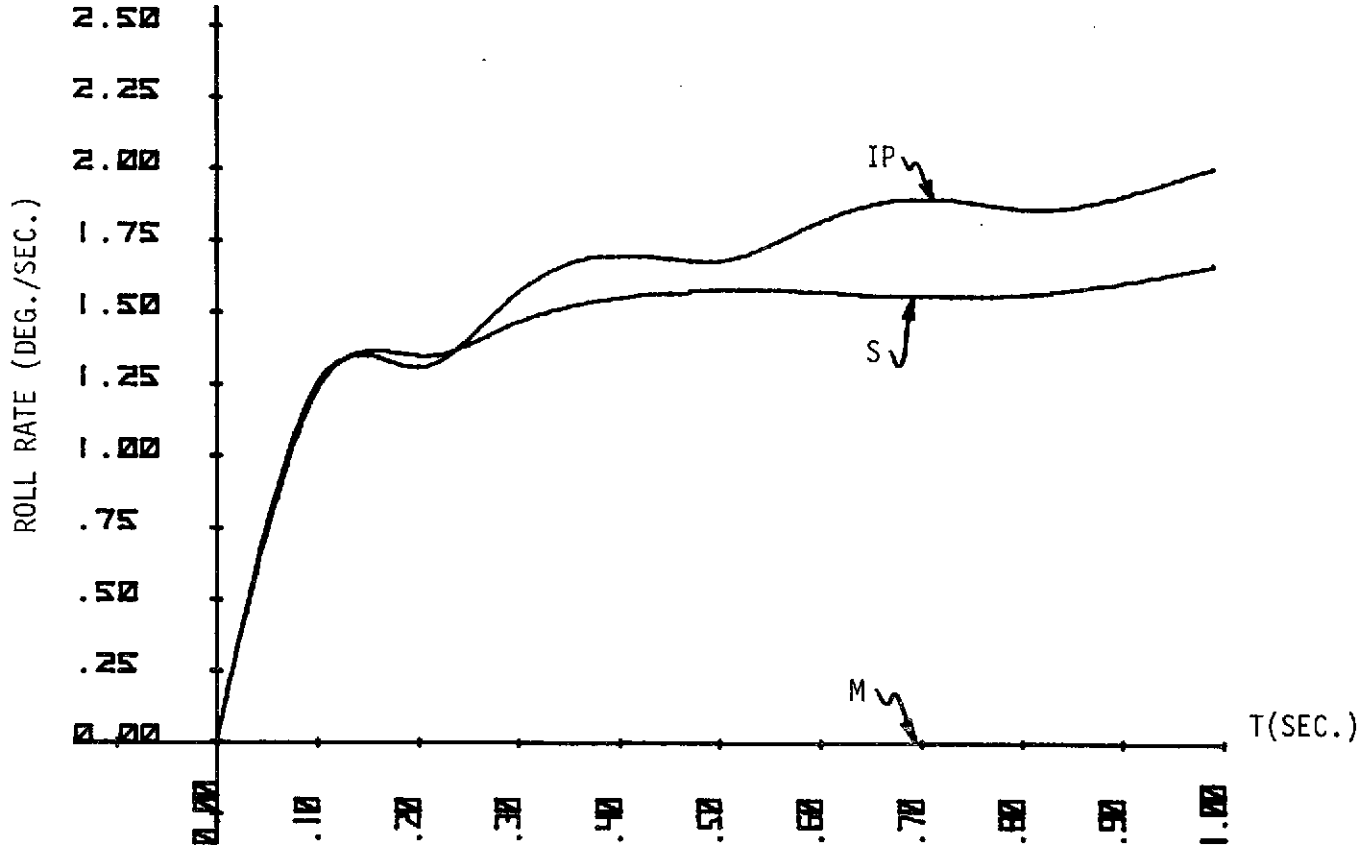

Flight Condition A; $\delta_a^p = 0°$, $\delta_r^p = 3°$; $\delta^a(0) = 0°$;

Rate and Magnitude Constrained

$\Delta\alpha = 8°/sec.$

Figure A 101

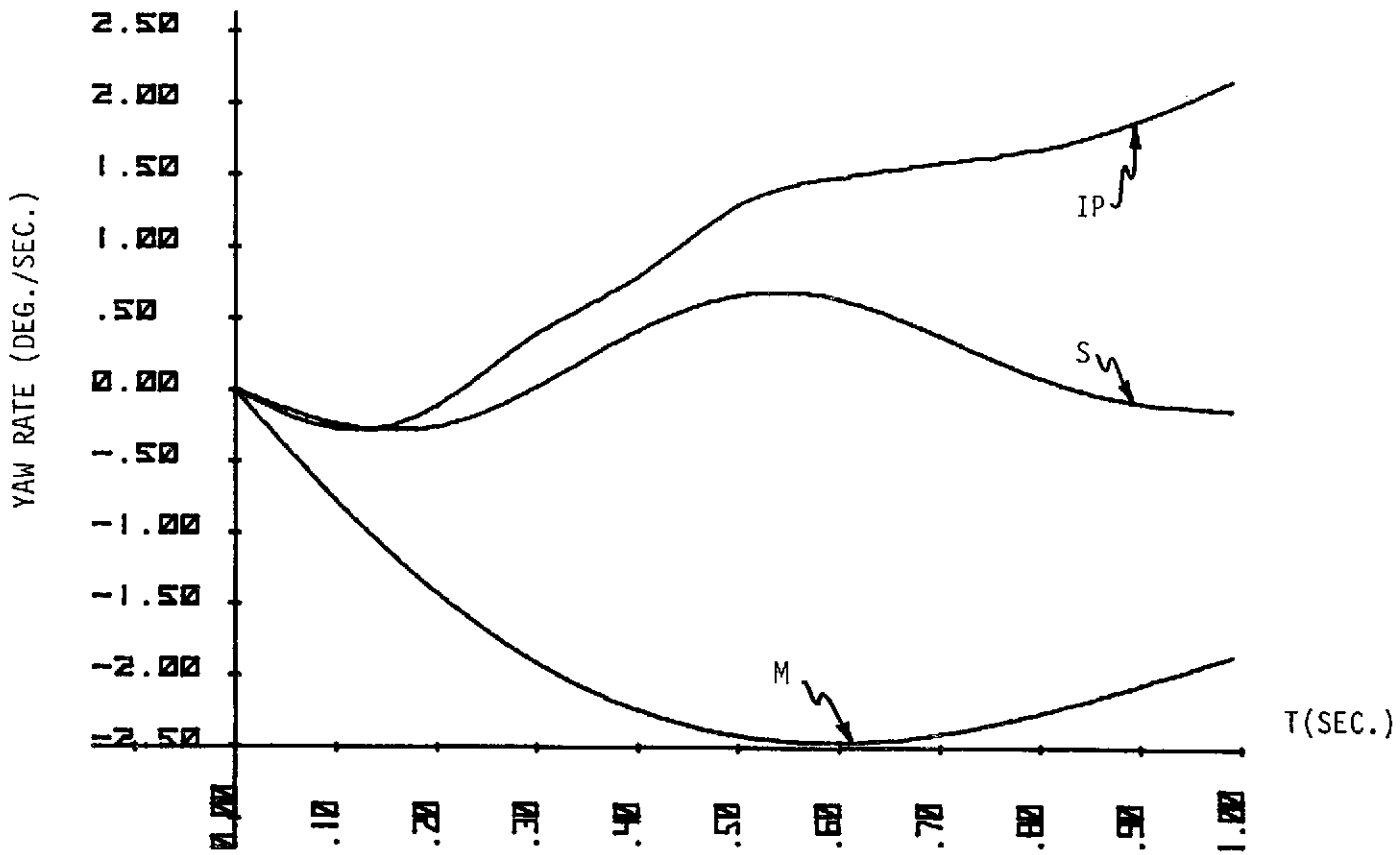

Flight Condition A; $\delta_a^p = 0°$, $\delta_r^p = 3°$; $\delta^a(0) = 0°$;

Rate and Magnitude Constrained

$\Delta\alpha = 8°/sec.$

Figure A 102

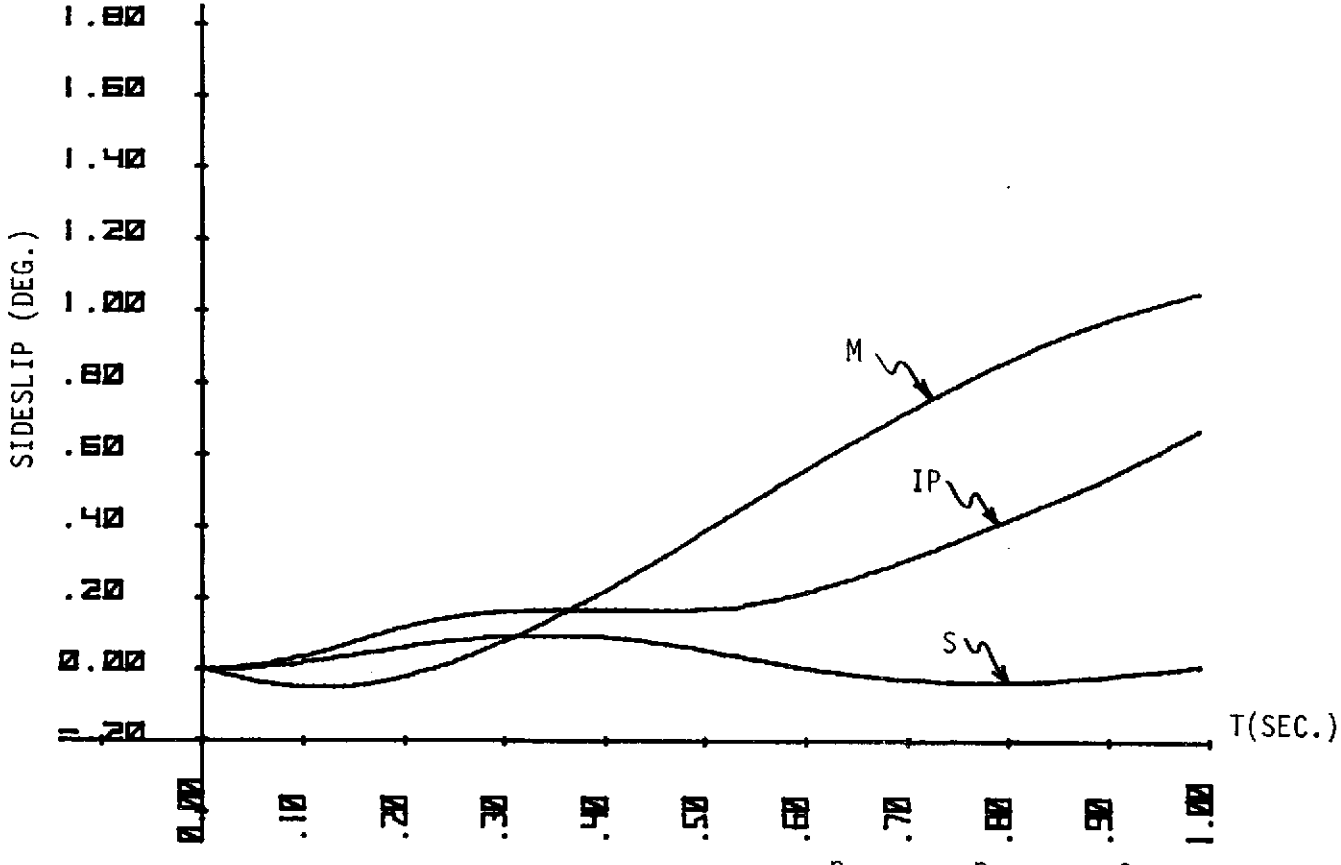

Flight Condition A; $\delta_a^p = 0°$, $\delta_r^p = 3°$; $\delta^a(0) = 0°$;

Rate and Magnitude Constrained

$\Delta\alpha = 8°/sec.$

Figure A 103

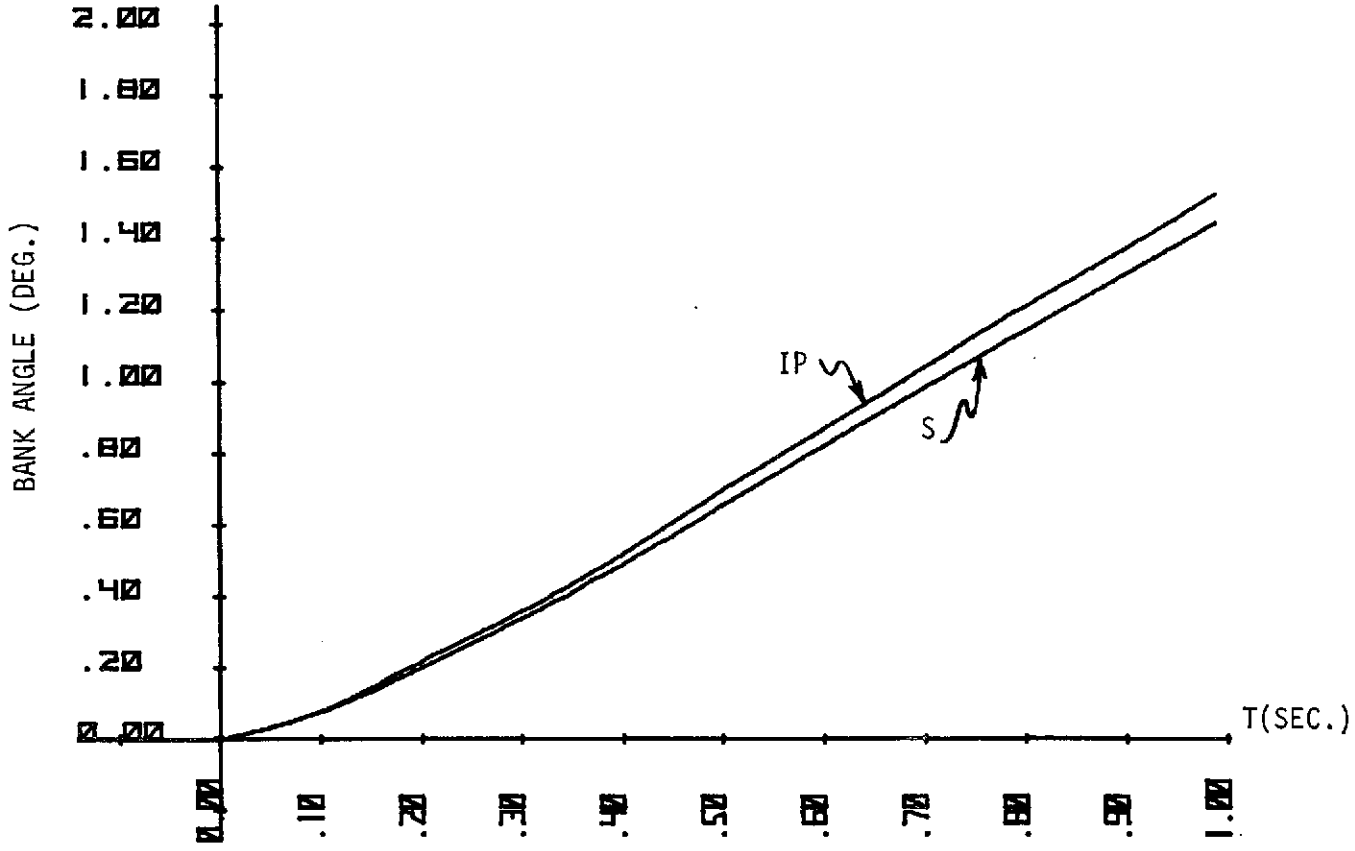

Flight Condition A; $\delta_a^p = 0°$, $\delta_r^p = 3°$; $\delta^a(0) = 0°$;

Rate and Magnitude Constrained

$\Delta\alpha = 8°/sec.$

Figure A 104